

University of Kentucky

UKnowledge

Theses and Dissertations--Radiation Medicine

Radiation Medicine


2021

DEVELOPMENT AND CLINICAL VALIDATION OF KNOWLEDGE-BASED PLANNING MODELS FOR STEREOTACTIC BODY RADIOTHERAPY OF EARLY-STAGE NON-SMALL-CELL LUNG CANCER PATIENTS

Justin David Visak

University of Kentucky, justinvisak18@gmail.com

Author ORCID Identifier:

 <https://orcid.org/0000-0002-8674-5657>

Digital Object Identifier: <https://doi.org/10.13023/etd.2021.038>

[Right click to open a feedback form in a new tab to let us know how this document benefits you.](#)

Recommended Citation

Visak, Justin David, "DEVELOPMENT AND CLINICAL VALIDATION OF KNOWLEDGE-BASED PLANNING MODELS FOR STEREOTACTIC BODY RADIOTHERAPY OF EARLY-STAGE NON-SMALL-CELL LUNG CANCER PATIENTS" (2021). *Theses and Dissertations--Radiation Medicine*. 2.
https://uknowledge.uky.edu/radmed_etds/2

This Doctoral Dissertation is brought to you for free and open access by the Radiation Medicine at UKnowledge. It has been accepted for inclusion in Theses and Dissertations--Radiation Medicine by an authorized administrator of UKnowledge. For more information, please contact UKnowledge@lsv.uky.edu.

STUDENT AGREEMENT:

I represent that my thesis or dissertation and abstract are my original work. Proper attribution has been given to all outside sources. I understand that I am solely responsible for obtaining any needed copyright permissions. I have obtained needed written permission statement(s) from the owner(s) of each third-party copyrighted matter to be included in my work, allowing electronic distribution (if such use is not permitted by the fair use doctrine) which will be submitted to UKnowledge as Additional File.

I hereby grant to The University of Kentucky and its agents the irrevocable, non-exclusive, and royalty-free license to archive and make accessible my work in whole or in part in all forms of media, now or hereafter known. I agree that the document mentioned above may be made available immediately for worldwide access unless an embargo applies.

I retain all other ownership rights to the copyright of my work. I also retain the right to use in future works (such as articles or books) all or part of my work. I understand that I am free to register the copyright to my work.

REVIEW, APPROVAL AND ACCEPTANCE

The document mentioned above has been reviewed and accepted by the student's advisor, on behalf of the advisory committee, and by the Director of Graduate Studies (DGS), on behalf of the program; we verify that this is the final, approved version of the student's thesis including all changes required by the advisory committee. The undersigned agree to abide by the statements above.

Justin David Visak, Student

Dr. Damodar Pokhrel, Major Professor

Dr. Lee Johnson, Director of Graduate Studies

DEVELOPMENT AND CLINICAL VALIDATION OF KNOWLEDGE-BASED
PLANNING MODELS FOR STEREOTACTIC BODY RADIOTHERAPY OF EARLY-
STAGE NON-SMALL-CELL LUNG CANCER PATIENTS

DISSERTATION

A dissertation submitted in partial fulfillment of the
requirements for the degree of Doctor of Philosophy in the
College of Medicine
at the University of Kentucky

By
Justin David Visak
Lexington, Kentucky
Director: Dr. Damodar Pokhrel, Associate Professor of Medical Physics
Lexington, Kentucky
2021

Copyright © Justin David Visak 2021
<https://orcid.org/0000-0002-8674-5657>

ABSTRACT OF DISSERTATION

DEVELOPMENT AND CLINICAL VALIDATION OF KNOWLEDGE-BASED PLANNING MODELS FOR STEREOTACTIC BODY RADIOTHERAPY OF EARLY-STAGE NON-SMALL-CELL LUNG CANCER PATIENTS

Lung stereotactic body radiotherapy (SBRT) is a viable alternative to surgical intervention for the treatment of early-stage non-small-cell lung cancer (NSCLC) patients. This therapy achieves strong local control rates by delivering ultra-high, conformal radioablative doses in typically one to five fractions. Historically, lung SBRT plans are manually generated using 3D conformal radiation therapy, dynamic conformal arcs (DCA), intensity-modulated radiation therapy, and more recently via volumetric modulated arc therapy (VMAT) on a C-arm linear accelerator (linac). Manually planned VMAT is an advanced technique to deliver high-quality lung SBRT due to its dosimetric capabilities and utilization of flattening-filter free beams to improve patient compliance. However, there are limitations in manual treatment planning as the final plan quality heavily depends on a planner's skill and available planning time. This could subject the plan quality to inter-planner variability from a single institution with multiple planners. Generally, the standard lung SBRT patient 'simulation-to-treatment' time is 7 working days. This delays clinic workflow and degrades the quality of treatment by eliminating adaptive re-planning capabilities. There is an ongoing effort to automate treatment planning by creating a model library of previously treated, high-quality plans and using it to prospectively generate new plans termed model-based knowledge-based planning (KBP). KBP aims to mitigate the previously mentioned limitations of manual planning and improve clinic workflow.

As part of this dissertation, lung SBRT KBP models were created using a commercially available KBP engine that was trained using non-coplanar VMAT lung SBRT plans with the final dose reported from an advanced Acuros-based algorithm. The dissertation begins with the development of a robust and adaptable lung SBRT KBP model for early-stage, centrally-located NSCLC tumors that is fully compliant with Radiation Therapy Oncology Group (RTOG)-0813 protocol's requirements. This new model provided similar or better plan quality to clinical plans, however it significantly increased total monitor units and plan complexity. This prompted the development and validation of

an automated KBP routine for SBRT of peripheral lung tumors via DCA-based VMAT per RTOG-0618 criteria. This planning routine helped incorporate a historical DCA-based treatment planning approach with a VMAT optimization automated KBP engine that helps reduce plan complexity. For both central and peripheral lung lesions, the validated models are able to generate high-quality, standardized plans in under 30 min with minimal planner effort compared to an estimated 129 ± 34 min of a dedicated SBRT planner's time. In practice, planners are expected to meticulously work on multiple plans at once, significantly increasing manual planning time. Thus, these KBP models will shorten the 'simulation-to-treatment' time down to as few as 3 working days, reduce inter-planer variability and improve patient safety. This will help standardize clinics and enable offline adaptive re-planning of lung SBRT treatment to account for physiological changes errors resulting from improper patient set-up.

Lastly, this dissertation sought to further expand these KBP models to support delivering lung SBRT treatments on a new O-ring linac that was recently introduced to support underserved areas and fast patient throughput. Despite learning from a C-arm modality training dataset, these KBP models helped the O-ring linac to become a viable treatment modality for lung SBRT by providing an excellent plan quality similar to a C-arm linac in under 30 min. These KBP models will facilitate the easy transfer of patients across these diverse modalities and will provide a solution to unintended treatment course disruption due to lengthy machine downtime. Moreover, they will relieve the burden on a single machine in a high-volume lung SBRT clinic. Further adaptation and validation of these KBP models for large lung tumors (> 5 cm) with multi-level dosing scheme and synchronous multi-lesion lung SBRT is ongoing.

KEYWORDS: Lung SBRT, Knowledge-based Planning, VMAT, Adaptive Re-Planning

Justin David Visak

(Name of Student)

3/19/2021

Date

DEVELOPMENT AND CLINICAL VALIDATION OF KNOWLEDGE-BASED
PLANNING MODELS FOR STEREOTACTIC BODY RADIOTHERAPY OF EARLY-
STAGE NON-SMALL-CELL LUNG CANCER PATIENTS

By
Justin David Visak

Damodar Pokhrel, PhD, DABR

Director of Dissertation

Lee Johnson, PhD, DABR

Director of Graduate Studies

3/19/2021

Date

DEDICATION

To Emily, my parents, friends, and family.

ACKNOWLEDGMENTS

When I first started as a graduate student at the University of Kentucky in 2017, I felt the full support of the department in all of my clinical and research endeavors. Whether specifically named or not, I would like to acknowledge the entire Radiation Medicine department staff for their support. More specifically, I would like to first acknowledge Dr. Damodar Pokhrel for advising me and helping to conceptualize this entire dissertation. He is dedicated to not only supporting me but all students in medical physics. He has played a large role in the success of this dissertation. With his unmatched guidance, it afforded me early success and has bolstered my knowledge of medical physics both clinically and academically.

The next two I would like to thank are Dr. Janelle Molloy and Dr. Marcus Randall. Dr. Molloy first presented me with this outstanding opportunity and worked closely with Dr. Randall to help formulate a way to help me complete my PhD. Without their support, my dissertation and this new program would not have left the ground state. Moreover, I would like to thank Dr. Ronald McGarry for always making time to discuss topics in his office with me and offering his unparalleled clinical expertise and support in lung SBRT throughout this entire PhD dissertation.

To the remaining members of my dissertation committee Dr. Jie Zhang and Dr. Guoqiang Yu, I would like to thank you for taking the time to support me and for steering this new PhD program down a successful path. Moreover, I would like to thank Dr. Wayne Cass for kindly agreeing to sit in on my final thesis defense as an outside examiner. Lastly, I would like to thank both Dr. Lee Johnson and Dr. Dennis Cheek. Both who have provided both academic teaching and clinical training throughout my entire time at UK.

TABLE OF CONTENTS

ACKNOWLEDGMENTS	iii
LIST OF TABLES	vii
LIST OF FIGURES	viii
CHAPTER 1. INTRODUCTION	1
1.1 Management of Lung Cancer.....	1
1.1.1 Lung Cancer Prevalence and Current Treatment Options	1
1.1.2 SBRT Rationale and Development.....	2
1.2 Overview of Lung SBRT Treatment Planning Techniques.....	4
1.2.1 Prescription and Dosing Criteria.....	4
1.2.2 Forward Planning Lung SBRT	5
1.2.3 Inverse Planning Lung SBRT	6
1.3 Knowledge-Based Planning.....	8
1.3.1 Advantages of Knowledge-Based Planning.....	8
1.3.2 Dose-Volume Estimation Algorithm	10
1.4 University of Kentucky SBRT Program.....	13
1.4.1 Lung SBRT Treatments	13
1.4.2 Expansion of Lung SBRT to Novel O-ring Linac	15
1.5 Purpose of Dissertation.....	16
CHAPTER 2. CLINICAL EVALUATION OF PHOTON OPTIMIZER (PO) MLC ALGORITHM FOR STEREOTACTIC, SINGLE-DOSE OF VMAT LUNG SBRT	18
2.1 Introduction.....	20
2.2 Methods and Materials.....	23
2.2.1 Patient Population and Treatment Planning.....	23
2.2.2 PO-VMAT Plan	25
2.2.3 Plan Analysis	25
2.3 Results.....	26
2.4 Discussion.....	29
2.5 Conclusion	33
CHAPTER 3. DEVELOPMENT AND CLINICAL VALIDATION OF A ROBUST KNOWLEDGE-BASED PLANNING (KBP) MODEL FOR STEREOTACTIC BODY RADIOTHERAPY (SBRT) TREATMENT OF CENTRALLY LOCATED LUNG TUMORS	35
3.1 Introduction.....	36
3.2 Materials and Methods.....	39
3.2.1 Patient Population and Target Definition	39
3.2.2 Clinical n-VMAT Plans	40

3.2.3	KBP Model Input and Training Datasets.....	41
3.2.4	Verification of KBP Model.....	42
3.2.5	Validation of KBP Model.....	44
3.3	Results.....	46
3.3.1	Dosimetric Criteria.....	46
3.3.2	Treatment Planning Time, Delivery Efficiency and Accuracy.....	48
3.3.3	Example Validation Case- Left Lower Lobe Tumor	49
3.3.4	Re-Optimized KBPs with 2.5 mm CGS	51
3.4	Discussion.....	53
3.5	Conclusion	56
CHAPTER 4. AN AUTOMATED KNOWLEDGE-BASED ROUTINE FOR STEREOTACTIC BODY RADIOTHERAPY OF PERIPHERAL LUNG TUMORS VIA DCA-BASED VOLUMETRIC MODULATED ARC THERAPY		58
4.1	Introduction.....	59
4.2	Methods.....	62
4.2.1	Patient Population and Clinical Plans	62
4.2.2	Development and Validation of KBP Model.....	62
4.2.3	Dosimetric Comparison Criteria.....	63
4.2.4	A Novel k-DCA Planning Routine	64
4.2.5	Independent Dose Verification	65
4.3	Results.....	65
4.3.1	Clinical Plans vs KBPs	65
4.3.2	Clinical Plans vs k-DCA Plans	66
4.3.3	OAR Sparing.....	67
4.3.4	Planning Efficiency and Deliverability.....	71
4.4	Discussion.....	72
4.5	Conclusion	75
CHAPTER 5. FAST GENERATION OF LUNG SBRT PLANS WITH A KNOWLEDGE-BASED PLANNING MODEL ON RING-MOUNTED HALCYON LINAC		76
5.1	Introduction.....	77
5.2	Materials and Methods.....	81
5.2.1	Patient Selection.....	81
5.2.2	Clinical Plans (c-Truebeam)	82
5.2.3	m-Halcyon Plans.....	83
5.2.4	k-Halcyon Plans	84
5.2.5	Plan Dosimetric Evaluation	84
5.3	Results.....	85
5.3.1	Target Coverage and Intermediate Dose Fall-Off	85
5.3.2	Dose to OAR.....	87
5.3.3	Planning Times and Plan Complexity.....	89

5.3.4	Left Upper Lobe Example Case.....	90
5.4	Discussion.....	91
5.5	Conclusion	94
CHAPTER 6. INNOVATIONS AND CLINICAL IMPACT.....		96
6.1	Chapter 2: Clinical Evaluation of Photon Optimizer (PO) MLC Algorithm for Stereotactic, Single-Dose of VMAT Lung SBRT	96
6.2	Chapter 3: Development and Clinical Validation of a Robust KBP Model for SBRT of Centrally Located Lung Tumors.....	97
6.3	Chapter 4: An Automated KBP Routine for SBRT of Peripheral Lung Tumors via DCA-Based VMAT	99
6.4	Chapter 5: Fast Generation of Lung SBRT Plans with KBP model on O-ring Halcyon Linac.....	101
CHAPTER 7. STUDY LIMITATIONS AND FUTURE RESEARCH DIRECTIONS		104
7.1	Study Limitations.....	104
7.2	Future Research Directions.....	106
CHAPTER 8. CLOSING ARGUMENTS		112
APPENDICES		114
APPENDIX 1. GLOSSARY.....		114
APPENDIX 2. KNOWLEDGE-BASED PLANNING INTERFACE		116
APPENDIX 3. EXAMPLE PLOTS AND STATISTICS.....		119
APPENDIX 4 EXAMPLE PATIENT WITH DVH AND ESTIMATION		122
REFERENCES		123
VITA.....		140

LIST OF TABLES

Table 2.1 Main tumor characteristics of the patients included in this study.....	24
Table 2.2 Analysis of the target coverage as outlined in RTOG 0915 for all 12 patients receiving a single dose of VMAT lung SBRT.....	26
Table 2.3 Analysis of OAR dosimetric parameters for all 12 lung SBRT patients treated with a single-dose of 30 Gy VMAT plan.....	27
Table 3.1 Selected constraints and their priority for the OAR used to generate the KBP model. Gen = generated.	44
Table 3.2 Patient cohort and tumor characteristics for both training and validation of this comprehensive and RTOG compliant KBP model.	45
Table 3.3 Evaluation of CI and GI for all plans generated via KBP model for validation.	46
Table 3.4 Evaluation of dosimetric lung data for all 20 lung SBRT validation cases. MLD = mean lung dose. V5, V10, V20 = volume of lung receiving 5 Gy, 10 Gy, 20 Gy or more.	47
Table 3.5 Treatment delivery efficiency and accuracy of KBP with respect to clinical n-VMAT plans.	49
Table 3.6 Average absolute differences of selected target coverage and DVH parameters for re-optimized KBPs with a 2.5 mm CGS vs original KBPs with 1.25 mm CGS.	52
Table 4.1 Evaluation of plan quality and target indices for all 20 lung SBRT validation cases generated using KBP or <i>k</i> -DCA routine.	66
Table 4.2 Evaluation of normal lung doses for validation cases generated using KBPs or <i>k</i> -DCA routine.....	69
Table 4.3 Evaluation of average treatment delivery parameters for validation cases that were generated using KBP or automated <i>k</i> -DCA routine.....	72
Table 5.1 Validation patient cohort and tumor characteristics. GTV = gross tumor volume, PTV = planning target volume.....	82
Table 5.2 Evaluation of plan quality and target coverage indices for all validation cases including <i>c</i> -Truebeam plans.....	86
Table 5.3 Evaluation of normal lung dosing for lung SBRT validation cases including original <i>c</i> -Truebeam plans.	89
Table 5.4 Evaluation of plan delivery metrics for lung SBRT validation cases including original <i>c</i> -Truebeam plans.	90

LIST OF FIGURES

Figure 2.1 Comparisons of select BEV corresponding MLC control points and isodose distribution in an axial view between PO and PRO algorithms.....	28
Figure 2.2 Comparison of dose volume histograms for target coverage and OARs.	29
Figure 2.3 Ratios of CI, GI, D2cm, GD and select OAR between PO plans vs. clinical PRO plans.	31
Figure 2.4 Average MFs and BOTs for PO and PRO MLC Algorithms.....	32
Figure 3.1 KBP model training input data selection workflow.	42
Figure 3.2 KBP model training workflow.	43
Figure 3.3 Box plot of maximal pairwise dose differences of KBP compared to n-VMAT plans.	48
Figure 3.4 Dose volume histogram comparison for target coverage and OAR dose.	50
Figure 3.5 Comparison of axial and coronal view SBRT isodose distribution for example patient corresponding to Figure 3.4	51
Figure 4.1 Proposed <i>k</i> -DCA treatment planning workflow for peripheral lung SBRT.	65
Figure 4.2 Average maximum doses of selected OAR for clinical plans, KBPs and <i>k</i> -DCA plans.....	68
Figure 4.3 Radiosurgical dose colorwash of the clinical plan, KBP and <i>k</i> -DCA plan for a selected validation case.....	70
Figure 4.4 Dose volume histogram for the clinical, KBP and <i>k</i> -DCA for corresponding example case presented in Figure 4.3	71
Figure 5.1 Beams-eye-view and description of the new stacked and staggered MLC design on the Halcyon Linac.....	80
Figure 5.2 Average doses to PTV and GTV (Gy) for lung SBRT validation cases including clinically treated <i>c</i> -Truebeam plans.....	87
Figure 5.3 Pairwise dose differences (Gy) of maximal and volumetric dose to OAR for <i>k</i> -Halcyon and <i>m</i> -Halcyon plans with respect to <i>c</i> -Truebeam plans.....	88
Figure 5.4 Cumulative dose-volume histogram and corresponding 3-plane view for an example LUL patient.	91

CHAPTER 1. INTRODUCTION

1.1 Management of Lung Cancer

1.1.1 Lung Cancer Prevalence and Current Treatment Options

Lung cancer is the second most prevalent form of cancer among both men and women.¹ The American Cancer Society estimated in 2020 there were 228,820 new cases of lung cancer which include approximately 135,720 deaths.¹ Of these cases, nearly 84% are non-small cell lung cancer (NSCLC).¹ Early stage (T1-T2N0-M0) NSCLC as defined by the eighth edition TNM stage classification includes tumors ≤ 7 cm, do not have or only present with regional metastasis in ipsilateral pulmonary/hilar nodes and no distant metastasis from the primary tumor site.² To manage these early-stage NSCLC patients, there are various forms of treatment options available including a combination of surgical resection, radiation therapy, chemotherapy, targeted agents and immunotherapy.

The most common treatment option for management of early stage I-II NSCLC without distant node involvement is surgical intervention and has demonstrated a 5-year survival rate between 56-92% based on meta-analysis.³ The standard of care for medically inoperable patients, with increasing popularity for operable patients, is lung stereotactic body radiotherapy (SBRT). Lung SBRT has an established and promising 3-year primary tumor control rate of 97% which may provide similar treatment advantages to surgery for less treatment related toxicity.⁴ For select patients, cisplatin-based chemotherapy can be given concomitantly or sequentially with other therapies based on TNM staging criteria.⁵ In addition to standard chemotherapy regimens, there is potential

for the inclusion of both gene expression targeted agents and immunotherapy check-point inhibitors as part of patient care.⁵

1.1.2 SBRT Rationale and Development

While surgical resection offers relatively high 5-year control rates, patients are often times medically inoperable because they present with an advanced stage tumor, inaccessible tumor location, or have a comorbidity due to lifestyle or other diseases (i.e., chronic obstructive pulmonary disease).⁶ Surgical intervention may also require a long-term recovery, extended hospital stay, or a potential surgical complication.^{7,8} For patients that are operable, they still may deny treatment due to this potential degradation of quality of life. Therefore, these select early-stage NSCLC patients may receive conventionally fractionated radiation therapy or lung SBRT; defined as a non-invasive cancer treatment in which numerous, small, highly-focused and accurate beams deliver a high dose of radiation (> 6 Gy per fraction), typically in under 5 treatments.⁴

Prior to the development of lung SBRT treatments, conventional fractionation radiotherapy delivered 60-70 Gy over 6-7 weeks to the tumor with poor five-year local control rates of approximately 30 to 50%.⁹ These unfavorable tumor local control rates led to the development of a high-dose radiotherapy technique for extracranial malignancies termed SBRT. At the time of development of the SBRT treatment procedure, Gamma Knife stereotactic radiosurgery using an external localization device was already widely used in the management of primary or metastatic intracranial lesions.¹⁰ The first major publication for extracranial SBRT was by Lax et al. where they proposed a method for high-dose radiotherapy of malignancies in the abdomen.¹¹ By applying pressure on the abdomen, a stereotactic body frame was described and showed that tumor movement in the liver and

lung could be reduced to 5-10 mm 90% of the time.¹¹ Moreover, they proposed an ultra-high dose can be safely delivered to the tumor using 6-8 non-coplanar beams with rapid dose fall-off around the target.¹² A follow-up study was presented describing 31 patients treated with 7.7 to 30 Gy per fraction in 1-4 fractions.¹³ It was concluded that this technique could offer a convenient SBRT treatment with minimal side-effects for the patients. These landmark studies served as the foundation for progression into modern SBRT techniques that will be described in the next section. Many other studies led to the eventual standardization of lung SBRT.¹⁴⁻¹⁸ In the early 2000s, Dr. McGarry and his colleagues began exploring the potential benefits of lung SBRT for early-stage NSCLC.¹⁹ One of the first studies reported by this Indiana University group was in 2003 that describes a phase I dose escalation trial starting at 8 Gy per fraction prescribed to the 70-80% isodose line for 3 fractions.¹⁴ Patient dose was escalated 2 Gy per fraction every 3-5 patients for a total of 37 patients (maximum up to 24 Gy per fraction for large tumors). It was determined that patients could tolerate 20 Gy per fraction for a total of 3 fractions (60 Gy total dose). In 2006, the same group launched a phase II trial to confirm the predicted toxicity from the previous trial along with an attempt to fully evaluate treatment scheme efficacy in a 2 cohort setting where patients received either 60 or 66 Gy in 3 fractions based on staging.¹⁸ Another important study, completed by Onishi et al., reported the long term follow data for 87 patients who were medically operable but instead treated with lung SBRT.¹⁶ During the follow-up interval, median 5-year local control rates were reported between 73-92% confirming that lung SBRT is potentially comparable to surgery for a non-invasive treatment with less treatment related side effects.¹⁶ Most recently, an ongoing study from the Veterans Affairs's Office of Research and Development titled Veterans Affairs Lung

Cancer Surgery or Stereotactic Radiotherapy (VALOR) aims to determine if surgery or SBRT is a superior treatment option for stage I NSCLC patients.²⁰

1.2 Overview of Lung SBRT Treatment Planning Techniques

1.2.1 Prescription and Dosing Criteria

In North America, the Radiation Therapy Oncology Group (RTOG) reports published between 2007-2009 are widely accepted as the modern lung SBRT practicing guidelines.²¹ In general, prescription selection is based on tumor geographical location, tumor size, staging and surgical candidacy status. These reports detail both tumor prescription and dosing limits to adjacent organs-at-risk (OAR) for lung SBRT treatments. For instance, the first report to be described is RTOG-0618 that provided treatment guidelines for patients with medically operable stage I/II patients with T1-3N0M0 NSCLC (T3 tumors must have chest wall primary tumors only > 2 cm away from proximal bronchial tree).²¹ This protocol originally had a starting fractionation scheme of 60 Gy in 3 fractions, but later it was reduced to 54 Gy in 3 fractions while including tissues heterogeneity corrections and prescribed dose to the tumor periphery (typically 70-80% isodose lines).²¹ Following this report, two reports detailing fractionation schemes specific to OAR sparing for medically inoperable central and peripheral located tumors were published.^{22,23} Centrally located lesions are strictly defined to be tumors within 2 cm or touching the ‘no-fly-zone’ of the proximal bronchial tree. RTOG-0813 provides recommendations starting with a fractionation scheme of 50 Gy in 5 fractions for medically inoperable, centrally located tumors including unique dosing limits to OAR due to toxicity concern.²² Conversely, RTOG-0915 is a 2-arm study with a dosing protocol consisting of 34 Gy in 1 fraction (Arm 1) or 48 Gy in 4 fractions (Arm 2) for peripherally located NSCLC

tumors.²³ Moreover, the most recent work of Videtic and colleagues suggests that there is virtually no differences in tumor local control rates and treatment related toxicity if Arm 1 of the RTOG-0915 protocol is used with a reduced prescription dose of 30 Gy in 1 fraction rather than 34 Gy. Therefore, for selected patients, in many clinics (including our own)²⁴ around the country this is now the standard prescription for a single treatment of lung SBRT.²⁵

1.2.2 Forward Planning Lung SBRT

To fully understand the intent of this dissertation, it is important to discuss all modern lung SBRT treatment planning techniques. 3D-conformal radiation therapy (3D-CRT) involves a planner upfront manually choosing treatment parameters for the desired SBRT plan followed by a dose calculation. This process is known as forward planning and requires a highly trained and experienced planner to generate a clinically acceptable lung SBRT plan. Historically, lung SBRT plans were generated using 3D-CRT. Typically, 5-13 static coplanar/non-coplanar beams shaped the targets with 5-10 mm multileaf collimator (MLC) margins. The planner then proceeds to manually optimize the beam angles, energies, weighting factors, and MLC apertures based on tumor size, location and proximity of the OAR. The results of this should generate a high-quality lung SBRT plan with fast dose fall-off outside the target.²⁶ Additionally, dynamic conformal arcs (DCA) can be used in lieu of or in combination with static gantry beams for lung SBRT treatments.²⁷ This benefits the patient as the target remains in the open field throughout the duration of treatment lessening the chance of interplay between the multi-leaf collimator position and tumor location while minimizing the concern of small field dosimetry errors.^{26,28} However, the major disadvantages of these techniques are there is less dose escalation

potential, less normal tissue sparing capabilities, and for static beams may require a relatively long treatment time that potentially degrades patient comfort.²⁹

1.2.3 Inverse Planning Lung SBRT

Inverse planning of lung SBRT is an advanced treatment planning approach compared to forward planning and its understanding is vital to this dissertation. In inverse planning, for a given beam geometry, the planner has the opportunity to input target doses and normal tissue limits/objectives that define a desired dose distribution upfront. The planner accomplishes this by inputting a series of target and OAR level dosing optimization objectives (e.g., maximum dose allowed to OAR, minimum dose coverage to target). To obtain this desired dose distribution, it requires complex sequencing and movement of the MLCs, gantry positions or dose rates and is not possible for a human to generate such a complex treatment plan. Therefore, using an optimization cost function minimization strategy, a planning software iteratively searches for a fluence map distribution that can replicate the pre-defined dose distribution when back-projected into the patient anatomy. There are two clinical techniques that use an inverse planning approach: intensity-modulated radiation therapy (IMRT) and volumetric modulated arc therapy (VMAT). IMRT for lung SBRT typically involves delivering treatment using 6-12 beams with a static gantry position and dose rate with modulating MLCs (i.e., sliding window or step and shoot methods). The advantage of using IMRT over 3D-CRT is it allows for dose escalation up to 30% without sacrificing normal tissue sparing.⁶ However, this significantly increases the total monitor units and leakage dose. Thus, the complexity of the treatment plan increases which increases overall treatment time.⁶

Most recently, VMAT paired with a flattening-filter-free (FFF) beam is utilized for fast delivery of lung SBRT treatments. To treat lung SBRT, 2-4 partial arcs are deployed with variable MLC openings, dose rate and gantry speed.³⁰ So far, VMAT has shown the benefits of providing the most conformal treatment with maximized normal tissue sparing capability. When these treatments are delivered with a FFF beam, the dose rate can be significantly increased, out-of-field target dose is reduced, and target coverage will be improved at the lung-tumor interface with respect to the traditional flattened beams.^{29,31} These benefits may improve patient convenience and ultimately provide a higher-quality treatment compared to 3D-CRT or IMRT. A few important drawbacks to utilizing a VMAT technique are it is the most susceptible to the previously described interplay effect and due to the gantry motion during treatment, it increases treatment delivery difficulty (including potential risk of patient collisions).^{8 26}

While an inverse planning approach can create a dosimetrically superior lung SBRT plan compared to traditional 3D-CRT methods, there are practical issues that arise that should be considered. These limitations are of the utmost importance as they heavily influence and motivate the purpose of this dissertation. Generating a high quality VMAT lung SBRT plan typically takes several rounds of iterative optimizations and is much of an art as it is a science.³² This is primarily due to a patient presenting with difficult planning geometry, unfavorable tumor location or a large tumor size abutting a dose limiting OAR.³³ Additionally, the final plan quality will depend on a planner's available treatment planning time, training and planning experience at their intuition.³⁴ In most radiotherapy centers, plans are created by a team of dosimetrists (some by well-trained SBRT physicists) and because the plan quality so heavily depends on an individual planner, an institution is

subjected to inconsistent plan quality known as inter-planner variability.^{35,36} In addition to variable final plan quality, the standard ‘simulation-to-treatment’ time across many SBRT clinics around the country is about 7 working days when manually generating a treatment plan. This long ‘simulation-to-treatment’ time significantly delays clinic workflow, patient start date, and eliminates a clinic’s ability to perform offline adaptive radiotherapy.^{37,38} This reduces patient safety, as it is not possible to account for day-to-day physiological changes or patient setup errors that occur during the course of lung SBRT. These drawbacks of the inverse planning prompted the development of an automated inverse planning technique termed knowledge-based planning (KBP) and serves as the fundamental rationale for this dissertation.

1.3 Knowledge-Based Planning

1.3.1 Advantages of Knowledge-Based Planning

Knowledge-based planning (KBP) is an effort to automate the inverse treatment planning process, reduce the burden on an individual planner/institution and improve the treatment plan quality.³² In general, KBP modeling algorithms and software work by using a model library of previously generated high-quality clinical plans to predict new treatment parameters for a prospective patient’s plan. This concept was first introduced and established by research groups from Duke University Medical Center and the Washington University in St. Louis.³⁹ A study by Chanyavanich et al. was one of the first publications to introduce this concept in the context of IMRT planning for prostate cancer.⁴⁰ Here they developed a knowledge-based approach by using a case similarity algorithm to query through a model of previously treated prostate IMRT plans and match their 2D beam’s eye view (BEV) projection image with a new prospective patient’s BEV via mutual

information.⁴⁰ Once the algorithm matched a prospective plan with a previous reference plan, the treatment parameters were imported into the new plan and the fluence map was deformable registered followed by a quick final plan optimization.⁴⁰ This study concluded that their proposed method could generate new plans that were similar or better quality than previously used clinical plans. Briefly, Moore and colleagues from the University of Washington in St. Louis developed a model based approach on the degree of overlap of OAR and the target used to predict mean dose values to those OARs for both head-and-neck or rectum treatments.⁴¹ These two important studies, among others, effectively validated that geometric locations of the target and OARs, paired with their respective dose maps, can generate prospective high-quality treatment plans using mathematical modeling.⁴²

Knowledge-based planning aims to mitigate some of the unavoidable limitations of manual inverse planning techniques for lung SBRT treatments and coincides with the benefits this dissertation proposes. The most important benefit of KBP is that it will remove inter-planner variability that centers with multiple lung SBRT planners are susceptible to.⁴³⁻⁴⁵ Additionally, KBP aids in creating high-quality and standardized treatment plans for specified treatment sites.⁴⁶⁻⁴⁸ If implemented effectively, plans will be created in a clinically relevant shorter planning time and potentially reduce the ‘simulation-to-treatment’ time to 3 working days. This will help reduce the planner burden at busy centers and may aid patients who require an immediate treatment start for aggressive lung tumors. For those cases, or to account for day-to-day physiological changes and daily patient set-up errors, a KBP model could enable a busy clinic to perform offline adaptive radiotherapy.⁴⁹ Having an effective KBP model will allow for underlying benefits that

include performing quality assurance on previous plans to better assess areas of future improvement.^{50,51} These benefits drove the conception and purpose of this dissertation to be later described.

1.3.2 Dose-Volume Estimation Algorithm

Recently, Varian Medical Systems (Palo Alto, CA) released a knowledge-based planning dose-volume-histogram algorithm RapidPlanTM that can predict OAR DVHs and optimization objectives including maximum, mean and a new line dose constraint with automatically generated priorities. This is achieved by mining specific data from a model library of previously treated high-quality plans. Our institution recently upgraded our treatment planning system and acquired a license for RapidPlan DVH estimates that can be used for lung SBRT planning.

The algorithm has two components, the model configuration and DVH estimate component.⁵² In the model configuration part, an appropriate numbers of previously treated high quality training plans⁵³ are input into the algorithm to begin data extraction. The exact number of plans to input is based on the complexity of the tumor site and other factors; too few plans can result in an undertrained model, conversely, too many plans could result in overfitting the KBP model. Once the plans are uploaded, the algorithm will parse out each OAR structure into four voxel regions: in-field, out-of-field, leaf transmission and overlap reason. For each region a Geometry Expected Dose (GED) histogram, cumulative DVH and other information will be calculated.⁵² The GED essentially provides a histogram relating the fractional volume of the particular OAR to a specified distance away from the target including dose received by each voxel at that specified distance. Once all relevant information has been extracted, the training phase of the algorithm begins.

For each OAR, a DVH estimation model will be trained that is the sum of four OAR-region estimation models (i.e., in-field model). There are different ways each region-specific model is trained depending on desired accuracy of prediction and available training dataset.³⁶ In general, the in-field region is trained using a principal component analysis (PCA) regression⁵⁴ and the remaining regions are trained using a mean and standard deviation (STD) method. Briefly, for regions using PCA, each DVH and GED histogram are sampled to represent feature points in a new feature space. The respective principal components scores (PCS) are found by performing a singular value decomposition (SVD) on the calculated covariance matrix from the feature space of points.⁵⁴ The eigenvectors and eigenvalues are then extracted via the SVD and the algorithm uses these values to determine the PCSs.⁵⁴ The extracted PCSs from the DVH and GED histogram are then used to find a linear relationship between two selected PCSs for each plan. Once this relationship is determined, a prospective patient plan's GED PCSs will be calculated in the algorithm by multiplying the new GED with the transformation matrix derived from the learning phase.⁵⁴ Next, the regression relationship is utilized to obtain the estimated DVH PCSs. These scores (which represent curves) are added to the average mean DVH of the database and the final estimated DVH can then be extracted using an inverse transformation. On a simpler note, the mean and STD DVH for the other regions are used to predict the new DVH (as specified by the vendor).⁵² Once the estimates are made, an upper and lower bound exists and the associated optimization objectives are derived by the algorithm based on user preference.

Once a model is fully trained, the user must verify and further validate the model with a separate set of training plans. This typically involves tweaking the model objectives,

input mapping of the clinical plans and overall fine adjustments of the model. Meaning, creating a model is simply not “plug-and-chug.” The goal of verifying a model in essence is to check the model’s overall fit and identify both geometric or dosimetric outliers.⁵⁵ This is accomplished by utilizing the algorithm provided fitting statistics (e.g., R^2 , modified Z-score, Cook’s distance), regression or geometric plots, and the cumulative DVH with its estimated prediction for each training plan (see Appendix). Currently, there is no standard way to verify the newly generated model and it is incumbent on the user to develop their own verification procedure (described in a later chapter). A separate set of validation plans (not used to train the model) should be re-optimized using the DVH estimation algorithm following further verification. To generate an acceptable KBP model, the vendor recommends using a minimum of 20 diverse plans⁵⁵ (e.g., varied tumor location and size), but it’s ultimately based on the user’s confidence to verify the model. These validation KBPs should be carefully examined that the DVH estimates are reasonable and the final KBP plan is of similar or better quality to the clinical treatment plan. This is a tedious and time intensive process as one minor tweak to either the training data or user objective will require all plans are re-validated with the KBP model in its current form. Therefore, it is mandatory on the user to learn how to determine which model adjustments will fulfill clinical requirements and further improve the model performance. Upon completion of all the previously mentioned steps, a KBP model will be ready to be deployed clinically.

In the context of lung SBRT, Chin et al. provided the first KBP RapidPlan model using 105 plans that included IMRT, VMAT and 3D-CRT treatments.⁴² As mentioned in the publication, their model was primarily trained using IMRT plans and concluded KBPs were of similar or better quality to their respective clinical plans. This study sought to

encompass all all tumor geographical locations with a single common RTOG prescription. As mentioned in later chapters, this is too broad of an approach with KBP modeling and uses an inferior planning technique; nonetheless this publication served as an important proof-of-concept for the field going forward. While other sites were preliminarily investigated, ^{33,48,56-60} minimal literature exists for lung SBRT KBP models with clinical application besides the manuscripts generated as part of this dissertation.⁶¹⁻⁶⁵

1.4 University of Kentucky SBRT Program

The University of Kentucky Medical Center has established constantly growing stereotactic radiosurgery (SRS) and SBRT programs that includes linac based brain and spine SRS, prostate, liver and thoracic SBRT treatments. In the context of this dissertation, the thoracic program herein will be described. For reference, all treatments including lung SBRT are currently manually optimized by many experienced dosimetrists at our institution. The results of this dissertation will enable many lung SBRT plans to be created via recently developed KBP models.

1.4.1 Lung SBRT Treatments

Following diagnosis and selection for lung SBRT treatment, a patient undergoes a computed tomography (CT) simulation using a respiratory motion management technique for treatment planning. In our center, patients are immobilized in a Body Pro-Lock™ platform (CIVCO system, Orange City, IA) in the head-first, supine position with arms above their head including abdominal compression. A free breathing 3D-CT scan is performed, and images are imported in the Eclipse treatment planning system (TPS). The region of tissue found to be grossly involved with the lung tumor, gross tumor volume (GTV), is then delineated by the treating physician.⁶⁶ To account for tumor motion and

patient set up errors, a margin of 1.0 cm superior/inferior and 0.5 cm laterally is applied to the GTV therefore delineating a planning target volume (PTV). If a patient is unable to undergo abdominal compression, a respiration correlated 4D-CT scan was acquired (along with the free breathing planning CT scan) and maximum intensity projection (MIP) images were derived. The free-breathing CT and MIP images were then co-registered, and an internal target volume (ITV) is created. Meaning, $ITV = GTV$. Per protocol guidelines, a 0.5 cm uniform margin is applied to the ITV to create the PTV to account for microscopic disease. All relevant OARs are contoured following target delineation. The University of Kentucky Medical Center almost exclusively uses a manually generated non-coplanar VMAT treatment technique for lung SBRT. These patients are primarily treated on a SBRT-dedicated Varian Truebeam linac (Varian Medical Systems, Palo Alto, CA) with a nominal 6MV-FFF beam and maximum dose rate setting of 1400 monitor units (MU) per minute. The major prescriptions utilized for lung SBRT treatments are 50 Gy in 5 treatments or 54 Gy in 3 treatments prescribed to the 60-80% isodose line with no hotspots allowed outside of the PTV (i.e., hotspots: 120-140%). Recently, for selected lung SBRT patients, 30 Gy in 1 treatment scheme is also becoming a rising prescription choice at UK.⁶⁷ Final plan dose is calculated using the advanced Acuros-based dose engine for tissues heterogeneities corrections. On the day of treatment, a physician is present at the machine to perform pre-treatment online cone-beam CT (CBCT) imaging for patient alignment and set up verification. The majority of cases are mostly single lesion; however, the University of Kentucky Medical Center has treated a growing number of lung SBRT patients who present with oligometastatic (< 5 lesions) lung tumors.^{68,69}

1.4.2 Expansion of Lung SBRT to Novel O-ring Linac

Recently, the University of Kentucky Medical Center installed a novel O-ring Varian Halcyon Linac (V3.0) and aims to expand the busy thoracic and other SBRT programs to this new platform. This linac was brought to market with the intention of increasing the speed of patient throughput and advance standard daily fractionated radiation treatments to the underserved community.⁷⁰ While not specifically designed for SBRT, the novel design of the linac with daily kV-CBCT imaging capability allows for high-quality lung SBRT treatments for selected patients after commissioning for hypofractionated treatments.⁷¹ Historically, the majority of treatments are delivered via a C-arm SBRT dedicated linac (Varian Truebeam) which is a vastly different design from the ring-mounted Halcyon. This linac is equipped with single-energy 6MV-FFF beam, is jawless and is a coplanar restricted modality. The Halcyon's 6X-FFF beam is slightly softer than Truebeam's with a mean energy and nominal depth of maximum dose of 1.3 MeV at 1.3 cm compared to 1.4 MeV at 1.5 cm, respectively. As of now, Halcyon only allows for a maximum dose rate setting of 800 MU/min whereas the Truebeam is capable of 1400 MU/min (for 6X-FFF). These mechanical limitations may present difficulty in manually planning lung SBRT VMAT treatments on Halcyon. A benefit of the new Halcyon design is the ring-mounted linac is capable of a fourfold increase of rotational gantry speed compared to Truebeam and is equipped with a new dual-layered stacked and staggered 1 cm wide MLC design.^{72,73} The new MLC design restricts the field size to $28 \times 28 \text{ cm}^2$ but is capable of complete MLC interdigitation whereas the Truebeam allows for a $40 \times 40 \text{ cm}^2$ maximum field size but does not have full leaf travel. While the larger field size is useful for many advanced staged disease sites, it does not serve a clinically practical

purpose for the relatively small target presentation in lung SBRT treatments. The Halcyon leaves are less rounded and subsequently have a smaller dosimetric leaf gap (0.1 mm) and ultra-low leakage and transmission (0.4%) compared to the standard millennium 120 MLC equipped on Truebeam linac.^{73,74} Target localization and patient set up verification may be improved on Halcyon as an advanced iteratively reconstructed on-board CBCT (iCBCT) scan can be acquired in under 15 seconds. Misalignments can then be corrected with automatically applied isocenter shifts via a “one-step patient set-up” approach without manually shifting the patients.⁷⁵

The Halcyon Linac has demonstrated that it can provide high-quality treatments for conventionally fractionated cranial, head and neck, prostate and breast treatments.⁷⁶⁻⁷⁹ Minimal literature exists on Halcyon for stereotactic treatments⁸⁰⁻⁸² and none which consider the benefits of using a lung SBRT-KBP model to improve treatments and ease the SBRT planner’s burden to overcome the treatment modality’s limitations.

1.5 Purpose of Dissertation

As previously discussed, manually inverse planning lung SBRT treatments leads an institution to clinical workflow delays, inconsistent plan quality and restricts offline adaptive replanning. Additionally, minimal literature exists for lung SBRT planning via KBP models with either a SBRT-dedicated C-arm or novel ring-mounted linac. There is no clear guidance or outlined procedure for developing and validating a high-performing, non-coplanar VMAT lung SBRT KBP model. These planning limitations and lack of literature provides the foundation for the core objective of this dissertation. **Therefore, the purpose of this dissertation is to develop, validate and explore the clinical benefits of fully RTOG criteria compliant, non-coplanar VMAT lung SBRT KBP models for**

medically inoperable centrally located and medically inoperable/operable peripherally located, early-stage, non-small-cell lung tumors. These fully RTOG compliant KBP models may be used to treat patients on both a traditional SBRT-dedicated C-arm linac or transfer patient to a novel O-ring mounted linac. We hypothesized that these region-specific models would help standardize SBRT plan quality in a busy SBRT clinics by removing inter-planner variability, improve clinic workflow by significantly shortening ‘simulation-to-treatment’ time to 3 working days, and enabling a clinic to perform offline adaptive replanning, as needed. Overall, the results of this dissertation will provide a clearer guidance for future KBP modeling, standardize a clinic’s lung SBRT program in academic and community centers, and improve patient safety.

Specifically, as part of the first aim of this dissertation, a robust lung SBRT KBP model for medically inoperable early-stage, centrally-located non-small-cell lung cancer was developed and validated. Following the first aim, the second aim of this dissertation developed and validated a robust lung SBRT KBP model for medically inoperable/operable early-stage, peripherally-located NSCLC patients using a novel DCA-VMAT based planning technique. Lastly, the third aim of this dissertation adapted and further generalized the model generated in the first aim to better support lung SBRT treatments on a novel O-ring linac.

Copyright © Justin David Visak 2021
<https://orcid.org/0000-0002-8674-5657>

CHAPTER 2. CLINICAL EVALUATION OF PHOTON OPTIMIZER (PO) MLC ALGORITHM FOR STEREOTACTIC, SINGLE-DOSE OF VMAT LUNG SBRT

Prior to generating the lung SBRT RapidPlan KBP models, it was necessary to dosimetrically characterize and validate the novel Photon Optimizer (PO) MLC positioning algorithm in the Eclipse TPS against the previously and clinically utilized Progressive Resolution Optimizer (PRO) algorithm. RapidPlan modeling does not support the PRO-MLC algorithm. The results of this chapter provided guidance in validating the most optimal PO-MLC algorithm that is used for generating lung SBRT KBP models. **Chapter 2** has been adapted from the recently published manuscript by: **Visak J**, McGarry RC, Pokhrel D. Clinical evaluation of photon optimizer (PO) MLC algorithm for stereotactic, single-dose of VMAT lung SBRT. Med Dosim. 2020; 45(4):321-326

Abstract

Recently implemented Photon Optimizer (PO) MLC optimization algorithm is mandatory for RapidPlan modeling in Eclipse. This report quantifies and compares the dosimetry and treatment delivery parameters of PO vs its predecessor Progressive Resolution Optimizer (PRO) algorithm for a single-dose of volumetric modulated arc therapy (VMAT) lung stereotactic body radiation therapy (SBRT). Clinical SBRT treatment plans for 12 early-stage non-small-cell-lung cancer (NSCLC) patients receiving 30 Gy in 1 fraction using PRO-VMAT were re-optimized using the PO-VMAT MLC algorithm with identical planning parameters and objectives. Average planning target volume (PTV) derived from the 4D-CT scans was 13.6 ± 12.0 cc (range: 4.3–41.1 cc). Patients were treated with 6MV flattening filter free (FFF) beam using Acuros-based calculations and 2.5 mm calculation grid-size (CGS). Both treatment plans were

normalized to receive same target coverage and identical CGS to isolate effects of MLC positioning optimizers. Original PRO and re-optimized PO plans were compared via RTOG–0915 protocol compliance criteria for target conformity, gradient indices, dose to organs at risks (OAR) and delivery efficiency. Additionally, PO-VMAT plans with a 1.25 mm CGS were evaluated. Both plans met RTOG protocol requirements. Conformity indices showed no statistical difference between PO2.5mm CGS and PRO2.5mm CGS plans. Gradient index ($p = 0.03$), maximum dose to 2 cm away from PTV in any direction (D_{2cm}) ($p < 0.05$) and gradient distance ($p < 0.05$) presented statistically significant differences for both plans with 2.5mm CGS. Some OAR showed statistically significant differences for both plans calculated with 2.5mm CGS, however no clinically significant dose differences were observed between the plans. Beam modulation factor was statistically significant for both PO1.25 mm CGS ($p = 0.001$) and PO2.5 mm CGS ($p < 0.001$) compared to clinical PRO2.5mm CGS plans. PO-VMAT plans provided decreased beam-on time by an average of 0.2 ± 0.1 min (up to 1.0 min) with PO2.5 mm and 1.2 ± 0.39 min (maximum up to 3.22 min) with PO1.25 mm plans compared to PRO2.5 mm plans. Overall, PO-VMAT single-dose of VMAT lung SBRT plans showed slightly increased intermediate-dose spillage but boasted overall similar plan quality with less beam modulation and hence shorter beam-on time. However, PO1.25mm CGS had less intermediate-dose spillage and analogous plan quality compared to clinical PRO-VMAT plans with no additional cost of plan optimization. Further investigation into peripheral targets with PO-MLC algorithm is warranted. This study indicates that PO1.25 mm CGS plans can be used for RapidPlan modeling for a single-dose of lung SBRT patients. PO-

MLC 1.25 mm algorithm is recommended for future clinical single dose lung SBRT plan optimization.

2.1 Introduction

Due to the recent technological advances in radiotherapy, stereotactic body radiotherapy (SBRT) treatment to solitary primary or metastatic lung lesions for medically inoperable non-small-cell lung cancer (NSCLC) patients is safe, effective and has a high cure rate comparable to surgery¹⁻⁴ including SBRT for elderly patients.⁵ Moreover, SBRT is better tolerated by patients with respect to surgery due to its minimal adverse effects.⁶ RTOG-0915 protocol (Arm 1) allowed a single-dose of 34 Gy SBRT treatment for early-stage I peripheral NSCLC patients when dosimetric compliance criteria were met.⁷ Videtic *et al*⁸ reported long-term follow up data which revealed no excess late toxicity in either arm (34 Gy in 1 fraction and 48 Gy in 4 fractions) and demonstrated consistent high rates of local control. They reported a median overall survival of 4 years for each arm suggesting similar efficacy. Their study concluded that single-fraction SBRT of 34 Gy remains a suitable treatment option for patients with early-stage inoperable lung cancer. In another study, Videtic *et al*⁹ compared 2 single-fraction SBRT dose schemes of 30 Gy and 34 Gy for 80 medically inoperable early stage-I NSCLC patients. Both treatment schedules provided equivalent tumor local-control and overall survival rates with minimal toxicity. Thus, a single-dose of 30 Gy is an equally effective treatment as 34 Gy for the selected NSCLC patients and is gaining popularity in the clinics.

It has been demonstrated that with respect to traditional SBRT planning methods, 3D conformal radiation therapy, VMAT provides equal or improved dosimetric delivery.¹⁰ Utilizing volumetric modulated arc therapy (VMAT) and flattening filter free (FFF) beams

have reduced SBRT treatment time significantly for a single-high dose of radiation and improved patient compliance.^{11, 12} Removal of the flattening filter from the gantry provides benefits by reducing head scatter, out-of-field dose, residual electron contamination, and delivers treatments with higher dose rates up to factors of 2.33 for 6X-FFF and 4 for 10X-FFF beams compared to the traditional flattened beams.^{10, 13} Because of the reduced treatment times, VMAT with FFF beams is particularly appealing for delivering a single high-dose of SBRT treatment to lung lesions, potentially minimizing intrafraction motion errors as well.

Recently, Varian Eclipse treatment planning system (TPS, Varian Medical Systems, Palo Alto CA, Version 13.5) has implemented a new multileaf collimator (MLC) optimization algorithm called Photon Optimizer (PO).¹⁴ PO-MLC algorithm was created to be more efficient for IMRT/VMAT optimization over its predecessor, Progressive Resolution Optimizer (PRO) algorithm. The main difference between PO and PRO algorithms is that PO uses a new model for defining structures. For the PO algorithm, the structures, dose-volume histogram calculations and dose sampling are defined spatially using a single matrix over the image instead of a point-cloud model defining structures that was used in the PRO algorithm. In this setting, the PO-MLC algorithm under-samples voxels at the periphery of the target. However, the PO-MLC setting in Eclipse uses multiresolution dose calculation approach to increase the dose calculation accuracy. Fixed voxel resolutions of 1.25 mm, 2.5 mm or 5 mm can be used during multiresolution optimization.

A few investigators have reported the dosimetric differences of PO-MLC algorithm for IMRT/VMAT planning in a digital phantom,¹⁵ conventional prostate, head and neck,

and brain treatments,¹⁶ knowledge-based planning to rectal cancer patients¹⁷ as well as fractionated lung SBRT patients and stereotactic brain treatments.¹⁸ For instance, the advantages and limitations of PO algorithm compared to its predecessor PRO for IMRT plans were evaluated by Binny *et al*¹⁶. Eleven plans including prostate, brain, and head and neck treatments were optimized using both PO and PRO-MLC algorithms in their study. For similar target coverage and dose to critical structures, they reported that the PO algorithm gave higher MLC variability and more monitor units. Liu *et al*¹⁸ compared PO with PRO algorithms for VMAT planning of fractionated lung SBRT and brain stereotactic treatments. Their retrospective study included 20 lung SBRT patients (10 received total dose of 54 Gy in 3 fractions and 10 patients received total dose of 50 Gy in 5 fractions) and 10 brain stereotactic patients received total dose of 25 Gy in 5 fractions. They reported for identical target coverage, PO algorithm provided comparable plan quality to PRO, with less MLC complexity, thus improving the treatment delivery efficiency, but contradicting the results presented by Binny *et al*.¹⁶ Although dosimetric differences with PO algorithm for lung SBRT plans have been studied previously by Liu *et al*¹⁸, the dosimetric impact and treatment delivery complexity of this algorithm with a FFF-beam in the treatment of single-high dose of 30 Gy in 1 fraction using non-coplanar VMAT lung SBRT planning with fine resolution dose calculation grid size (CGS) of 1.25 mm has not yet been reported.

Single-fraction lung SBRT (30 Gy in 1 fraction) is an extreme form of hypofractionation used in our clinic for extracranial lesions where the dose calculation accuracy could potentially suffer by tumor size, tumor location and the presence of inhomogeneities in the lung. Moreover, due to under sampling of the voxels at the periphery of tumor volume by the PO-MLC algorithm, there is a potential for higher

nontarget normal tissue dose to the organs-at-risk (OAR) adjacent to the tumor periphery. This consequence will be amplified when delivering a single high-dose of radiation. This prompted us to quantify the effect of PO-MLC algorithm for our clinical implementation of a single-high dose of 30 Gy in one fraction protocol using our non-coplanar VMAT lung SBRT approach. Dose to radiosensitive nontarget OAR is a major worry in VMAT lung SBRT treatments,^{19, 20} specifically while delivering a single-large fraction dose as described here. Therefore, herein, we have retrospectively evaluated 12 consecutive early-stage NSCLC patient's plans who underwent VMAT-SBRT treatment in our clinic using the PRO algorithm. For comparison, the clinical PRO-VMAT plans were re-optimized with the PO algorithm with identical beam geometry and planning objectives. Additionally, PO-VMAT plans were re-optimized with a fine resolution of 1.25 mm CGS for evaluation. The original PRO-VMAT and re-optimized PO-VMAT plans were compared by lung SBRT protocol compliance criteria for the target conformity, gradient indices and dose to OAR per RTOG requirement.⁷

2.2 Methods and Materials

2.2.1 Patient Population and Treatment Planning

After obtaining approval from our institutional review board, this retrospective study included 12 patients with early stage non-small-cell lung cancer. The patients were immobilized using Body Pro-LokTM platform (CIVCO system, Orange City, IA) in the supine position, arms above their head. All planning computed tomography (CT) images were acquired on a GE Lightspeed 16 slice CT scanner (General Electric Medical Systems, Waukesha, WI). CT images were acquired with 512×512 pixels at 2.5 mm slice thickness. All patients underwent a free breathing 3D-CT scan followed by a 10-phase 4D-CT scan

using Varian’s Real Time Position Management Respiratory Gating System (version 1.7). Internal target volumes (ITV) were delineated on the 3D CT images with reference to the MIP images and the planning target volume (PTV) was created by adding a 5 mm uniform margin around the ITV. Mean PTV derived from 4D-CT scan was 13.6 ± 12.0 cc (range, 4.3-41.1 cc). The critical structures, such as bilateral lungs excluding the ITV (normal lung), spinal cord, ribs, heart, trachea and bronchus, esophagus, and skin were delineated on the free-breathing CT images for dose recording. The main tumor characteristics of the patients included in this retrospective study are shown in **Table 2.1**.

Table 2.1 Main tumor characteristics of the patients included in this study.

Parameters	Mean \pm SD (range or no. of patients)
PTV (cc)	13.6 ± 12.0 (4.3 – 41.1)
Prescription dose	30 Gy in 1 fraction
Normal lung volume (cc)	4035 ± 1388 (2396 – 6976)
Laterality (left/right)	(8/4 patients)

An isocenter was placed at the geometric center of tumor in each patient. Highly conformal, VMAT treatment plans were generated on the free-breathing 3D-CT images using 2-6 non-coplanar partial arcs ($\pm 5-10^\circ$, couch kicks were used) for the Truebeam linear accelerator (Varian, Palo Alto, CA) with standard millennium MLC and a 6MV-FFF (1400MU/min) beam. All clinical plans were optimized in Eclipse (version 13.6) with PRO algorithm using a fixed 2.5 mm voxel resolution. For each arc, collimator angles were chosen such that the opening of the MLC outside the target was minimized for each patient. Additionally, the jaw tracking option was chosen during VMAT plan optimization to further minimize the non-target dose. Advanced Acuros-based dose calculation algorithm^{14,21-23} and dose to medium reporting mode was used. A dose of 30 Gy in 1 fraction was prescribed and at least 95% of the PTV received the prescription dose with the maximum

dose to the PTV limited to 130% (hotspots fell within the ITV) of the prescription dose. In addition to optimization ring structures, the generalized normal tissue objective (NTO) parameters were used to control the gradients for each target. Planning objectives for the target coverage and OAR sparing were per RTOG 0915 guidelines.⁷

2.2.2 PO-VMAT Plan

The clinical PRO-VMAT treatment plans for all lung SBRT patients were re-optimized using a recently implemented PO-VMAT MLC algorithm in Eclipse. Identical beam geometry and planning objectives were used in the PO and PRO plan including the NTO parameters, ring structures and convergence criteria. The PO plan received the same target coverage as the clinical PRO. Moreover, PO plans were re-optimized with a fine resolution of 1.25 mm CGS for further evaluation.

2.2.3 Plan Analysis

The dose volume histograms (DVHs) and isodose curves of clinical PRO and PO plans were compared. The conformity index (CI) and gradient index (GI) were defined as the ratios of prescription isodose volume and 50% prescription isodose volume to the PTV volume, respectively. The gradient distance (GD) was calculated as the average distance (in any direction) from the PTV margin to the 50% prescription isodose volume whereas the maximal dose to 2 cm away from the PTV in any direction (D_{2cm}) was calculated per RTOG 0915 criteria. The dose to the normal lung was evaluated using V5Gy, V10Gy, V20Gy, mean lung dose (MLD) and maximum dose to 1000 cc of lungs. Furthermore, dosimetric differences were evaluated for spinal cord, heart, trachea, bronchial tree, esophagus, ribs and skin following RTOG-0915 requirements. Total number of monitor units (MU), modulation factor (MF) and beam-on time were compiled. The MF was

defined as the total number of MU divided by the prescription dose in cGy. Beam-on time was calculated using total MU divided by the delivered dose rate in minutes. Paired sample t-test (Microsoft Excel, Microsoft Corp., Redmond, WA) was used to evaluate parameters for clinical PRO 2.5mm CGS vs PO2.5mm CGS plans using a p-value < 0.05 (two-sided). Similarly, PRO2.5mm CGS vs PO1.25mm CGS plans were also compared.

2.3 Results

The PO2.5mm CGS plans provided similar plan quality compared to the original clinical PRO2.5mm CGS optimized plans. As displayed in **Table 2.2**, PTV parameters per RTOG 0915 criteria were evaluated. It was confirmed by the study that PO2.5mm CGS plans were able to reproduce similar conformality for single fraction lung SBRT plans. However, it is important to note the higher level of intermediate dose spillage with PO algorithm as shown by the systematically higher values of GI, D_{2cm} and GD (see statistically significant differences p < 0.05 of these RTOG parameters). This indicates an increase of intermediate dose-spillage in PO 2.5mm optimized plans.

Table 2.2 Analysis of the target coverage as outlined in RTOG 0915 for all 12 patients receiving a single dose of VMAT lung SBRT.

Parameter	PO2.5 mm CGS	PRO2.5 mm CGS	p-value
CI	1.08 ± 0.073 (0.99 – 1.24)	1.06 ± 0.08 (0.97 – 1.30)	n. s.
GI	5.48 ± 1.09 (3.92 – 7.40)	5.21 ± 0.98 (3.81 – 7.24)	0.03
D _{2cm} (%)	50.08 ± 5.01 (38.520 – 59.50)	47.4 ± 4.64 (37.7 – 55.1)	< 0.05
GD (cm)	1.03 ± 0.177 (0.78 – 1.37)	0.98 ± 0.16 (0.77 – 1.28)	< 0.05

The absolute differences of the averages between the PO2.5mm CGS and PRO2.5mm CGS for various OAR parameters per RTOG 0915 protocol were analyzed and displayed in **Table 2.3**. All values for re-optimized PO2.5mm CGS plans met RTOG 0915 protocol's requirement with an approximate average absolute difference of less than 1.0

Gy. There was a statistically significant difference in dose to 1 cc of rib, dose to 10 cc of skin and the V20Gy in lungs (see, $p < 0.05$). This reinforces that PO optimized plans exhibit more intermediate dose-spillage due to the new matrix-based sampling technique. The dose to 1 cc of rib parameter difference can be explained by the close proximity of PTV volumes with respect to the ribs in some patients' plans. It was determined that although there were a few statistically significant values between the OAR sparing, no clinically significant differences were discerned due to the small average absolute dose difference between each OAR.

Table 2.3 Analysis of OAR dosimetric parameters for all 12 lung SBRT patients treated with a single-dose of 30 Gy VMAT plan.

OAR	DVH Parameter	Absolute Difference (Gy)	p-value
Ribs (Gy)	Maximum	0.88 ± 0.82 (0.16 – 3.02)	n. s.
	Dose to 1 cc	0.95 ± 0.86 (0.04 – 3.24)	< 0.05
Cord (Gy)	Maximum	0.23 ± 0.23 (0.0 – 0.72)	n. s.
	Dose to 0.35 cc	0.22 ± 0.19 (0.0 – 0.66)	n. s.
Heart (Gy)	Maximum	0.48 ± 0.62 (0.01 – 2.02)	n. s.
	Dose to 15 cc	0.30 ± 0.24 (0.04 – 0.70)	n. s.
Esophagus (Gy)	Maximum	0.31 ± 0.21 (0.01 – 0.66)	n. s.
	Dose to 3 cc	0.28 ± 0.29 (0.0 – 1.09)	n. s.
Skin (Gy)	Maximum	0.84 ± 0.86 (0.01 – 2.94)	n. s.
	Dose to 10 cc	0.16 ± 0.13 (0.02 – 0.50)	< 0.05
Normal lung (%)	V20Gy	0.06 ± 0.04 (0.00 – 0.13)	< 0.05

The beams eye views (BEV) of MLCs (one control point of one arc) and the corresponding axial views of isodose distributions through the isocenter of a selected patient are shown for the plans optimized with PO2.5mm CGS and PRO2.5mm CGS in **Figure 2.1**. The MLC positions correlate to the same control point for each separately optimized plan. The PO2.5mm CGS optimized plan shows a larger MLC aperture opening with respect to the PRO2.5mm CGS optimized plan. It can be observed that even with a significantly different

MLC aperture, PO-VMAT optimized plans were able to reproduce similar plan quality to PRO-VMAT plans with less modulation and overall smaller treatment time.

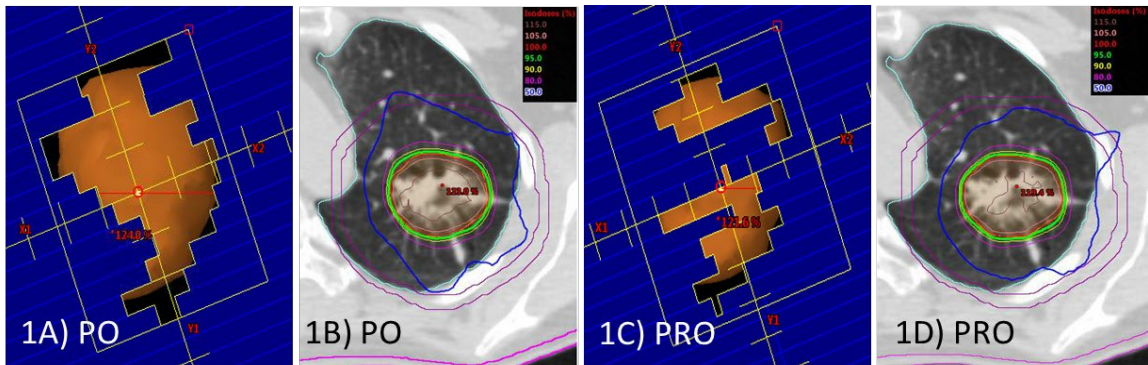


Figure 2.1 Comparisons of select BEV corresponding MLC control points and isodose distribution in an axial view between PO and PRO algorithms.

Comparisons of the selective BEV corresponding MLC control points (one control point of arc 1) and isodose distribution in an axial view between the PO (Figure 1C and 1D) and PRO (Figure 1A and 1B) algorithms for an example patient # 5 (this patient was treated using 2-partial non-coplanar arcs). PTV size was 41.1 cc at the middle of left upper lobe. Although both MLC optimizers provided similar target coverage and OAR doses, PO delivers treatment relatively faster and potentially more accurately due to the decreased MLC modulation. The PO control points showing larger MLC opening at the PTV margin, compared to the corresponding PRO control points, was associated with relatively smaller MU, MF and shorter beam-on time.

An example DVH comparison for the target coverage for the ITV, PTV and a few OAR are shown for the same example patient #5 in **Figure 2.2**. This patient's ITV and PTV were 10.1 cc and 41.1 cc, respectively and the corresponding PTV diameter of 4.22 cm. For the similar PTV coverage, PO algorithm provided slightly higher dose to the ITV, while providing similar OAR sparing.

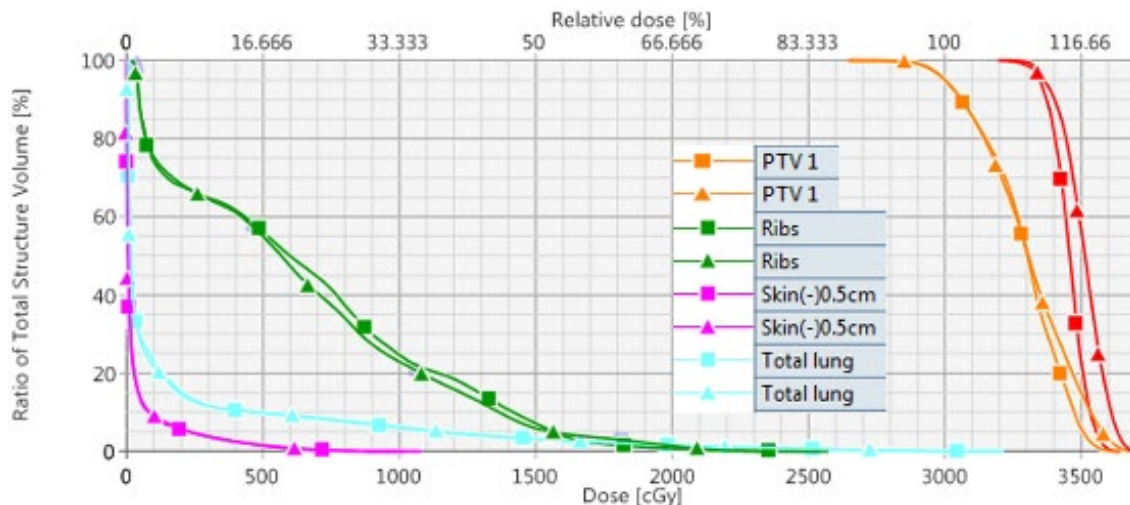


Figure 2.2 Comparison of dose volume histograms for target coverage and OARs. Comparison of dose volume histogram for the target coverage and the OAR is shown. The ITV (red), PTV (orange) and a few OAR such as total normal lung (light blue), ribs (green) and skin (pink) are shown for the same patient #5. The square symbols representing the clinical PRO plan, and the triangle symbols representing the PO-MLC plan. Both plans were normalized to have at least 95% of PTV receiving 100% of the prescribed dose. In this case, the dosimetrically equivalent plans were generated using PRO vs PO algorithm, as demonstrated, with similar target coverage and dose to the OAR.

2.4 Discussion

In this report, we investigated the potential improvement of treatment delivery efficiency while utilizing recently implemented PO-MLC algorithm in the treatment of single large dose of VMAT lung SBRT patients. For similar target coverage, intermediate dose spillage and dose to the OAR, our PO VMAT plan provided lower number of MU, smaller MF and shorter beam-on time compared to PRO plan. Most importantly, the beam-on time was improved by 1.0 min, on average (maximum up to 3.12 min) with PO-MLC algorithm, compared to clinical PRO-MLC algorithm in Eclipse.

While agreeing with those retrospective previous reports, our single-dose of lung SBRT plans with PO-MLC algorithm exhibited similar target coverage and OAR sparing compared to clinical PRO plans. Additionally, our PO1.25mm CGS significantly reduced

beam-on time. Huang *et al*²⁴ compared the dosimetric impact of PRO-MLC algorithm and CGS for lung SBRT patients using 6X-FFF and 10X-FFF beams. AcurosXB and AAA algorithms were analyzed with 2.5 mm and 1 mm CGS for a total dose of 48 Gy in 4 fractions. They have shown that the dose differences become larger while using higher energy beam and smaller CGS. However, for the similar target coverage, while re-optimizing PO algorithm with finer resolution of 1.25 mm CGS (smallest resolution available in Eclipse) we have observed a few clinically interesting results. For instance, in **Figure 2.3** we have shown the ratios of the RTOG target coverage parameters (see left panel) and a few OAR dose differences (see right panel) between the PO2.5mm CGS and PO1.25mm CGS as a function of clinical PRO2.5mm CGS plans. It was observed that for the similar target coverage, there was less intermediate dose spillage (shown by smaller differences of GI and GD and similar for D2cm) with PO1.25mm CGS (compared to PO2.5mm CGS). This may indicate PO algorithm with fine resolution will offer similar dosimetric results with respect to the traditional PRO2.5mm CGS plans. Furthermore, in some cases the absolute dose differences predicted by PO plans for skin and ribs were significantly higher up to 2.4 Gy and 3.8 Gy, respectively. Due to these select cases, we (see **Figure 2.3**, right panel) suggest the planner to carefully evaluate each plan for dose to OAR. We believe the large error bars and higher predicted maximum and volumetric dose in the ribs by the plans optimized with PO1.25mm CGS seen in **Figure 2.3** were manifested by a single lung SBRT plan. In this plan, the target size was relatively small (5.0 cc) directly abutting the rib cage. As a consequence of this tumor location, a relatively higher density rib was directly in the beam's path for the entire duration of the arc rotation, causing difficulty to accurately predict dose with larger CGS (2.5mm). Therefore, we believe that

the higher dose predicted in the PO1.25mm CGS was a more accurate representation of the actual dose to the ribs due to the finer sampling along the periphery of the target. The dose to 1cc of ribs and 10 cc of skin was evaluated and found to have similar variable dose as seen by the maximal dose to the ribs (see **Figure 2.3**). However, 10 cc of skin dose was similar between the plans. We predict those dosimetric differences (maximal dose to ribs and skin) and dose to 1 cc of ribs could be clinically significant and need careful assessment by the planner on the per-patient basis

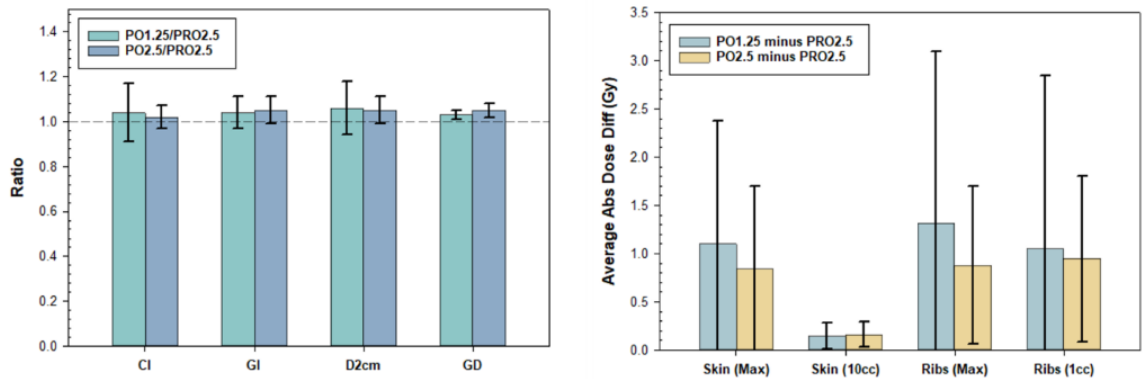


Figure 2.3 Ratios of CI, GI, D2cm, GD and select OAR between PO plans vs. clinical PRO plans.

Ratios of CI, GI, D2cm and GD between the PO plans vs clinical PRO plans (left panel) and the corresponding absolute maximum and volumetric dose differences to skin and ribs (right panel) for all 12 patients treated with a single high-dose of VMAT lung SBRT. For similar target coverage, PO algorithm predicted higher maximum doses to the skin and ribs, including calculating with the fine resolution of 1.25mm CGS.

Comparison of MFs and beam-on times of VMAT lung SBRT plans with PO1.25mm, PO2.5mm and PRO2.5mm CGSs are shown in **Figure 2.4**. For the given complexity of single-large dose of VMAT lung SBRT, it was observed that PO1.25mm CGS provided the smallest MF and shortest beam-on time among the plans. For a similar dose distribution, significant reduction of beam delivery complexity was observed with PO1.25mm CGS (average MF = 2.65 ± 0.51 , range: 1.71-3.4) vs. PO2.5mm CGS (average

MF = 2.73 ± 0.48 , range: 2.15-3.53) vs. clinical PRO2.5mm CGS (average MF = 3.19 ± 0.71 , range: 2.28-4.8). These plans presented with all p-values < 0.001. The resulting reduction of average beam on time with PO1.25mm CGS plans compared to PO2.5mm and PRO2.5mm CGS were 0.2 ± 0.1 min (up to 1.0 min) and 1.2 ± 0.39 min (up to 3.22 min) respectively. Therefore, by optimizing the VMAT lung SBRT plan with PO1.25mm CGS, the smaller openings of the MLCs were eliminated that led to less beam modulation and consequently shorter beam on time, a feature desirable for single dose of lung SBRT. This suggests more accurate dose delivery due to the reduction in small-field dosimetry uncertainty.²⁵ Reducing the number of small MLC openings is important for improving treatment delivery accuracy and reduce small-field dosimetry error in the beam model.

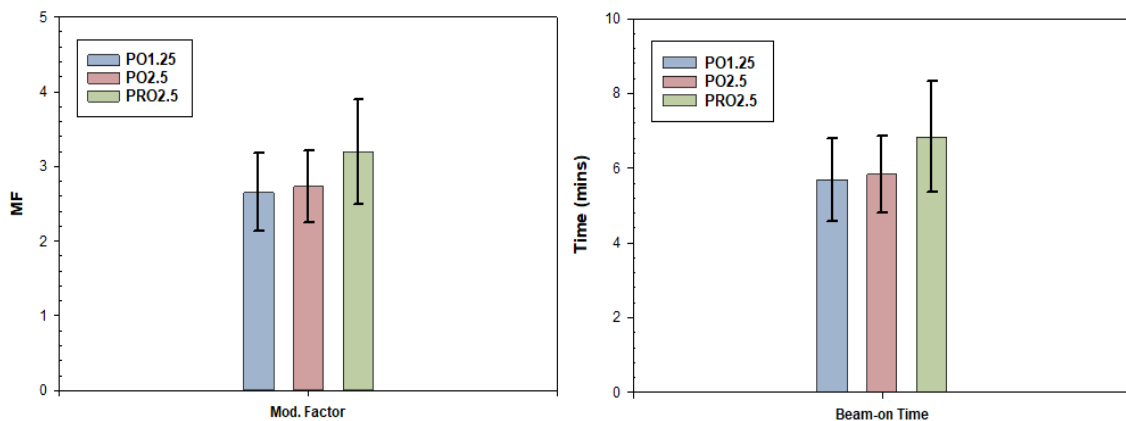


Figure 2.4 Average MFs and BOTs for PO and PRO MLC Algorithms

Left panel: average MFs for PO and PRO-MLC algorithms for 1.25 mm and 2.5 mm CGS for all 12 patients treated with single-dose of VMAT lung SBRT plan. The corresponding beam-on time for PO vs PRO algorithms (right panel); significant improvement of the beam-on time was observed with PO1.25mm CGS with no additional cost of plan optimization.

Utilizing PO-MLC algorithm with fine resolution of 1.25mm CGS during VMAT lung SBRT plan optimization potentially reduces MLC complexity and beam-on time while providing similar target coverage and similar dose to the OAR. However, in some cases PO-MLC algorithm predicted higher dose to critical structures such as ribs and skin,

therefore, we suggest carefully evaluating OAR doses on a case-by-case basis. Therefore, to minimize MLC complexity and consequently beam-on time (based on the presented results) we strongly recommend utilizing PO-MLC algorithm with fine resolution of 1.25mm CGS (if available) for single-dose of VMAT lung SBRT plan optimization, thus potentially reducing beam modulation, and transmission and perhaps minimizing unwanted dose to the patients. This study allows for future work in the development and validation of a new lung SBRT RapidPlan model using non-coplanar VMAT geometry that supports advanced Acuros-based dose calculations. It was not previously understood if the PO-MLC algorithm would be capable of producing high quality non-coplanar VMAT lung SBRT treatments for a single dose of 30 Gy. Some work has been already done by Snyder *et al*²⁶ that successfully generated a RapidPlan model for lung SBRT treatments using predominately IMRT plans (VMAT and 3DCRT were also included in the model for 3-5 fractions lung SBRT plans) with Varian Anisotropic Analytical Algorithm dose calculation algorithm. Our new RapidPlan model aims to include these extreme hypofractionated SBRT plans including other highly conformal non-coplanar VMAT lung SBRT plans with different fractionation schemes.

2.5 Conclusion

In summary, the potential benefits of utilizing the PO-MLC algorithm on Truebeam with 6MV-FFF beam for single high-dose of VMAT lung SBRT with curative therapeutic biological effective dose to lung lesions has been presented. The use of PO-MLC algorithm for single-dose of VMAT lung SBRT plans optimization showed slightly increased intermediate-dose spillage but boasted overall similar plan quality with less beam modulation. Even though PO-MLC algorithm under-sampled voxels at the periphery of the

target, utilizing fine resolution dose CGS of 1.25 mm overcomes the deficiency of PO2.5mm CGS and provided lung SBRT plans quality similar to that of clinical PRO2.5mm CGS plans. Shorter beam-on time can potentially reduce intrafraction motion errors and improve patient compliance. Smaller beam-modulation and faster treatment delivery with PO-MLC algorithm suggest that PO1.25mm CGS is suitable for single-dose of VMAT lung SBRT patients with relatively smaller tumor sizes (< 2cm). This indicates that RapidPlan modeling can be performed using PO-VMAT plans with fine resolution of 1.25mm CGS for a single-dose of lung SBRT treatments.

Copyright © Justin David Visak 2021
<https://orcid.org/0000-0002-8674-5657>

CHAPTER 3. DEVELOPMENT AND CLINICAL VALIDATION OF A ROBUST KNOWLEDGE-BASED PLANNING (KBP) MODEL FOR STEREOTACTIC BODY RADIOTHERAPY (SBRT) TREATMENT OF CENTRALLY LOCATED LUNG TUMORS

Upon confirmation that the PO-MLC algorithm that was suitable for KBP modeling of lung SBRT treatments, the first model was developed and validated for centrally located lung tumors with full RTOG-0813 compliance. **Chapter 3** has been adapted from the recently published manuscript by: **Visak J**, McGarry RC, Randall ME, Pokhrel D. Development and clinical validation of a robust knowledge-based planning model for stereotactic body radiotherapy treatment of centrally located lung tumors. *J Appl Clin Med Phys.* 2020; 22(1); 1-10

Abstract

The purpose of this study is to develop a robust and adaptable knowledge-based planning (KBP) model with commercially available RapidPlan™ for early-stage, centrally-located non-small-cell lung tumors (NSCLC) treated with stereotactic body radiotherapy (SBRT) and improve a patient's 'simulation to treatment' time. The KBP model was trained using 86 clinically treated high quality non-coplanar volumetric modulated arc therapy (n-VMAT) lung SBRT plans with delivered prescriptions of 50 or 55 Gy in 5 fractions. Another twenty independent clinical n-VMAT plans were used for validation of the model. KBP and n-VMAT plans were compared via RTOG-0813 protocol compliance criteria for conformity (CI), gradient index (GI), maximal dose 2 cm away from the target in any direction (D2cm), dose to organs-at-risk (OAR), treatment delivery efficiency and accuracy. KBP plans were re-optimized with larger calculation grid size (CGS) of 2.5 mm to assess feasibility of rapid adaptive re-planning. KBPs were similar or better than n-

VMAT plans based on a range of target coverage and OAR metrics. Planning target volume (PTV) for validation cases was 30.5 ± 19.1 cc (range 7.0–71.7 cc) KBPs provided an average CI of 1.04 ± 0.4 (0.97–1.11) versus n-VMAT plan's average CI of $1.01 \pm (0.97–1.17)$ ($p < 0.05$) with slightly improved GI with KBPs ($p < 0.05$). D2cm was similar between the KBPs and n-VMAT plans. KBPs provided lower lung V10Gy ($p = 0.003$), V20Gy ($p = 0.007$) and mean lung dose ($p < 0.001$). KBPs had overall better sparing of OAR at the minimal increased of average total monitor units and beam-on time by 460 ($p < 0.05$) and 19.2 seconds, respectively. Quality assurance phantom measurement showed similar treatment delivery accuracy. Utilizing 2.5 mm CGS in the final optimization improved planning time (mean, 5 minutes) with minimal or no cost to the plan quality. RTOG compliant adaptable RapidPlan model for early-stage SBRT treatment of centrally located lung tumors was developed. To conclude, all plans met RTOG dosimetric requirements in less than 30 minutes of planning time, potentially offering shorter 'simulation to treatment' times. OAR sparing via KBPs may permit tumoricidal dose escalation with minimal penalties. Same day adaptive re-planning is plausible with 2.5 mm CGS optimizer setting.

3.1 Introduction

Stereotactic body radiotherapy (SBRT) for early stage localized non-small cell lung cancer (NSCLC) has become a significant treatment option to traditional surgical intervention providing primary tumor local control rates in excess of 97% (median, 3 year).^{1,2} Historically, lung SBRT was delivered using 7-13 co/non-coplanar static beams or dynamic conformal arcs (DCA), followed by intensity modulation radiation therapy (IMRT) and more recently with volumetric modulated arc therapy (VMAT).^{1,3,4} VMAT

provides more conformal dose-distribution to the target better sparing of organs-at-risk (OAR) and much faster treatment delivery. The dosimetric advantages of VMAT can be enhanced using 6MV-flattening filter free (6MV-FFF) beam for lung SBRT because of its higher dose rates and reduction of out-of-target dose with respect to traditional flattened beams.⁵ This provides clinical benefits to the patients as it improves target coverage at the lung-tumor interface and shorter treatment time; potentially improving patient convenience and reducing intrafraction motion errors.⁶ In North America, the Radiation Therapy Oncology Group (RTOG) reports provides recommendations to clinicians for SBRT dosing schemata and contouring guidelines based on operable eligibility and tumor geographical location. This study concentrates on SBRT for early stage NSCLC patients with centrally located tumors following RTOG-0813 guidelines.⁷ In addition to centrally located lung tumors, our clinic uses this protocol for risk-adapted prescriptions for tumors located adjacent to critical structures such as the ribs.

Generating an optimal SBRT treatment using a VMAT approach requires multiple iterations and heavily depends on a planner's skill. This potentially results in inconsistent plan quality known as inter-planner variability.^{8, 9} Automation of inverse planning via knowledge-based planning (KBP) aims to remove inter-planner variability, improve plan quality and decrease planning time.¹⁰ KBP uses a model library of previously generated high quality clinical plans to predict new treatment parameters, effectively generating new plans based on a clinic's treatment planning history.¹¹ Varian RapidPlan (Varian Medical Systems, Palo Alto, CA) model is a KBP engine that utilizes a knowledge-based dose-volume histogram (DVH) algorithm to estimate the dose volume histogram (DVH) that can produce optimization objectives such as maximum, minimum and new line dose

constraints with associated priority values.¹² KBP has demonstrated the ability to create improved or equivalent plans for prostate, head and neck, spine, breast and thoracic sites.^{8,13-18} However, there is very limited literature available for lung SBRT treatments,^{14, 15,}¹⁷ specifically utilizing highly conformal non-coplanar VMAT (n-VMAT) planning geometry.

In this report, a RapidPlan model is described to generate adaptable n-VMAT based KBP treatment plans for early-stage NSCLC patients with medically inoperable centrally located tumors that follows RTOG-0813 dosing schemata and contouring guidelines. Our model is exclusively trained with clinically treated high quality n-VMAT lung SBRT plans using the advanced AcurosXB final dose calculation algorithm. We use the advanced AcurosXB algorithm for heterogeneity corrections for lung SBRT treatments as it provides an more accurate dose calculation in heterogeneous patient anatomy by modeling secondary build-up in tissue/low density interfaces than traditionally used superposition/convolution algorithms.^{19, 20} The KBP model may permit the improvement of ‘simulation to treatment’ time from our current average 7 working days to 3 days while maintaining plan consistency and reducing inter-planner variability. This may enable same or next day adaptive treatments (if needed) that aim to account for day-to-day changes in physiological characteristics or setup errors as they occur during a treatment course. A previous study using a smaller CGS of 1.25 mm vs 2.5 mm in manually optimized VMAT lung SBRT plans with the Photon Optimizer (PO) algorithm demonstrated minimal dosimetric differences between the two plans but has not yet been evaluated in a lung SBRT KBP setting.²¹ This led to further evaluation of the concept by generating KBPs with a CGS of 2.5 mm which drastically decreasing treatment planning time (mean, 5 minutes)

and observe if they provide similar plan quality to the KBPs plans optimized with a 1.25 mm CGS.

3.2 Materials and Methods

3.2.1 Patient Population and Target Definition

Following approval from our Institutional Review Board (IRB), 106 clinically treated high quality n-VMAT lung SBRT plans generated for patients with early stage centrally located tumors as defined by RTOG-0813 were selected for training and validation. Eighty-six plans were used for training this model and the remaining 20 were used for validation. Patients received a total of 50 Gy or 55 Gy in 5 fractions. Details of the patient setup and simulation are published in detail elsewhere.⁶ Motion control of the target lesion was accomplished primarily by abdominal compression. If a patient had a contraindication to abdominal compression e.g., abdominal aortic aneurysm, extensive abdominal surgery etc., a 4D CT simulation was done to create an internal target volume (ITV). For patients with abdominal compression, the gross tumor volume (GTV) was contoured on lung windows and a planning target volume (PTV) was added with margins of 1.0 cm superior/inferior and 0.5 cm laterally. For patients with 4D CT planning, an ITV was created from the maximum intensity projections (MIP) on lung windows and a uniform 0.5 cm PTV margin was added uniformly per RTOG 0813 requirements. No clinical target volume (CTV) was allowed. Organs at risk such as spinal cord, ipsilateral brachial plexus, skin, esophagus, heart, trachea, total lungs minus PTV, ribs and bronchial tree were delineated per RTOG-0813 compliance criteria for dose tracking.

3.2.2 Clinical n-VMAT Plans

For all patients, n-VMAT SBRT plans were generated in the Eclipse treatment planning system (Varian Medical Systems, Palo Alto CA) using 3–6 (mean, 4) partial non-coplanar arcs (with ± 5 - 12° couch kicks) on Truebeam Linac (Varian Palo Alto, CA) consisting of standard millennium 120 MLC and 6MV-FFF (1400MU/min) beam. Jaw tracking option was enabled for each arc and optimal collimator angles were selected to minimize non-target dose and enhance plan conformity. Clinical plans were optimized using Photon Optimizer (v13.6 or v15.6) algorithm with either 1.25 mm or 2.5 mm voxel resolution. The final dose calculation was performed using advanced AcurosXB algorithm with dose to medium reporting mode. A dose of 50 Gy or 55 Gy in 5 treatments was prescribed to cover at least 95% of the PTV receiving 100% of the prescribed dose ensuring that all hotspots were within the PTV. Before approval, each plan was rigorously evaluated by our treating physicians via RTOG-0813 compliance criteria and institutional guidelines including dose to OAR listed below:

- Conformity index (CI): ratio of 100% isodose line volume to PTV volume, typically $1.0 < CI < 1.2$.
- Gradient index (GI): ratio of 50% isodose line volume to PTV volume, typically $3.0 < GI < 6.0$ based on tumor size
- D2cm (%): maximum dose in any direction 2 cm away from the PTV, typically $50\% < D2cm < 70\%$ based on tumor size.
- Gradient distance (GD): average distance from 100% isodose line to 50% isodose line, indicator of intermediate dose spillage and sharp fall-off.
- Total monitor units (MU).

- Modulation factor (MF): total number of monitor units divided by the prescription dose in cGy.
- Beam-on time (BOT).
- Dose to OAR: Maximal and volumetric dose to OAR.

3.2.3 KBP Model Input and Training Datasets

An extensive iterative training approach was developed to create this novel and comprehensive KBP model for SBRT of centrally located lung tumors. Eighty-six n-VMAT plans were retrospectively selected and verified to be high quality by evaluating the numbers of partial arcs and total MU consistency based on historical treatment planning practice. Original (unaltered) clinical VMAT plans were used for model training. The primary focus of this plan selection process was examination of RTOG-0813 criteria. Each plan contour was individually verified to be consistent and correct. A total lung minus PTV structure was added for each patient's plan if the structure was not previously created. Calculation models consisting of dose calculation algorithm, VMAT MLC optimizer and CGS were verified to be AcurosXB for a 2.5 mm resolution voxel size and photon optimizer for a 1.25 mm or 2.5 mm voxel size, respectively. Optimal collimator angle and jaw tracking options were verified prior to input of the training plans. To make the model fully comprehensive for RTOG compliance, it was necessary to track and select plans of varying target size and tumor geographical locations (e.g., lower lobe vs upper lobe, right lung vs left lung) encompassing both lungs (see **Table 3.2**). **Figure 3.1** shows a summarized workflow of initial plan selection criteria.

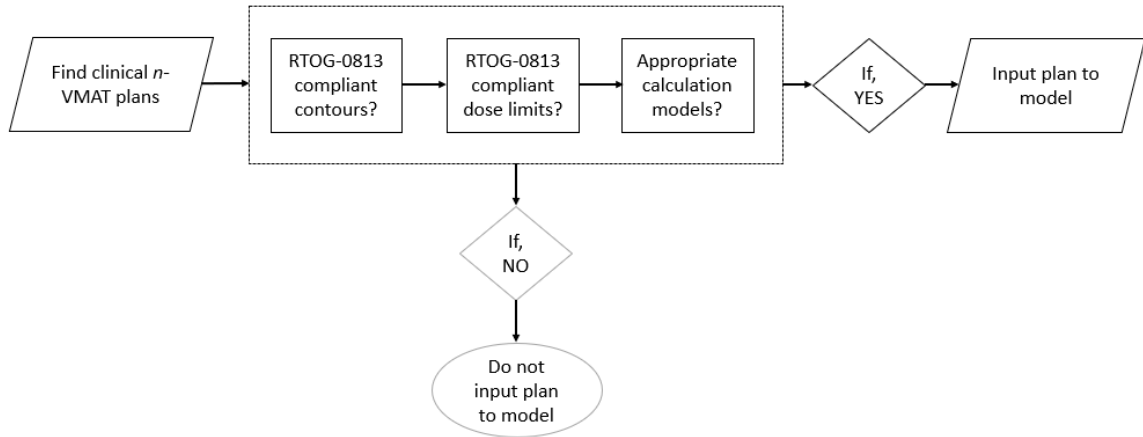


Figure 3.1 KBP model training input data selection workflow.

KBP-model training input data selection workflow for centrally located lung SBRT: A total of 86 high quality clinical n-VMAT plans were selected to train this model that met RTOG-0813 requirements for contouring and OAR dose tolerances while using Acuros-based dose calculation.

3.2.4 Verification of KBP Model

Verification of a model is a process to evaluate the goodness of fit of the model to ensure proper generation of each OAR DVH estimate. Model verification was accomplished by using data provided by the RapidPlan engine to evaluate the R^2 fitting values and chi-squared values for each DVH estimate provided in the model-training log. If these values are suboptimal, this is due to the presence of outlier plans in the model. There are two different types of outliers in the plans: dosimetric and geometric.¹⁴The RapidPlan engine aids in the removal of outliers; for each OAR it provides in-field DVH plots, geometric box plots, principal component analysis-regression and residual plots coupled with a window of different statistics used to gauge a plan's quality of fit into a model. The provided regression and residual plots were evaluated for each OAR were used for manual verification of potential outliers.²²This approach was combined with observing the Cook's

distance that indicated influential data points in a regression model and the modified Z-score, which measures the difference of an individual geometric parameter from the median value in the training set.²⁵ Once true outliers were identified; the entire plan or specific outlying structure was removed from the model and all data was re-extracted. A summary of the KBP model refinement process is shown in **Figure 3.2**.

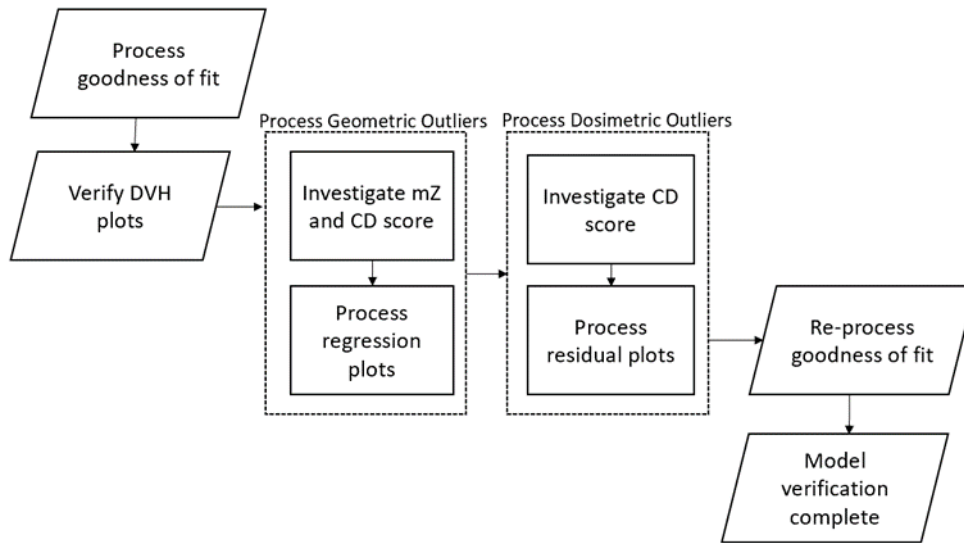


Figure 3.2 KBP model training workflow.

KBP-model training workflow: The model was trained by locating and removing the geometric and dosimetric outliers iteratively.

Constraints were placed on a given OAR following successful verification of the model to create a fully robust model for centrally located lung tumors and risk adapted tumor location such as those tumors abutting the rib (see **Table 3.1**). These constraints were chosen based on RTOG-0813 guidelines and our historical treatment planning practice.

Table 3.1 Selected constraints and their priority for the OAR used to generate the KBP model. Gen = generated.

Structure	Constraint type	Vol [%]	Dose	Priority
Brachial plexus	Upper	5.0	2360 cGy	Gen.
	Upper	0	2720 cGy	Gen.
Bronchial Tree	Upper	0.0	105%	Gen.
	Line (prefer target)	Gen.	Gen.	Gen.
Spinal cord	Upper	0	2100 cGy	
	Upper (fixed volume, gen dose)	2.0	Gen.	Gen.
	Line	Gen.	Gen.	Gen.
D2cm	Upper	0.0	50%	110
	Line (prefer target)	Gen.	Gen.	Gen.
Esophagus	Upper	0	105%	Gen.
	Line (prefer OAR)	Gen.	Gen.	Gen.
Heart	Upper	0.0	105%	Gen.
	Line (prefer target)	Gen.	Gen.	Gen.
Ribs	Upper	0	4000 cGy	Gen.
	Upper (fixed dose, gen vol.)	Gen.	3200 cGy	Gen.
	Line (prefer target)	Gen.	Gen.	Gen.
Skin	Line (prefer target)	Gen.	Gen.	Gen.
Trachea	Line (prefer target)	Gen.	Gen.	Gen.

3.2.5 Validation of KBP Model

A total of 20 clinical n-VMAT plans that were not used to generate the RapidPlan model were selected for final verification including recently treated lung SBRT patients where dedicated manual planning time was recorded (**Table 3.2**). These plans were specifically selected to encompass both lungs' geometry and variable target sizes to fully test the functionality of our model's robustness. However, plan quality was not evaluated prior to selection to ensure the model could produce optimal plans for various case complexities. The overall validation set included 16 patients who received 50 Gy and 4 patients who received 55 Gy in 5 fractions, respectively. These plans were re-optimized with the RapidPlan model with identical planning geometry as the clinical n-VMAT plans.

KBPs were created from a single optimization with no manual intervention. Target dose coverage for the KBPs was normalized for identical or better target coverage compared to previously used clinical n-VMAT plans.

To fully assess the performance of this new KBP model, we evaluated the target conformity, dose-fall off and intermediate dose spillage. Additionally, dose limiting criteria for organs such as spinal cord, skin, esophagus, trachea, heart, lungs minus PTV, ribs and bronchial tree were evaluated. Paired student t-test (Microsoft Excel, Microsoft Corp., Redmond, WA) was used to evaluate KBP vs clinical n-VMAT plans. Plan complexity was assessed by calculating MF. We also recorded the beam-on time which is proportional to the changes in MF. Quality assurance phantom measurements of both n-VMAT and KBPs were performed using an Octavius detector 1500 and phantom with 7.1 mm center-to-center detector spacing (PTW, Freiburg, Germany) to better assess the treatment delivery accuracy. KBPs were initially optimized using a 1.25 mm CGS in the PO MLC algorithm configuration. To assess the feasibility of using this KBP model for the same day adaptive re-planning, KBPs were re-optimized with a 2.5 mm CGS. Plan quality and re-optimization time were assessed by comparing to the original KBPs plans.

Table 3.2 Patient cohort and tumor characteristics for both training and validation of this comprehensive and RTOG compliant KBP model.

Tumor location	Training Set		Validation Set	
	Patients	PTV (cc)	Patients	PTV (cc)
Overall cohort	n = 86	35.7 ± 26.7 (4.4–158.3)	n = 20	30.5 ± 19.1 (7.0–71.7)
Right lower lobe (RLL)	n = 23	42.9 ± 35.2 (10.4–158.3)	n = 5	29.4 ± 19.8 (7.5–58.9)
Right upper lobe (RUL)	n = 30	29.1 ± 20.1 (4.4–78.7)	n = 6	30.3 ± 23.8 (7.0–71.7)

Table 3.2(continued)

Left lower lobe (LLL)	n = 16	34.1 ± 27 (9.4–105.3)	n = 4	24.1 ± 8.6 (12–33.1)
Left upper lobe (LUL)	n = 17	39.1 ± 19.2 (9.0–70.8)	n = 5	37.0 ± 16.1 (12.5–51.3)

3.3 Results

3.3.1 Dosimetric Criteria

Knowledge based plans were able to provide similar or better target coverage than clinical n-VMAT plans (**Table 3.3**). Knowledge based plans had a slightly higher conformity index of 0.03 ($p < 0.05$) on average, indicating better overall target coverage than n-VMAT plans including enhancing minimum dose to GTV. The gradient index was on average lower by 0.28 for KBP ($p < 0.05$) suggesting the KBP model was able to provide a more homogenous dose to the target with sharper and lower intermediate dose spillage. While a difference in D2cm was not statistically significant, there was a lower difference in the gradient distance ($p < 0.05$) suggesting KBPs had a sharper 50% isodose fall off.

Table 3.3 Evaluation of CI and GI for all plans generated via KBP model for validation.

Target	Parameter	KBP	n-VMAT	p-value
PTV	CI	1.04 ± 0.4 (0.97–1.11)	1.01 ± (0.97–1.17)	p = 0.002
	GI	4.12 ± 0.9 (3.10–6.53)	4.40 ± 0.7 (3.39–6.01)	p = 0.003
	HI	1.25 ± 0.05 (1.15–1.35)	1.24 ± 0.06 (1.16–1.39)	p = n. s.
	D2cm (%)	51.2 ± 0.4 (0.41–0.57)	50.2 ± 0.4 (44.6–61.6)	p = n. s.
	GD (cm)	1.01 ± 0.2 (0.72–1.35)	1.11 ± 0.2 (0.78–1.62)	p < 0.001
	D99% (Gy)	49.1 ± 2.2 (46.6–54.5)	49.6 ± 2.0 (47.4–53.9)	p = 0.004
	Mean (Gy)	57.1 ± 2.4 (54.4–62.4)	55.8 ± 2.4 (52.7–61.4)	p = 0.003
GTV	Max (Gy)	62.1 ± 3.0 (58.1–69.5)	62.3 ± 2.8 (57.2–67.5)	p = n. s.
	Min (Gy)	56.0 ± 3.1 (50.8–62.6)	54.9 ± 3.3 (50.1–61.9)	p = 0.05
	Mean (Gy)	59.6 ± 2.5 (56.2–65.6)	59.1 ± 2.8 (55.4–65.8)	p = n. s.

Dose to normal lung was tracked using mean lung dose, and the volume receiving 5 Gy (V5) 10 Gy (V10) and 20 Gy (V20) or more. These results are shown in **Table 3.4**. KBPs had an average lower V5Gy by 0.6%, ($p < 0.001$), V10Gy by 0.5% ($p < 0.001$) and MLD by 0.12 Gy ($p < 0.001$) suggesting a potentially lower risk of radiation induced pneumonitis. In addition to normal lung tissue doses, all other OAR compliance criteria were assessed per RTOG-0813 (**Figure 3.3**). In many lung SBRT cases, risk-adapted prescription to targets adjacent to the ribs are used. The greatest sparing achieved in the KBPs was shown in the ribs ($p < 0.001$) for an average of 2.62 Gy (maximum up to 9.67 Gy).

Table 3.4 Evaluation of dosimetric lung data for all 20 lung SBRT validation cases. MLD = mean lung dose. V5, V10, V20 = volume of lung receiving 5 Gy, 10 Gy, 20 Gy or more.

DVH Parameter	KBP	n-VMAT	p-value
V5Gy (%)	10.7 ± 5.1 (3.4–19.7)	11.3 ± 5.2 (3.2–21.0)	p < 0.001
V10Gy (%)	6.6 ± 3.8 (2.4–14.1)	7.1 ± 4.1 (2.3–15.4)	p < 0.001
V20Gy (%)	2.7 ± 1.8 (0.7–6.7)	2.8 ± 1.9 (0.8–7.7)	p = 0.007
MLD (Gy)	2.29 ± 1.2 (0.95–4.9)	2.41 ± 1.2 (0.8–5.2)	p < 0.001

Our study showed ipsilateral brachial plexus, esophagus, heart, trachea and bronchial tree received an insignificant average lower dose in KBPs compared to the clinical n-VMAT plans. Additionally, KBPs on average presented an insignificant but slightly higher skin dose to spinal cord by 0.46 Gy ($p = 0.32$).

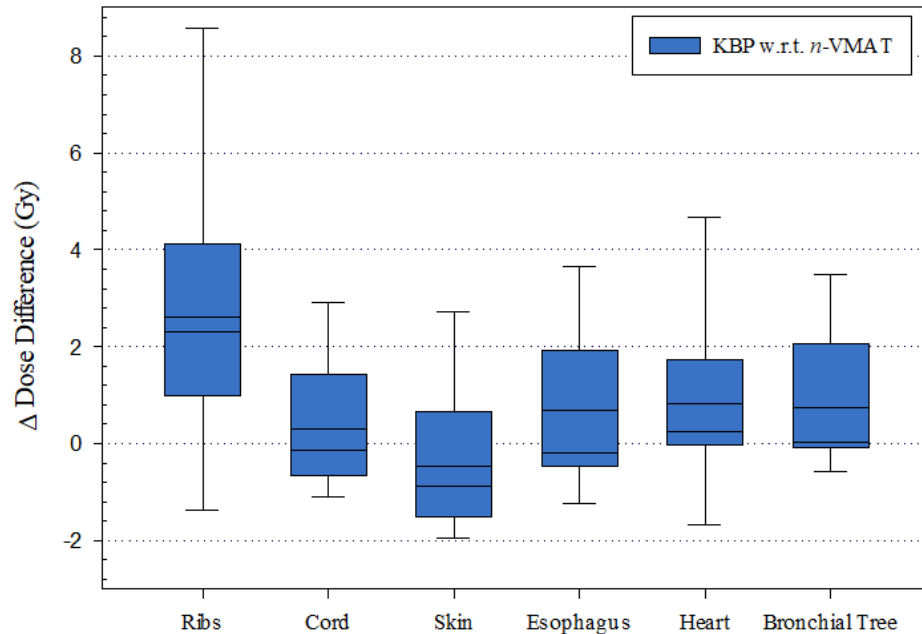


Figure 3.3 Box plot of maximal pairwise dose differences of KBP compared to n-VMAT plans.

Box plot of maximal pairwise dose differences of KBP compared to n-VMAT plans displaying median, 10th, 25th, 75th, and 90th percentiles with error bars. Negative values indicate that KBPs provided less sparing relative to n-VMAT plans. All 20 lung SBRT cases used for validation were included. Prescription was 50 or 55 Gy in 5 fractions. KBP model was able to spare maximum rib dose on average by 2.62 Gy (maximum up to 9.67 Gy). Maximum skin dose was on average higher by 0.46 Gy ($p = n. s.$) but not clinically significant in KBPs.

3.3.2 Treatment Planning Time, Delivery Efficiency and Accuracy

Knowledge based plans were generated and ready for treatment plan review on average in under 30 minutes, providing a clinically relevant reduction in treatment planning time. For an experienced planner with dedicated SBRT planning time, manual plans were created in 129 ± 34 min, on average (range, 95–183 min). **Table 3.5** displays treatment and delivery efficiency metrics for KBPs and n-VMAT plans. Knowledge based plans on average only increased total monitor units by 460 ($p = 0.008$). When considering nominal maximal dose rates of 6MV-FFF beam (1400MU/min), this results in similar beam on time.

The minimal values of MF and BOT were increased by 0.46 ($p = 0.008$), and 19.2 seconds ($p = 0.008$), respectively. However, KBPs were still able to provide enhanced GTV dose and lower dose to OAR.

Table 3.5 Treatment delivery efficiency and accuracy of KBP with respect to clinical n-VMAT plans.

Treatment delivery parameter	KBP	n-VMAT	p-value
Total monitor units	3480 ± 531 (2553–4639)	3020 ± 674 (1961–4104)	p = 0.008
Modulation factor	3.48 ± 0.53 (2.53–4.64)	3.02 ± 0.67 (1.92–4.10)	p = 0.008
Beam-on time (min)	2.49 ± 0.34 (1.81–3.31)	2.15 ± 0.48 (1.37–2.93)	p = 0.008
γ -pass rate [2%/2mm]	94.4 ± 2.7 (90.6–100.0)	95.4 ± 2.3 (90.9–99.4)	p = 0.11

In the patient-specific quality assurance measurements, the gamma analysis of 2%/2 mm criteria was used to assess the plan delivery accuracy differences between KBP vs clinical n-VMAT plans. KBPs presented with a similar average pass rates of 94.4 ± 2.7% (range, 90.6–100.0%) compared to n-VMAT plans with an average pass rates of 95.4 ± 2.3% (range, 90.9–99.4%) ($p = 0.11$) plans suggesting that comparable treatment delivery accuracy can be achieved with KBPs.

3.3.3 Example Validation Case- Left Lower Lobe Tumor

Dose volume histograms of both the KBP and n-VMAT plan for a validation case with a left lower lobe tumor of a lung SBRT patient were generated (**Figure 3.4**). This patient was selected as the example case as it best represented the average expectation of improvement using the KBP model. With better target coverage (minimum dose to GTV was increased by 2.3 Gy), the KBP model was able to lower volumetric dose to lungs including MLD, ribs, heart, and bronchial tree. In this case, the maximum rib dose was

reduced by 4.2 Gy compared to clinical n-VMAT plan. Both plans were normalized so at least 95% of PTV received 100% of the prescribed dose.

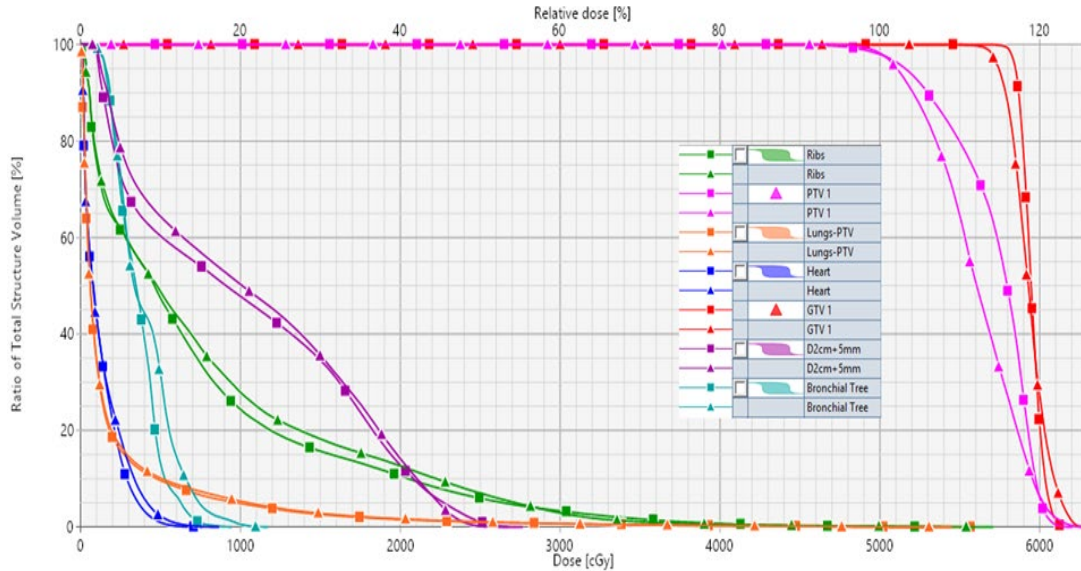


Figure 3.4 Dose volume histogram comparison for target coverage and OAR dose. Dose volume histogram comparison for the target coverage for the GTV (red) and OAR such as total normal lung minus PTV (orange), heart (dark blue), ribs (green) and bronchial tree (dark blue) are shown for an example patient KBP plan (square), and n-VMAT (triangle). Prescription dose was 50 Gy in 5 fractions. KBP provided superior target coverage and lower dose to the OAR.

The dosimetrically superior plan was generated using the KBP model, as demonstrated with slightly better target coverage and volumetrically lower dose to the OAR including lower maximal dose to rib (**Figure 3.5**).

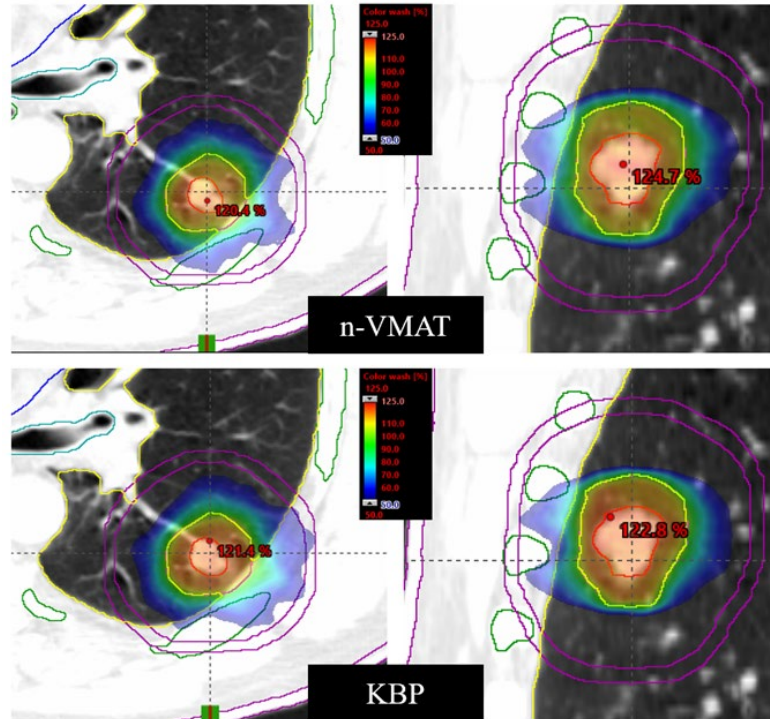


Figure 3.5 Comparison of axial and coronal view SBRT isodose distribution for example patient corresponding to Figure 3.4

Comparison of KBP vs a clinical n-VMAT plan for the example validation case. The axial and coronal views of SBRT isodose distributions for the clinical n-VMAT plan (upper panel) and the corresponding KBP plan (lower panel) are shown. Tumor was located in the left lower lobe and treated for 50 Gy in 5 fractions. Similar, CI, GI, D2cm, GD and V_{20Gy} were obtained. A few critical structures shown were ribs, skin, bronchial tree, ipsilateral normal lung as well as D2cm ring (purple contour). Tighter 50% dose color wash showing lower rib dose providing slightly better target coverage with KBP plan.

3.3.4 Re-Optimized KBPs with 2.5 mm CGS

The KBP calculation time was dictated by the CGS used in the optimization window. The original KBPs were calculated with 1.25 mm CGS. However, while using 2.5 mm CGS the treatment planning time was reduced to approximately 5 minutes. This setting could support even faster adaptive re-planning in emergent clinical situations. Therefore, KBPs were re-optimized with a 2.5 mm CGS for plan evaluation. **Table 3.6** displays sample

target coverage and normal tissue sparing dose volume histogram metrics. It was found that these plans could be created in 5 minutes, on average, with minimal loss of dosimetric plan quality. Conformity index and gradient index showed no statistical difference between 1.25 mm vs 2.5 mm CGS re-optimized plans. Therefore, KBPs indicate similar conformal and homogenous target dose coverage with a 2.5 mm CGS. Gradient distance ($p = 0.45$) was slightly increased with 2.5 mm CGS configured KBPs signifying an increase in intermediate dose spillage, however, clinically acceptable and similar V20Gy values were observed (**Table 3.6**).

Table 3.6 Average absolute differences of selected target coverage and DVH parameters for re-optimized KBPs with a 2.5 mm CGS vs original KBPs with 1.25 mm CGS.

Plan metrics	Average difference: 1.25 minus 2.5 mm CGS KBPs	p-value
Conformity index	0.02 ± 0.02 (0.0–0.06)	$p = 0.46$
Gradient index	0.32 ± 0.59 (0.0–2.4)	$p = 0.93$
Gradient distance (cm)	0.03 ± 0.08 (0.0–0.19)	$p = 0.04$
DVH Metrics		
V20Gy (%)	0.08 ± 0.07 (0.0–0.3)	$p = 0.53$
Maximum rib dose (Gy)	0.57 ± 0.44 (0.8–1.5)	$p < 0.001$
Maximum cord dose (Gy)	0.41 ± 0.50 (0.0–2.33)	$p = 0.45$

As shown in **Table 3.6**, our study found that maximum dose differences for the rib and spinal cord were not clinically significantly different (similar results were found for other OAR, not shown here) indicating that 2.5 mm CGS can be used for safe and effective adaptive re-planning of lung SBRT cases (for selected patients) using this KBP model.

3.4 Discussion

A fully RTOG-0813 compliant, n-VMAT based KBP model using Varian RapidPlan was developed and validated for centrally located lung tumors treated with SBRT. This novel model was fully trained with high quality clinical plans that adhere to contouring, prescription schemata and dose limits set forth by RTOG-0813 without prior alteration to input to the model. It is likely that any clinic that complies with RTOG protocol constraints and are RapidPlan capable can potentially adapt this model to provide high quality n-VMAT lung SBRT treatments. To our best knowledge, this novel model is the first RapidPlan model created exclusively for centrally located tumors using a non-coplanar VMAT approach with the more accurate Acuros-based dose calculation engine. This comprehensive KBP model can encompass centrally located lung tumors as well as those near the ribs.

One of the major benefits of using this RapidPlan model is its possibility of improving clinic workflow of ‘simulation to treatment’ time from 7 to 3 working days. While this study recorded an average dedicated planning time of approximately 129 minutes for an experienced planner, in our clinic the majority of our standard 7 working day ‘simulation to treat time’ comes from planning. We do not have dedicated SBRT planners and this standard time-slot accounts for not only planner workload but also inter-planner variability. Our institution’s planners simultaneously plan multiple treatments per day and do not have the time to meticulously optimize each lung SBRT plan unlike a dedicated planner. Additionally, patients who present for re-treatment, have an implanted pacemaker or any other unique planning difficulty can increase planning time up to a week. Therefore, the KBP model may allow adaptive re-planning for selected patients with

incorrect patient set-up on the machine, weight loss or tumor shrinkage that will maintain high quality SBRT treatment delivery in a timely manner. As expected, for most tumors, this model can generate a plan of similar or better quality much faster than manual planning approach, while removing inter-planner variability and standardizing the clinic workflow. This concept was expanded further by evaluating the effects of the photon optimizer CGS on a KBP model to evaluate the dosimetric trade-off with decreased treatment planning time. This appears to be the first study evaluating CGS effects in the context of lung SBRT KBP planning. It is shown that by utilizing 2.5 mm CGS same day adaptive re-planning is plausible as planning time was decreased to approximately 5 minutes with minimal dosimetric impact.

Moreover, the validation cases have shown that slight tumor dose escalation can be achieved in select lung SBRT cases with similar plan quality to clinical plans and no penalty to dose limiting organs (DLO). For example, this KBP model can potentially reduce maximum dose to the rib by 2.62 Gy, on average, while also reducing dose in the ipsilateral brachial plexus, esophagus, heart, bronchial tree and trachea with no significant increases to other DLO like spinal cord. Normal lung tissue dosing was also reduced in KBPs indicated by the reported V5Gy, V10Gy, V20Gy and MLD. Again, these possible indicators of radiation induced pneumonitis.²³⁻²⁵ This dosimetric OAR sparing and slight dose escalation of tumor dose was achieved with minimal increase of plan complexity and overall beam on time. Plan deliverability and small field dosimetry errors were minimal as seen by similar quality assurance pass rates between the two plans. This indicates that the optimizer in the KBP model was not significantly modulating the treatment plans more to achieve better OAR sparing.

In the past, some investigators have generated KBP models for lung SBRT treatments.^{14,15,17} However, this model is different as it is the first to exclusively consider centrally located tumors, eliminating varied normal tissue DLO limits due to variable tumor location and prescriptions as seen in other models. For instance, this work differs from Chin *et al.* because they trained their model with a majority of IMRT plans with the less accurate analytical anisotropic algorithm (AAA) in their training datasets, resulting in different dosimetric sparing capabilities.¹⁴ They reported an average maximum dose increase to the esophagus of 1.1 Gy in their VMAT validation whereas our KBP model reduced the maximum esophageal dose by 0.7 Gy, on average. Another study by Delaney, *et al.* generated a lung SBRT model for peripheral lesions that considered both a 55 Gy in 5 fractions and 54 Gy in 3 fractions dosing schema.¹⁵ Using different prescriptions causes changes in normal tissue dose limits that can be detrimental to OAR sparing because of their different biological response to the organs. Our work differs from Delaney *et al.* as it fully covers centrally located tumors for a single prescription. The study by Hof, *et al.* created a lung VMAT SBRT model to retroactively evaluate patients who developed greater than grade 3 toxicities in tumors greater than 5 cm in diameter.¹⁷ They used a subset of their patients (tumors > 5 cm) who did not develop toxicities as a training dataset. Due to lung toxicity, lung SBRT treatments are typically not done for tumors larger than 5 cm, so the KBP model described herein was designed for prospective treatment of standard tumor sizes with centrally located lesions.

A limitation to our work (a common issue in other models) is that some patients' geometries do not lend themselves to have a treatment ready lung SBRT plan in a single optimization. This limitation can be broadened to the idea that it is extremely difficult to

create a KBP model that is fully robust. We found that in atypical cases treatment plans might need to be manually optimized further following automatic plan generation. While we feel that using 86 plans for training was sufficient, a few more atypical plans could be added to the model to better improve robustness of this model. However, there is also a risk of overfitting the model if too many plans are used for training the model. Future directions include adding more atypical cases into to further expand this model to tackle those extremely difficult cases. Our methods described in this work will be expanded next to generate and further validate a robust lung SBRT RapidPlan model for medically inoperable/operable early-stage, peripherally located NSCLC patients using a recently developed dynamic conformal arc-based VMAT planning method that further minimizes MLC complexity and improves SBRT treatment delivery efficiency and accuracy.²⁶

3.5 Conclusion

This study created a lung SBRT KBP model via RapidPlan that can quickly generate a high-quality n-VMAT lung SBRT treatment plan for centrally located lung tumors per RTOG-0813 protocol. This KBP model is fully comprehensive covering all ranges of tumor sizes and tumor geographical locations while maintaining adaptability for other clinics. Using this model, a lung SBRT treatment plan can be generated in less than 30 minutes, on average providing the ability to increase clinic workflow by reducing ‘simulation to treatment’ time down to as few as 3 working days. This activates a clinic’s ability for online adaptive treatments to selected lung SBRT patients. Treatment planning time of KBPs was further reduced to 5 minutes while using PO 2.5 mm CGS rather than 1.25 mm in the plan optimization without compromising plan quality. This supports same or next day adaptive re-planning for selected lung SBRT patients. In addition to improving

clinical workflow, our model was able to enhance hypoxic tumor core dose while better sparing critical structures compared to clinical VMAT plans. Moreover, it eliminates inter-planner variability, benefiting standardizing lung SBRT treatment planning and improving patient safety. Clinical implementation of this KBP model will effectively improve overall clinic workflow and provide high quality, consistent and highly conformal KBP lung SBRT treatments.

Copyright © Justin David Visak 2021
<https://orcid.org/0000-0002-8674-5657>

CHAPTER 4. AN AUTOMATED KNOWLEDGE-BASED ROUTINE FOR STEREOTACTIC BODY RADIOTHERAPY OF PERIPHERAL LUNG TUMORS VIA DCA-BASED VOLUMETRIC MODULATED ARC THERAPY

In the previous **Chapter 3**, a KBP model was developed to aid in the fast treatment planning of prospective centrally located lung SBRT patients. During the creation of this model, it was discovered that KBP unintendingly increases total MU and plan complexity. Therefore, utilizing a traditional DCA-based approach before an automatic VMAT optimization, a novel routine was developed to design a new KBP model that minimally impacts current treatment planning workflow and improves the overall plan quality. This KBP model will significantly reduce the overall plan complexity relative to both manual and knowledge-based techniques. Herein, **Chapter 4** describes this novel routine and has been adapted from the recently published manuscript by: **Visak J**, Ge GY, McGarry RC, Randall M, Pokhrel D. An Automated knowledge-based planning routine for stereotactic body radiotherapy of peripheral lung tumors via DCA-based volumetric modulated arc therapy. *J Appl Clin Med Phys.* 2020; 22(1); 1-10

Abstract

This study aimed to develop a knowledge-based planning (KBP) routine for stereotactic body radiotherapy (SBRT) of peripherally located early-stage non-small-cell lung cancer (NSCLC) tumors via dynamic conformal arc (DCA)-based volumetric modulated arc therapy (VMAT) using the commercially available RapidPlan™ software. This proposed technique potentially improves plan quality, reduces complexity and minimizes interplay effect and small field dosimetry errors associated with treatment delivery. KBP model was developed and validated using 70 clinically treated high quality non-coplanar VMAT lung SBRT plans for training and 20 independent plans for validation.

All patients were treated with 54 Gy in 3 treatments. Additionally, a novel *k*-DCA planning routine was deployed to create plans incorporating historical 3D-conformal SBRT planning practices via DCA-based approach prior to VMAT optimization in an automated planning engine. Conventional KBPs and novel *k*-DCA plans were compared with clinically treated plans per RTOG-0618 requirements for target conformity, tumor dose heterogeneity, intermediate dose fall-off and organs-at-risk (OAR) sparing. Treatment planning time, treatment delivery efficiency and accuracy were recorded. KBPs and *k*-DCA plans were similar or better than clinical plans. Average planning target volume for validation was 22.4 ± 14.1 cc (7.1–62.3 cc). KBPs and *k*-DCA plans provided similar conformity to clinical plans with average absolute differences of 0.01 and 0.01, respectively. Maximal doses to OAR were lowered in both KBPs and *k*-DCA plans. KBPs increased monitor units (MU) on average 1316 ($p < 0.001$) while *k*-DCA reduced total MU on average by 1114 ($p < 0.001$). This routine can create *k*-DCA plan in less than 30 minutes. Independent Monte Carlo calculation demonstrated that *k*-DCA plans showed better agreement with planned dose distribution. In summary, a *k*-DCA planning routine was developed in concurrence with a knowledge-based approach for the treatment of peripherally located lung tumors. This novel method minimizes plan complexity associated with model-based KBP techniques and improve plan quality and treatment planning efficiency.

4.1 Introduction

Stereotactic body radiation therapy (SBRT) of lung tumors is an alternative treatment modality to surgery for early stage non-small-cell lung cancer (NSCLC) patients, boasting local control rates greater than 97% at 3-years.¹⁻³ These outstanding clinical outcomes were predominantly based on traditional lung SBRT treatments performed with 7 to 13

coplanar/non-coplanar 3D-conformal static beams or with a few dynamic conformal arcs (DCA).^{4, 5} With modern advances in technology, lung SBRT can be delivered using intensity modulated radiation therapy (IMRT) or volumetric modulated arc therapy (VMAT). VMAT offers the most conformal dose distribution with higher chances of sparing organs-at-risk (OAR).⁶ When coupled with a 6 MV flattening filter free (FFF) beam, VMAT benefits are enhanced by providing higher dose rates, reduction of out of field dose and improved coverage at the lung-tumor interface when compared to traditionally flattened beams.^{7, 8}

The generation of a high quality VMAT lung SBRT plan can require multiple iterations of optimization due to difficult patient geometry, tumor size or location.⁹ In general, inverse planning heavily depends on a planner's experience, treatment planning time and planner's skill. Inter-planner variability potentially leads to inconsistent plan quality and reduced patient safety.¹⁰ Efforts have been made to increase treatment planning efficiency and plan quality using a form of inverse planning automation known as knowledge-based planning (KBP).¹¹ Model-based KBP is a commonly utilized automatic planning strategy that gathers historical treatment planning data to predict achievable tumor coverage and OAR doses for a prospective patient.¹² This form of KBP has demonstrated success in creating dosimetrically similar or better plans when compared to manual planning across many treatment sites with limited but recently increasing literature for lung SBRT.¹²⁻¹⁸

However, a major concern with using KBP for lung SBRT is its tendency to increase total monitor units (MU) and overall plan complexity^{12,18} which can increase treatment delivery complexity leading to unintended consequences particularly with

VMAT plans. This includes the interplay effect between MLC motion and the tumor motion due to breathing cycle.¹⁹ VMAT lung SBRT for small tumor sizes (< 3 cm) could result in small field dosimetry errors.²⁰ These drawbacks are compounded by very high MLC modulation observed in knowledge-based planning. More traditionally planned 3D-conformal and DCA methods may improve the level of confidence in the treatment. MLC interplay effect and small field dosimetry errors are reduced improving delivery, efficiency and accuracy in these plans.¹⁹

Recently, Pokhrel and colleagues have shown that DCA-based VMAT lung SBRT planning can provide a dosimetrically similar or better plan with reduced complexity when compared to a standard clinical VMAT lung SBRT plans.²¹ Utilizing their approach, in this study we have developed a novel and automated KBP routine using Varian's RapidPlan™ knowledge-based planning engine that couples the benefits of a DCA-based dose technique with modern knowledge-based VMAT optimization. To deploy this new and clinically useful technique, it was first necessary to develop and validate a robust non-coplanar VMAT lung SBRT RapidPlan model for medically inoperable/operable early-stage, peripherally located NSCLC patients. This model was created to fully comply with the RTOG-0618 lung SBRT protocol's dosing requirements. Its novelty is furthered because the model uses more accurate advanced Acuros-based dose calculation for heterogeneity corrections to better predict dose at soft tissue tumor and low-density lung interfaces.^{7, 22, 23}

4.2 Methods

4.2.1 Patient Population and Clinical Plans

Approval from our institutional review board was obtained to utilize 90 clinically treated patients' treatment plans for peripherally located early stage, NSCLC tumors that met the criteria set forth by RTOG-0618. Motion management for these patients was primarily performed using abdominal compression unless the patient presented with a comorbidity that did not allow for compression, in these cases a 4D-CT scan was performed. A gross tumor volume (GTV) was delineated in a lung window and a planning target volume (PTV) was created with added margins of 1.0 cm superior/inferior and 0.5 cm laterally per protocol guidelines. With the 4D-CT scan, the PTV was generated using a 0.5 cm isotropic margin around the internal target volume (ITV). OARs were contoured per RTOG-0618 guidelines. Clinical non-coplanar VMAT plans were created in Varian's Eclipse treatment planning system (TPS) on a Truebeam Linac (Varian Medical Systems, Palo Alto, CA). Details of patient set up have previously been published elsewhere.⁷ All patients received a total dose of 54 Gy in 3 fractions prescribed to the 70-80% isodose line.

4.2.2 Development and Validation of KBP Model

The new KBP model was trained and validated using 90 previously treated high quality non-coplanar VMAT lung SBRT plans. Seventy plans were selected for training and the remaining 20 plans were used for validation. Prior to input, training and validation datasets were manually verified to have correct calculation models and grid sizes (e.g., PO MLC algorithm and Acuros-XB algorithm enabled). Training contours and overall plan quality were then evaluated for compliance per RTOG-0618 guidelines. Once the KBP model was verified, normal tissue constraints and dose objectives were iteratively selected.

To ensure the KBP model was fully functional and robust, 20 independent patients were specifically selected to include both lungs' geometries, differing tumor locations and variable tumor sizes. This validation dataset included: 6 RUL, 6 LUL, 3 LLL and 5 RLL patients with an average tumor sizes of 17.0 ± 9.9 cc (7.8–37.5 cc), 19.5 ± 12.1 cc (7.1–42.9 cc), 38.7 ± 18.2 cc (18.0–62.3 cc), and 22.6 ± 10.2 cc (7.8–37.6 cc) respectively. Validation plans were re-optimized with the RapidPlan model using identical treatment geometry as the clinical plans to create the KBP's. Plans were normalized to have identical or better target coverage than the original plans.

4.2.3 Dosimetric Comparison Criteria

Re-optimized plans were evaluated for target conformity, dose gradient and intermediate dose spillage as described by RTOG-0618. Target conformity was assessed using the conformity index defined as the ratio of the 100% isodose line volume to PTV volume. Dose gradient was assessed using the RTOG recommended gradient index (GI) defined the ratio of the 50% isodose line volume to the PTV volume. The maximum dose 2 cm away from the PTV (D2cm) in any direction and the gradient distance (GD), defined as the average distance between the 100% and 50% isodose lines, were used to quantify degree of intermediate dose fall-off.

Volumetric and maximum doses to organs at risk outlined by RTOG-0618 were evaluated. These dose limiting organs (DLO) include the spinal cord, skin, esophagus, trachea, heart, bronchial tree, ribs and normal lung. The total monitor units divided by prescription dose in cGy defined as the modulation factor (MF), including beam-on time, was used to assess plan complexity. An in-house data collection method using the Visual Eclipse Scripting Application Programming Interface (ESAPI) (Varian Medical Systems,

Palo Alto, CA), Microsoft Excel (Microsoft corp., Redmond, WA) and MATLAB (Math Works, Natick, MA) was developed for rapid collection of the aforementioned data. A paired student t-test was used to assess statistical agreement ($p < 0.05$ statistically significant).

4.2.4 A Novel *k*-DCA Planning Routine

To integrate the benefits of both traditional planning techniques and modern lung SBRT treatment practices using VMAT optimization, a novel routine was developed to improve the plan quality and patient safety in prospective treatments. This routine creates a *k*-DCA plan using a combination of manual and automated planning approaches with minimal deviation from traditional planning workflow. To begin, planning geometry is manually determined by deploying dynamic conformal arcs and collimator angles. An MLC is then added to each field and is fit with a 2 mm margin around the PTV on each DCA. Within the PO algorithm (v15.0 or higher) exists the new MLC aperture shaper controller (ACS). Following creation of planning geometry, the ACS is adjusted from its default setting of 'low' to 'very high.' This is modified to aid in the reduction of MLC modulation in the final plan. Once this aperture setting is applied, a 3D DCA-based dose is calculated, and field weights are adjusted to give a practical starting point and a base dose for the future VMAT optimization. Following the DCA-based dose calculation, the VMAT optimizer is launched and DVH estimates are automatically generated by enabling the novel KBP model (see section 2B) within the VMAT optimization window. VMAT optimization is performed using the newly and automatically generated dose optimization objectives and priorities via the KBP model. **Figure 4.1** outlines this process.

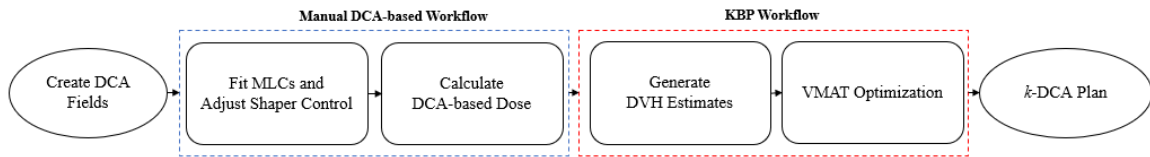


Figure 4.1 Proposed *k*-DCA treatment planning workflow for peripheral lung SBRT.

4.2.5 Independent Dose Verification

To verify knowledge-based plans independently, patient-specific quality assurance was performed using an in-house Monte Carlo (MC) program.^{24, 25} This was performed in lieu of traditional based quality assurance measurements as recent technological advancements in online/offline-adaptive re-planning strategies may not allow enough time to perform a conventional physical measurement.²⁶ The in-house MC code uses a vendor provided phase space file to base its functionality off the PENELEOPE MC code.²⁷ Rather than physical measurement of multi-leaf collimators at the machine, a vendor provided schematic was used to model in the MC code and independent dose verification. More details of this algorithm used for this physics second check tool can be found in the cited literature above.

4.3 Results

4.3.1 Clinical Plans vs KBPs

Knowledge-based plans produced similar or better target coverage than clinical plans (**Table 4.1**). Slight dose escalation to the GTV was achieved with KBPs with an average of 2.2 Gy ($p < 0.001$). PTV minimum coverage was maintained while slightly increasing the PTV mean dose ($p < 0.001$) with no increase in intermediate dose-spillage with KBPs. This is reflected in both the lower D2cm and the average reduction of 0.1 cm

in the gradient distance ($p < 0.001$). For a similar CI, there was significant improvement of GI with KBPs ($p < 0.001$) compared to clinical plans indicating less intermediate dose spillage in normal lung (**Table 4.1**).

4.3.2 Clinical Plans vs k -DCA Plans

When the proposed automatic planning routine to create a k -DCA plan was deployed, a higher target dose was achieved at minimal costs to plan quality when compared to clinical plans. The GTV minimum dose was escalated on average 3.7 Gy in k -DCA plans. This is due to the increased average MLC aperture size and less MLC modulation through the target. PTV target metrics showed higher dose with an increase of mean dose by an average of 2.9 Gy ($p < 0.001$) with no clinically significant differences in PTV minimum coverage. Despite the higher delivered GTV dose, the CI differences between the k -DCA plans and clinical plans were insignificant. As expected, and following the trend of KBPs, k -DCA plans were more homogenous indicated by the lower GI ($p = 0.005$) and delivered less intermediate dose spillage reflected in a lower value of GD ($p = 0.004$). D2cm was slightly increased in k -DCA plans with respect to clinical plans but this increase was not statistically significant (**Table 4.1**).

Table 4.1 Evaluation of plan quality and target indices for all 20 lung SBRT validation cases generated using KBP or k -DCA routine.

Target	Parameter	Clinical	KBP	k -DCA	Clinical vs. KBP	Clinical vs. k -DCA	KBP vs. k -DCA
GTV	Min (Gy)	58.3 ± 2.1	60.3 ± 2.3	62.0 ± 2.1	p = 0.002	p < 0.001	p = 0.002
	Mean (Gy)	62.4 ± 1.4	64.6 ± 1.9	66.9 ± 1.6	p = 0.004	p < 0.001	p < 0.001
	Max (Gy)	65.5 ± 1.2	67.7 ± 1.5	69.3 ± 1.6	p = 0.001	p < 0.001	p < 0.001

Table 4.1 (continued)

PTV	D99%(Gy)	52.3 ± 0.4	52.5 ± 0.4	52.0 ± 0.6	p = n. s.	p = n. s.	p = 0.002
	Mean (Gy)	59 ± 0.7	61.5 ± 0.8	61.9 ± 0.7	p < 0.001	p < 0.001	p = 0.01
	CI	1.02 ± 0.03	1.01 ± 0.02	1.03 ± 0.03	p = n. s.	p = n. s.	p = 0.001
	HI	1.21 ± 0.02	1.27 ± 0.02	1.28 ± 0.02	p < 0.001	p < 0.001	p < 0.001
	GI	4.56 ± 0.8	3.95 ± 0.5	4.23 ± 0.6	p < 0.001	p = 0.005	p < 0.001
	D2cm (%)	49.3 ± 5.6	48.6 ± 4.7	50.6 ± 4.6	p = n. s.	p = n. s.	p = 0.025
	GD (cm)	1.04 ± 0.1	0.94 ± 0.1	0.98 ± 0.1	p < 0.001	p = 0.004	p = 0.05

4.3.3 OAR Sparing

All OAR dosing criteria was assessed per RTOG-0618 protocol's requirements for all 20 lung SBRT validation cases. Clinically relevant maximal doses to OAR are shown in **Figure 4.2**. Both KBPs and *k*-DCA plans provided less maximum dose to these select structures.

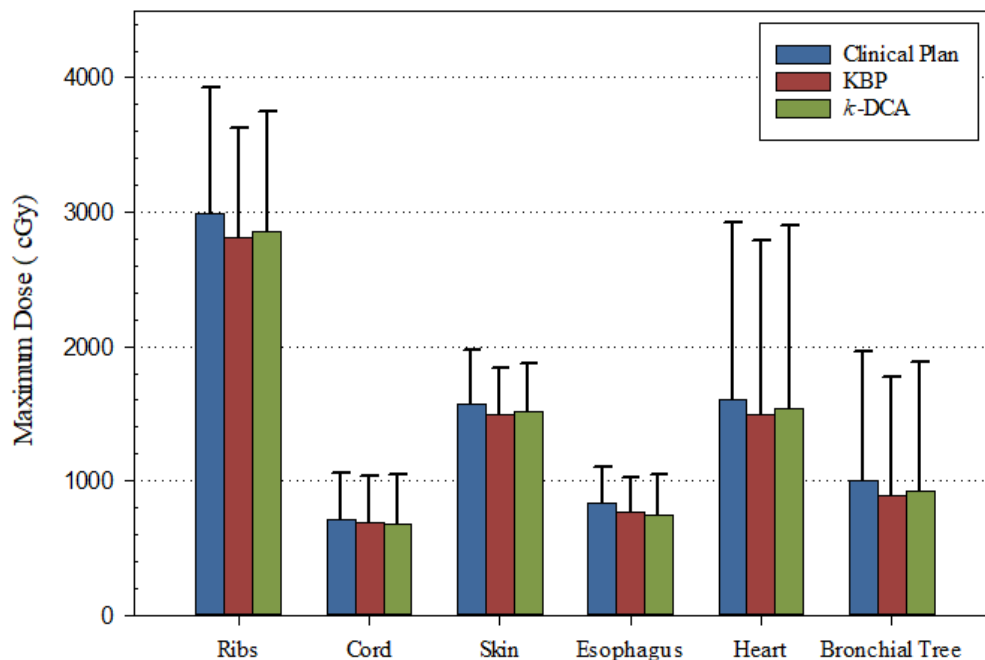


Figure 4.2 Average maximum doses of selected OAR for clinical plans, KBPs and *k*-DCA plans.

Average maximum doses of selected OAR for clinical plans, KBPs and *k*-DCA plans for all 20 lung SBRT validation cases. In all cases both KBPs and *k*-DCA plans were able to successfully lower the maximum doses delivered to the OAR. KBPs lowered the maximum rib dose by an average of 1.8 Gy and *k*-DCA reduced the maximum esophageal dose by 0.9 Gy when compared to clinical plans.

Better OAR sparing can be achieved while still maintaining slight dose escalation to the tumor using the newly developed KBP model or automated *k*-DCA routine. The maximum ipsilateral brachial plexus doses were not clinically significant (not shown). Volumetric doses were also tracked with notable sparing of 1.0 cc of the ribs in KBPs with average dose reduction of 0.65 ± 1.28 Gy (0.92–4.0 Gy) and 15 cc of heart in *k*-DCA plans with an average dose reduction of 0.97 ± 2.2 Gy (0.2–9.0 Gy) when compared to clinical plans.

Table 4.2 Evaluation of normal lung doses for validation cases generated using KBPs or *k*-DCA routine.

Target	Parameter	Clinical	KBP	<i>k</i> -DCA	Clinical vs. KBP	Clinical vs. <i>k</i> -DCA	KBP vs. <i>k</i> -DCA
Lungs-PTV	V5Gy (%)	12.0 ± 4.8	11.0 ± 4.4	11.1 ± 4.5	p < 0.001	p = 0.006	p = n. s.
	V10Gy (%)	7.3 ± 3.1	6.7 ± 3.0	6.9 ± 3.0	p < 0.001	p = n. s.	p = n. s.
	V20Gy (%)	2.8 ± 1.3	2.6 ± 1.2	2.5 ± 1.2	p < 0.001	p < 0.001	p = 0.005
	MLD (Gy)	2.48 ± 0.9	2.25 ± 0.9	2.30 ± 0.9	p < 0.001	p = 0.001	p = n. s.

Normal lung tissue sparing was tracked for V5Gy, V10Gy and MLD because literature suggested these better predict radiation-induced pneumonitis than V20Gy²⁸⁻³⁰ (Table 4.2). For V5Gy, V10Gy, V20Gy and MLD, KBPs were able to significantly reduce (all p-values < 0.001) the dose to normal lung when compared to clinical plans. This suggests that in most cases KBPs show reduced normal lung doses and could potentially allow for re-treatment in future as needed. Clinical plans delivered higher doses to normal lung tissue across all metrics when compared to *k*-DCA plans, however only V5Gy (p = 0.006) and V20Gy (p < 0.001) were statistically significant. This could correlate to a potential lower risk of radiation-induced pneumonitis via *k*-DCA plans.

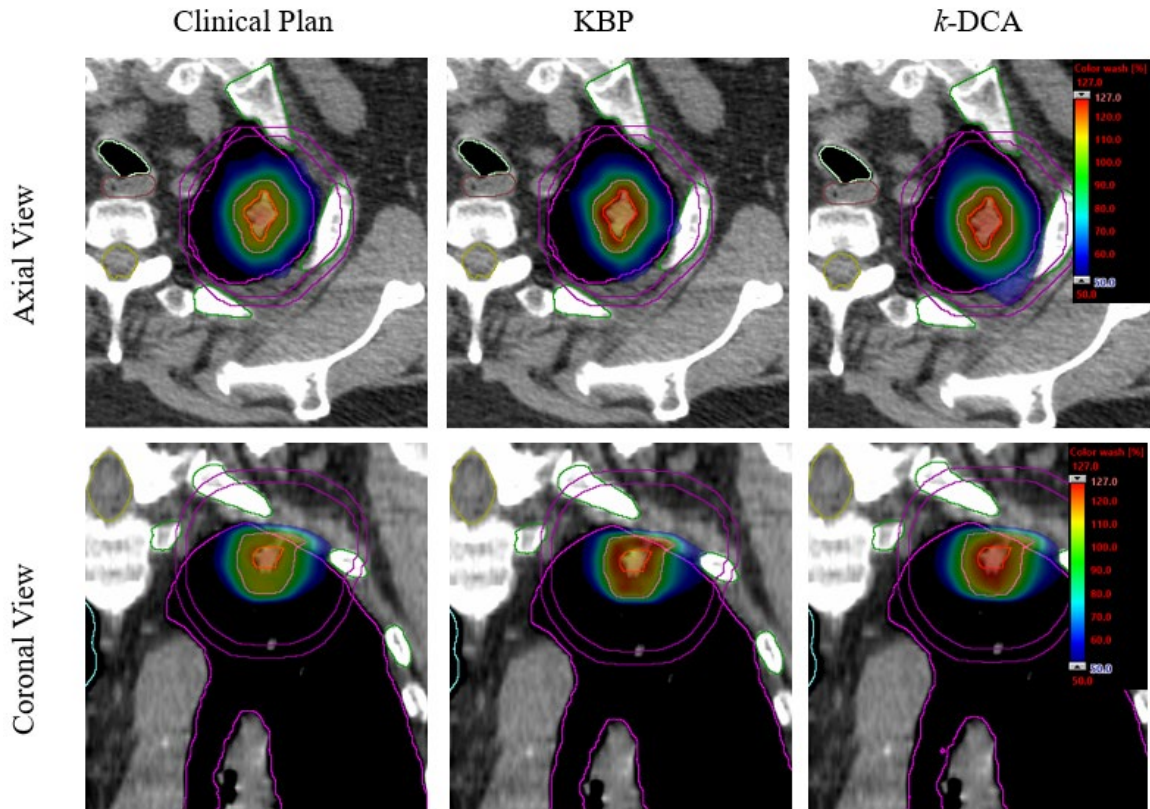


Figure 4.3 Radiosurgical dose color wash of the clinical plan, KBP and k -DCA plan for a selected validation case.

Radiosurgical dose colorwash of the clinical plan, KBP and k -DCA plan for a selected validation case. Trachea (light green), esophagus (brown), spinal cord (yellow) and ribs (dark green) are shown. Clinical plan shows a smaller central hotspot than both KBPs and k -DCA plan. 50% isodose colorwash was slightly larger in the k -DCA plan but still clinically acceptable. The largest central hotspot was seen in the k -DCA plan improving dose to GTV.

A dose color wash distribution with both the axial and coronal views of an example validation case is shown (**Figure 4.3**). Corresponding dose-volume histogram is shown in **Figure 4.4**. Select OAR are also shown for reference to the tumor location. Highly conformal radiosurgical dose distribution with a tighter 50% isodose color wash (blue) can be observed in both clinical and KBPs, however, there was a reduced central hotspot in both plans when compared to the k -DCA plan. This reflects our findings that k -DCA routine was able to increase minimum dose to GTV. This larger central hotspot displayed

in the $-k$ -DCA was achieved with minimal to no additional costs in OAR dosing. It is shown that the 50% isodose color wash was slightly larger in the k -DCA axial slice but still easily met RTOG-0618 criteria.

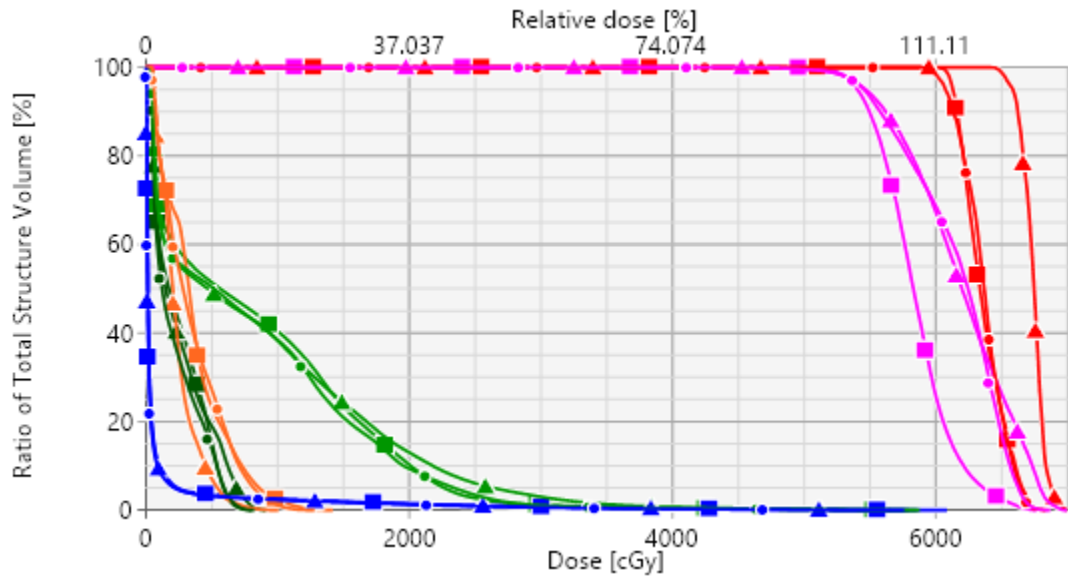


Figure 4.4 Dose volume histogram for the clinical, KBP and k -DCA for corresponding example case presented in Figure 4.3

Dose volume histogram for the clinical plan (squares), KBP (circles) and k -DCA (triangle) plans corresponding to example case presented in **Figure 4.3**. PTV (pink), GTV (red), ribs (green), brachial plexus (orange), trachea (dark green) and lungs-PTV (blue) are presented. Note for similar OAR sparing, the k -DCA plan significantly increased GTV dose.

4.3.4 Planning Efficiency and Deliverability

The k -DCA plans were generated using plan geometry identical to previously treated plans in less than 30 minutes. **Table 4.3** displays the average values of various treatment delivery parameters across all 20 lung SBRT validation cases. The most important result to note here is the significant reduction of total monitor units in the k -DCA plans due to less MLC modulation through the target. On average, k -DCA plans delivered 1133 and 2460 less MU than clinical plans and KBPs, respectively. This correlates to a

lower modulation factor, indicating less plan complexity and shorter beam on time. This validates that *k*-DCA plans are able to create similar or better-quality plans than manually generated clinical plans and KBPs with significantly less MLC modulation. Additionally, the in-house MC second check algorithm reported that the clinical plans (1.8%) and KBPs (2.4%) on averaged showed less agreement with planned TPS dose with respect to *k*-DCA plans (1.0%). This indicates the novel *k*-DCA planning routine may more accurately deliver treatment. Additionally, the better MC agreement will provide more confidence in treatment delivery accuracy for online/offline adaptive lung SBRT.

Table 4.3 Evaluation of average treatment delivery parameters for validation cases that were generated using KBP or automated *k*-DCA routine

Treatment delivery parameter	Clinical	KBP	<i>k</i> -DCA	Clinical vs KBP	Clinical vs <i>k</i> -DCA	KBP vs <i>k</i> -DCA
Total monitor units (MU)	5488 ± 1018	6804 ± 963	4344 ± 687	p < 0.001	p < 0.001	p < 0.001
Modulation factor (MF)	1.02 ± 0.2	1.26 ± 0.2	0.80 ± 0.1	p < 0.001	p < 0.001	p < 0.001
Beam-on time (min)	3.9 ± 0.7	4.9 ± 0.7	3.1 ± 0.5	p < 0.001	p < 0.001	p < 0.001
MC agreement (%)	±1.76	± 2.40	± 1.03	p = 0.03	p = n. s.	p = 0.002

4.4 Discussion

A novel automatic planning routine was developed to generate a non-coplanar VMAT lung SBRT *k*-DCA plans in less than 30 minutes. Both conventional and the *k*-DCA planning routine generates a similar or better-quality plan than manually planning. This method reduces inter-planner variability and lowers the plan complexity when compared to original clinical and conventional knowledge-based plans. Better target

coverage and more DLO sparing was achieved with *k*-DCA plans because it merges the benefits of both a historical DCA-based lung SBRT planning approach with a powerful automatic inverse planning engine. Using the 3D DCA-based dose as a starting point and optimal machine generated DVH estimates, we have shown that a more accurate lung SBRT plan can be generated in short period of time compared to typical model-based knowledge-based planning. Due to less MLC modulation through the target, *k*-DCA plans could potentially reduce interplay effect and small-fields dosimetry errors as demonstrated by better agreement with MC calculation. Nonetheless, it remains incumbent on the treating physician to review plans in detail to help ensure accuracy and appropriateness of the objectives of the treatment since there can be intangible goals of the plan that a computer cannot recognize.

Other investigators have created RapidPlan KBPs for lung SBRT and some evaluated plan complexity.^{12, 16-18} The most recent study by Yu *et al.* compared clinical VMAT SBRT plans with both the University of California, San Diego's publicly shared RapidPlan VMAT lung SBRT model and robotic CyberKnife plans.¹² They reported on average an increase of 1025 MU in KBPs when compared to manual clinical plans for a prescription dose of predominately 50 Gy in 5 fractions.¹² This reflects similar findings in our study but using our automated *k*-DCA planning routine we were able significantly reduce the total MU (see **Table 4.3**). A study by Delaney *et al.* produced two RapidPlan models intended to treat peripheral lung tumors in either 54 Gy in 3 treatments or 55 Gy in 5 fractions.¹⁷ For their 55 Gy evaluation patient group, they report average increase of 222 MU for their 5 × 11 Gy model and 188 MU for their combined prescription model compared to manually generated PO optimized plans.¹⁷ Additionally, they reported an

increase of monitor units in their 54 Gy evaluation group of 384 MU and 242 MU for their prescription specific and combined model, respectively. While not as dramatic as the results shown by Yu *et al.*,¹² there is an apparent increase of MU when using KBPs which could be accounted for by different choice of planning constraints and model input datasets, similar to one demonstrated by Kubo *et al* for conventionally fractionated prostate radiotherapy.³³ With our previous institutional experience, we believe that selecting normal tissue constraints is a critical process in the creation of a KBP model and it will influence the performance of the model as much as the initial input dataset selection. Our previous clinical experience with building a KBP model designed to treat central locations with 50 Gy in 5 fractions scheme also shown increased MU by an average of 261. However, our automated *k*-DCA planning routine was able to overcome this issue and maintained significantly lower total MU and consequently shorter beam-on time. Other KBP models were generated but did not report total number of MUs.^{16,18}

This automated *k*-DCA planning routine appears to be the first of its kind and its novelty is further enhanced when validated independently with MC dose calculations. The use of the MC code opens the possibility of using this routinely in the clinic for either online adaptive re-planning or next day offline adaptive re-planning of lung SBRT treatment. It has previously been shown that 30 Gy in a single fraction can be delivered to the lung lesion in a 15-minute time slot.³¹ Delivering a single fraction treatment subjects the plan to delivery potential errors that could greatly enhanced the interplay effect, so our *k*-DCA routine could potentially limit this effect by providing less MLC modulation across the target and improve small-field dosimetry.³² Further validation and clinical

implementation of this KBP model and automated k -DCA routine for SBRT patient treatment is underway.

4.5 Conclusion

A novel lung SBRT KBP model for the treatment of peripherally located early-stage NSCLC tumors as defined by RTOG-0618 was developed and validated. In conjunction with this model, a first of its kind automated k -DCA planning routine was developed to generate high-quality lung SBRT plans with less complexity. Utilizing this process, a high-quality lung SBRT treatment plan can be generated in as little as 30 minutes with less inter-planner variability, allowing for same day or next day adaptive re-planning, if desired. Due to less MLC modulation through the target and faster treatment delivery, a k -DCA plan could potentially reduce treatment delivery complexity and intra-fraction motion errors; improve patient comfort and treatment delivery accuracy.

Copyright © Justin David Visak 2021
<https://orcid.org/0000-0002-8674-5657>

CHAPTER 5. FAST GENERATION OF LUNG SBRT PLANS WITH A KNOWLEDGE-BASED PLANNING MODEL ON RING-MOUNTED HALCYON LINAC

The previously described KBP models in **Chapters 3** and **4** were trained and intended to treat lung SBRT patients using a non-coplanar VMAT technique with a SBRT-dedicated C-arm linac. However, with the recently introduced coplanar restricted O-ring Halcyon linac, it was of great interest to demonstrate whether the previously built KBP model that was fully trained using highly conformal non-coplanar VMAT plans can be used to develop an effective KBP model for this novel modality. Therefore, the KBP model from **Chapter 3** was adapted to support coplanar treatments geometry with the Halcyon linac. In addition to reducing ‘simulation-to-treatment’ time, this model intends to reduce the burden on high-volume lung SBRT clinics and assess the feasibility of quickly transferring patients between treatment platforms. This provides a solution to unintended longer machine downtime. Hence, **Chapter 5** has been adapted from the recently submitted manuscript by: **Visak J**, Webster A, Bernard ME, McGarry RC, Randall M, Pokhrel D. Fast Generation of Lung SBRT Plans with a Knowledge-based Planning on Ring-Mounted Halcyon Linac. (**Under Review**, J Appl Clin Med Phys, submitted on January 10, 2021).

Abstract

This study demonstrates fast treatment planning feasibility of stereotactic body radiation therapy (SBRT) for centrally located lung tumors on Halcyon Linac via a previously validated knowledge-based planning (KBP) model to support offline adaptive radiotherapy. Twenty previously treated non-coplanar volumetric modulated arc therapy (VMAT) lung SBRT plans (*c*-Truebeam) on SBRT dedicated C-arm Truebeam Linac were selected. Patients received 50 Gy in 5 fractions. *c*-Truebeam plans were re-optimized for

Halcyon manually (*m*-Halcyon) and with KBP model (*k*-Halcyon). Both *m*-Halcyon and *k*-Halcyon plans were normalized for identical or better target coverage than clinical *c*-Truebeam plans and compared for target conformity, dose heterogeneity, dose fall-off, and dose tolerances to the organs-at-risk (OAR). Treatment delivery parameters and planning times were evaluated. *k*-Halcyon plans were dosimetrically similar or better than *m*-Halcyon and *c*-Truebeam plans. *k*-Halcyon and *m*-Halcyon plan comparisons are presented with respect to *c*-Truebeam. Differences in conformity index were statistically insignificant in *k*-Halcyon and on average 0.02 higher ($p=0.04$) in *m*-Halcyon plans. Gradient index was on average 0.43 ($p=0.006$) lower and 0.27 ($p=0.02$) higher for *k*-Halcyon and *m*-Halcyon, respectively. Maximal dose 2cm away in any direction from target was statistically insignificant. *k*-Halcyon increased maximal target dose on average by 2.9 Gy ($p<0.001$). Mean lung dose was on average reduced by 0.10 Gy ($p=0.004$) in *k*-Halcyon and increased by 0.14 Gy ($p<0.001$) in *m*-Halcyon plans. *k*-Halcyon plans lowered bronchial tree dose on average by 1.2 Gy. Beam-on-time was increased by 2.85 min and 1.67 min, on average for *k*-Halcyon and *m*-Halcyon. *k*-Halcyon plans were generated in under 30 minutes compared to estimated dedicated 180 ± 30 minutes for *m*-Halcyon or *c*-Truebeam plans. To summarize, *k*-Halcyon plans were generated in under 30 minutes with excellent plan quality. This adaptable KBP model supports high-volume clinics in the expansion or transfer of lung SBRT patients to Halcyon.

5.1 Introduction

Surgical resection is an important treatment for early stage non-small-cell lung cancer (NSCLC) patients. However, many patients are inoperable due to comorbidities,

refuse surgical resection, or present with a high chance of post-operative morbidity.^{1,2} For these NSCLC patients, stereotactic body radiation therapy (SBRT) has become an extremely effective curative treatment modality.² Compared to poor tumor local-control rates from conventional lung radiotherapy (60-70% local failure rates), lung SBRT has provided very high local-control rates up to 97% (median, 3 years actuarial) with less treatment related toxicity compared to surgery.¹⁻⁴ To deliver high-quality lung SBRT treatments, a precise delivered dose must be highly conformal around the tumor with a steep dose gradient to limit intermediate dose spillage.⁵ This can be accomplished using traditional 3D conformal radiation therapy (3D-CRT), intensity-modulated radiation therapy (IMRT), or more recently via manually generated volumetric modulated arc therapy (VMAT) plans.⁶⁻⁸ Delivering lung SBRT with VMAT provides enhanced dosimetric benefits and faster treatments that may aid in patient compliance.^{7,8} Currently, VMAT lung SBRT treatment is being delivered with flattening filter free (FFF) beams using a SBRT-dedicated C-arm Linac.^{2, 9-11} FFF beams provide significantly higher dose rates, less out-of-field scatter dose, less electron contamination and better target coverage at the tumor-lung interface in comparison to flattened beams.¹¹ These additional benefits translate to superior treatment in a shorter overall treatment time.

For fast patient throughput and the advancement of standard radiation treatments to the under-served communities, Varian Medical Systems (Palo Alto, CA) recently introduced a new jawless, single energy, ring-mounted coplanar restricted Halcyon (V2.0) medical linear accelerator.¹² The Halcyon Linac is equipped with a 6X-FFF beam with a maximum dose rate setting of up to 800 MU/min, much lower than the 6MV-FFF (up to

1400 MU/min) beam on a SBRT-dedicated Truebeam Linac. The Halcyon Linac has a relatively softer beam with a mean energy and nominal maximum depth dose of 1.3 MeV and at 1.3 cm, compared to the corresponding 6MV-FFF beam on Truebeam of 1.4 MeV and 1.5 cm. Additionally, Halcyon's ring-mounted gantry design offers a fourfold increase in gantry rotation speed when compared to Truebeam and is equipped with a new design of 1 cm wide dual-layered stacked and staggered MLC (see **Figure 5.1**).¹³⁻¹⁴ This design restricts the field size to $28 \times 28 \text{ cm}^2$, however, the stacked and staggered MLC design offers complete leaf interdigitation and allows for MLC travel all the way to 28 cm. With a less rounded MLC leaf design, the Halcyon boasts a small dosimetric leaf gap of 0.1 mm and ultra-low leakage and transmission around 0.4%.^{14,15} This novel MLC design offers leaf speeds of up to 5.0 cm/s with an effective equivalent 5 mm MLC resolution at the treatment isocenter. Additionally, target localization is potentially improved with the Halcyon onboard imager because it has an advanced image reconstruction algorithm that can iteratively reconstruct a pre-treatment conebeam CT.¹⁶ This reconstruction can be acquired in less than 15 seconds due to the increased gantry speed. Moreover, the new "one-step patient set up" approach includes automatically applied isocenter shifts that will significantly reduce patient set up times.¹² One drawback to the Halcyon is that all treatment plans are restricted to coplanar beam geometry whereas SBRT-dedicated C-arm linacs allow for larger range of non-coplanarity.

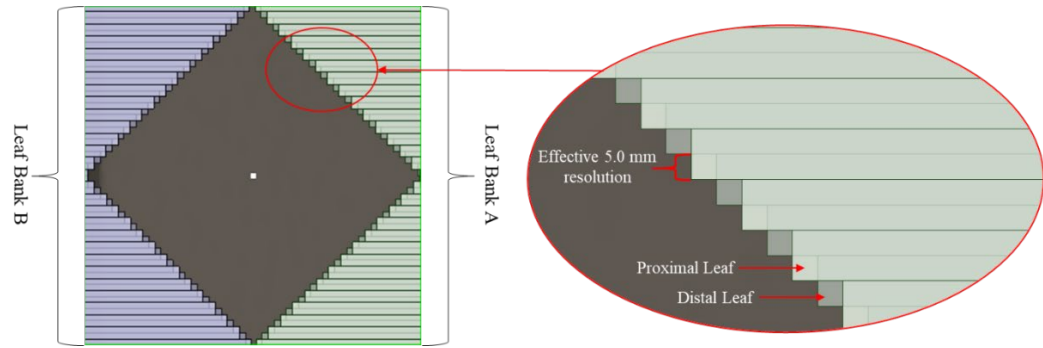


Figure 5.1 Beams-eye-view and description of the new stacked and staggered MLC design on the Halcyon Linac

Currently, highly conformal clinical VMAT lung SBRT plans are generated using a manually optimized inverse planning technique. An issue with manual planning is that the quality of the final plan depends on individual patient anatomy, planning experience and available treatment planning time.^{17,18-24} This potentially leads to inter-planner variability (i.e., plans with varied dosimetric quality). Knowledge-based planning (KBP) has become a clinically feasible approach for generating high-quality treatment plans and aims to mitigate the issues associated with manual planning by standardizing treatment plans and removing inter-planner variability.¹⁸ This is commonly accomplished by using a model library of previously generated high quality clinical plans to predict new treatment parameters.¹⁹ KBP improves plan quality and drastically reduces treatment planning and will shorten ‘simulation-to-treatment’ time down to as few as 3 working days.²⁵ Our center uses Varian RapidPlan dose-volume histogram estimation algorithm as our KBP engine. In the past, a few investigators have shown that KBP may help to create dosimetrically superior or similar lung SBRT plans when compared to manual planning for traditional SBRT-dedicated C-arm linac treatments.²¹⁻²⁵

Halcyon has been shown to provide fast and effective treatment in the setting of conventionally fractionated cranial, head and neck, prostate, and breast treatments.²⁶⁻²⁸ However, due to the lack of lung SBRT training datasets on Halcyon, there is no literature that describes training and clinically validating a KBP model for lung SBRT. This prompted us to evaluate the feasibility of generating lung SBRT plans for centrally located tumors per RTOG-0813 criteria²⁹ on the Halcyon Linac using a previously validated KBP model using high-quality non-coplanar Truebeam VMAT plans. It has previously been demonstrated that lung SBRT using a coplanar geometry produces similar patient outcomes compared to non-coplanar treatments and that it is feasible to treat lung SBRT on the Halcyon linac.^{30,31} The aim of this study was to evaluate the capabilities of KBP modeling techniques to produce coplanar VMAT plans of similar or better quality on ring-mounted Halcyon when compared to traditional non-coplanar lung SBRT treatments delivered on a C-arm Truebeam. We additionally sought to demonstrate whether the Halcyon can overcome coplanar restrictions with the aid of a previously trained KBP model in the treatment of centrally located lung tumors using SBRT.

5.2 Materials and Methods

5.2.1 Patient Selection

Institutional review board approval was obtained to conduct this retrospective study. The previously validated in-house lung SBRT KBP model that was built using highly-conformal non-coplanar VMAT plans with a patient cohort of 86 patients was adopted for this study. Details of the model generation have been published.²⁵ Twenty new patients who were previously treated to 50 Gy in 5 fractions for early-stage I-II NSCLC on

SBRT-dedicated Truebeam Linac using non-coplanar VMAT plans were retrospectively selected to further validate this model on Halcyon Linac.

5.2.2 Clinical Plans (*c*-Truebeam)

Patients in this cohort were primarily immobilized using the Body Pro-Lock™ system (CIVCO system, Orange City, IA) in the supine position with their arms above the head and abdominal compression. A free-breathing 3DCT scan was then performed and a gross target volume (GTV) was delineated followed by a planning target volume (PTV) with expanded margins of 1.0 cm superior/inferior and 0.5 cm laterally from the GTV. If a patient was unable to undergo abdominal compression, a respiration-correlated 4DCT scan using the Varian RPM system (version 1.7) was performed. Maximum intensity projection (MIP) images were derived from the 4DCT scan, and the images were co-registered to the free-breathing 3DCT images to delineate an internal target volume (ITV), therefore the GTV=ITV. The PTV was created by expanding the ITV by 0.5 cm in all directions per SBRT protocol guidelines. As specified by the RTOG-0813 requirements, all relevant organs-at-risk (OAR) were contoured (e.g., total lungs, spinal cord, ribs, heart, esophagus brachial plexus, and skin). For the robust validations of this model, we have included variable tumor sizes and locations on both lungs' geometries as shown in **Table 5.1**.

Table 5.1 Validation patient cohort and tumor characteristics. GTV = gross tumor volume, PTV = planning target volume.

Tumor location	Pop.	GTV size (cc)	PTV size (cc)
Overall patient cohort	n = 20	9.7 ± 13.4 (0.1–61.2)	32.6 ± 25.8 (7.5–114.3)
Right lower lobe (RLL)	n = 6	13.5 ± 21.7 (0.1–61.2)	37.0 ± 36.9 (7.5–114.3)
Right upper lobe (RUL)	n = 5	12.8 ± 8.1 (1.6–22.1)	43.1 ± 22.1 (11.2–71.7)

Table 5.1 (continued)

Left lower lobe (LLL)	n = 4	4.2 ± 1.7 (2.8–7.0)	24.1 ± 8.6 (12–33.1)
Left upper lobe (LUL)	n = 5	6.6 ± 5.5 (1.0–14.8)	23.7 ± 14.5 (9.7–51.3)

All patients were treated with a highly conformal plan using non-coplanar VMAT geometry on Truebeam Linac using a 6MV-FFF beam with a maximum dose rate of 1400 MU/min. On average 3-6 non-coplanar partial arcs (± 5 – 12° couch rotations) were utilized with average arc lengths of approximately 200° and patient-specific collimator angles were selected to minimize the MLC tongue and groove effect (jaw-tracking enabled). Truebeam couch and SBRT board were inserted. Isocenter was placed in the center of the PTV and the dose was prescribed to the 60-80% isodose line and normalized to ensure at least 95% of the PTV received the full prescription dose of 50 Gy in 5 fractions. All hot-spots (average: 120-140%) were constrained to be within the GTV. Clinical plans were inversely optimized using the photon optimizer (PO version 13.0 or 15.0) with final dose calculation performed using AcurosXB with a 1.25 mm calculation-grid size (CGS) with tissue heterogeneity corrections.^{32,33} Dose to medium reporting mode was enabled per our linac calibration. These patients were treated every other day. On the treatment day, an online pre-treatment cone-beam CT scan was performed for patient set-up corrections.

5.2.3 *m*-Halcyon Plans

For comparison, all *c*-Truebeam lung SBRT plans were manually reoptimized on Halcyon (*m*-Halcyon) with identical arc lengths and collimator rotations but using coplanar geometry. The Truebeam couch was removed and the Halcyon couch and SBRT board were inserted. As previously described, *m*-Halcyon plans were reoptimized with the same

calculation algorithms (with corresponding CGS) and identical planning objectives when compared to *c*-Truebeam plans. No jaw tracking option is available on this jawless Halcyon. The *m*-Halcyon plans received the same target coverage as the clinical *c*-Truebeam plans.

5.2.4 *k*-Halcyon Plans

c-Truebeam plans were reoptimized automatically on Halcyon (*k*-Halcyon) using a previously validated KBP RapidPlan model. The planning geometry of the *k*-Halcyon is identical to *m*-Halcyon. *k*-Halcyon plans used the same calculation algorithms and corresponding CGS but with the automatic planning constraints generated by the previously validated non-coplanar KBP model. The *k*-Halcyon plans received the same target coverage as the clinical *m*-Halcyon plans.

5.2.5 Plan Dosimetric Evaluation

All plans were dosimetrically evaluated for target conformity, gradient indices and dose to OAR with RTOG-0813 protocol's requirements. This included the ratio of prescription isodose volume to the PTV volume, conformity index (CI), and the ratio of the 50% isodose volume to the PTV volume known as the gradient index (GI). Additionally, the maximal dose at 2 cm away from the PTV in any direction (D2cm) was assessed for intermediate dose fall-off. Supplemental to the RTOG-0813 criteria, our institution records the gradient distance (GD) defined as the average distance between the 100% and 50% isodose line to further quantify intermediate dose spillage. Moreover, the heterogeneity index (HI), ratio of PTV maximal dose in cGy and prescription dose were used to assess hot spots of each plan. In addition to target and plan complexity metrics, dose to OAR was tracked and documented for maximal and volumetric dosing per RTOG-

0813 criteria. These structures include spinal cord, ipsilateral brachial plexus, skin, total lung-PTV, esophagus, heart and trachea. Plan complexity was simply assessed by recording total number of monitor units (MU) and modulation factor (MF). The MF is defined as the total number of MU divided by the prescription dose in cGy and the corresponding beam-on time (BOT) was calculated using total MU divided by the delivered dose rate for each plan. Moreover, overall treatment planning time and results of independent dose verification via a second physics check Monte Carlo (MC) routine were recorded.³⁴ To collect and statistically compare these metrics, an in-house data collection routine was developed using Eclipse Visual Scripting (Varian Medical Systems, Palo Alto) and MATLAB (Math Works, Natick, MA). Statistical analysis was performed with Microsoft Excel (Microsoft Corp., Redmond, WA) using a paired student t-test with $p < 0.05$ signifying statistical significance.

5.3 Results

5.3.1 Target Coverage and Intermediate Dose Fall-Off

Plan quality and target coverage indices are displayed in **Table 5.2**. All results are presented for both *m*-Halcyon and *k*-Halcyon plans with respect to *c*-Truebeam plans. Both *m*-Halcyon and *k*-Halcyon produced clinically insignificant differences in conformity indices indicating similar target coverage. The *m*-Halcyon plans, on average, produced less homogenous plans as indicated by the increase of 0.27 in GI ($p = 0.02$) whereas *k*-Halcyon plans provided more homogeneity in target coverage by reducing the GI on average 0.43 ($p < 0.005$). Across both plans D2cm differences were statically insignificant, however the GD was much higher in *m*-Halcyon plans and lower in *k*-Halcyon plans. This potentially

indicates less intermediate dose spillage when using knowledge-based planning with Halcyon Linac.

Table 5.2 Evaluation of plan quality and target coverage indices for all validation cases including *c*-Truebeam plans.

Target	Parameter	<i>k</i> -Halcyon	<i>m</i> -Halcyon	<i>c</i> -Truebeam	<i>k</i> -Halcyon vs. <i>m</i> -Halcyon	<i>k</i> -Halcyon vs. <i>c</i> -Truebeam	<i>m</i> -Halcyon vs. <i>c</i> -Truebeam
PTV	CI	1.01 ± 0.02	1.03 ± 0.04	1.01 ± 0.04	p = n. s.	p = n. s.	p = 0.04
	HI	1.19 ± 0.02	1.16 ± 0.03	1.14 ± 0.04	p < 0.001	p < 0.001	p = n. s.
	GI	4.22 ± 1.2	4.92 ± 1.3	4.65 ± 1.2	p < 0.001	p = 0.005	p = 0.02
	D2cm (%)	50.8 ± 4.9	51.4 ± 5.0	50.5 ± 4.4	p = n. s.	p = n. s.	p = n. s.
	GD (cm)	1.06 ± 0.2	1.17 ± 0.2	1.11 ± 0.2	p < 0.001	p = 0.02	p = 0.002

Figure 5.2 displays the average near minimum (D99%) and mean PTV dose including the average minimum, mean, and maximal doses to GTV for all three plans. Qualitatively, the near minimum dose to PTV was similar across all three plans (p = n. s.), however *k*-Halcyon was able to increase dose across all other metrics indicating slight dose escalation may be achievable on the Halcyon using KBP model. The PTV mean dose was 55.8 ± 1.61 Gy (53.7–60.6 Gy), 57.8 ± 1.81 Gy (55.7–65.0 Gy) and 55.7 ± 3.0 Gy (53.9–68.3 Gy) for *m*-Halcyon, *k*-Halcyon and *c*-Truebeam plans, respectively. Additionally, on average *k*-Halcyon plans provided higher GTV minimum dose by 1.2 Gy (p = 0.04), maximum up to 7.6 Gy in some cases.

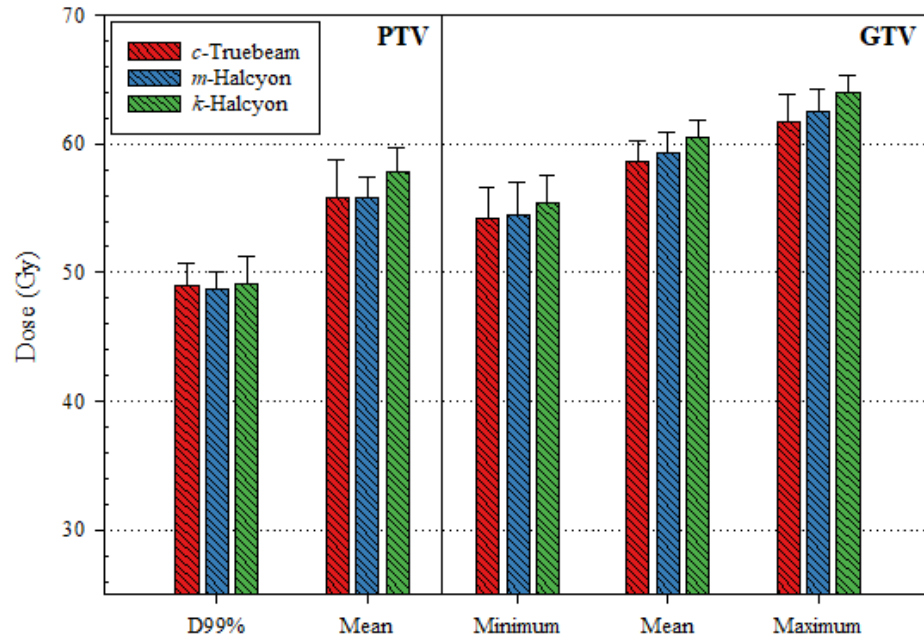


Figure 5.2 Average doses to PTV and GTV (Gy) for lung SBRT validation cases including clinically treated *c*-Truebeam plans.

Average doses to PTV and GTV (in Gy) for 20 lung SBRT validation cases including clinically treated *c*-Truebeam plans. Near minimum PTV (D99%) dose was similar across *c*-Truebeam, *m*-Halcyon and *k*-Halcyon plans. In general, *k*-Halcyon provided higher average dose to PTV and GTV relative to both *m*-Halcyon and *k*-Halcyon plans.

5.3.2 Dose to OAR

Maximal and volumetric doses to OAR were recorded per protocol guidelines and the pairwise differences (in Gy) with respect to clinical *c*-Truebeam plans are presented in **Figure 5.3**. Positive values indicate that both *m*-Halcyon and *k*-Halcyon plans provided higher doses to OAR compared to *c*-Truebeam plans. In many cases, *k*-Halcyon plans helped reduce doses to OAR more than *m*-Halcyon plans, although these small differences may not be clinically significant. However, this finding supports the premise that *k*-Halcyon plans on average will be dosimetrically similar or superior to clinical *c*-Truebeam

plans and to *m*-Halcyon. One interesting value to note is that *k*-Halcyon on average reduced the maximum rib dose by 1.9 Gy ($p = 0.003$), maximum up to 6.3 Gy in some cases.

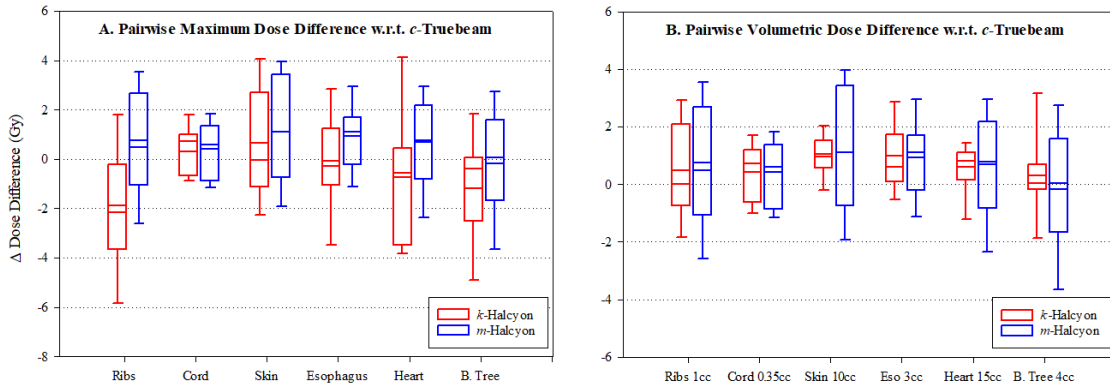


Figure 5.3 Pairwise dose differences (Gy) of maximal and volumetric dose to OAR for *k*-Halcyon and *m*-Halcyon plans with respect to *c*-Truebeam plans.

Pairwise dose differences (in Gy) of maximal and volumetric dose to OAR for *k*-Halcyon and *m*-Halcyon plans with respect to *c*-Truebeam plans. Positive values indicate respective plans on average provided a higher dose to OAR compared to *c*-Truebeam plans. *k*-Halcyon plans across many dosing metrics delivered lower OAR doses than *m*-Halcyon including an average 0.74 Gy reduction in maximal dose to heart.

Dose to normal lung was evaluated using V5Gy, V10Gy, V20Gy and mean lung dose (Gy) as all of these metrics have been correlated to radiation-induced pneumonitis and recently, may correlate with overall survival in stage I lung cancer.³⁵⁻³⁷ These results are shown in **Table 5.3**. *k*-Halcyon plans on average reduced all normal lung dosing metrics whereas *m*-Halcyon increased values when compared to *c*-Truebeam plans. The largest differences in dose to normal lung were recorded for V5Gy. There was a 0.4% decrease and a 0.6% increase of dose for *k*-Halcyon and *m*-Halcyon, respectively.

Table 5.3 Evaluation of normal lung dosing for lung SBRT validation cases including original *c*-Truebeam plans.

Lungs-PTV	<i>k</i> -Halcyon	<i>m</i> -Halcyon	<i>c</i> -Truebeam	<i>k</i> -Halcyon vs. <i>m</i> -Halcyon	<i>k</i> -Halcyon vs. <i>c</i> -Truebeam	<i>m</i> -Halcyon vs. <i>c</i> -Truebeam
V5Gy (%)	12.0 ± 5.6	13 ± 5.6	12.4 ± 5.6	p < 0.001	p = n. s.	p < 0.001
V10Gy (%)	6.9 ± 4.2	7.6 ± 4.4	7.2 ± 4.3	p < 0.001	p = 0.01	p < 0.001
V20Gy (%)	2.7 ± 2.1	3.0 ± 2.3	2.8 ± 2.2	p < 0.001	p = 0.002	p = 0.02
MLD (Gy)	2.5 ± 1.2	2.7 ± 1.3	2.6 ± 1.2	p < 0.001	p = 0.004	p < 0.001

5.3.3 Planning Times and Plan Complexity

The *k*-Halcyon planning time was less than 30 minutes. This is compared to the estimated dedicated planning time of 180 ± 30 min (for an experienced planner) to manually create a high-quality non-coplanar VMAT lung SBRT plan on either linac. This estimation solely accounts for dedicated planning time and no other parts of the planning workflow such as contouring. In practice, this is not feasible as the planners frequently work on multiple plans simultaneously, must wait for physician's time for contouring, or other various checks prior to the final plan approval. Plan complexity was assessed using total MU and its derived metrics that include MF and the corresponding BOT (**Table 5.4**) as described above. There was no statistically significant difference in MU between *m*-Halcyon and *c*-Truebeam plans; however, MU increased for *k*-Halcyon plans by 939 MU on average ($p < 0.001$) compared to *c*-Truebeam plans. This corresponds to an increased MF of 0.94 ($p < 0.001$) indicating *k*-Halcyon plans are modulated higher than both manual

plans. Despite this increase of modulation, no clinically significant differences in agreement between the Eclipse TPS and the 2nd check MU calculated dose were observed. Due to maximum dose rate restrictions (800 MU/min), BOT inherently increases by 2.86 min and 1.66 min, on average, in *k*-Halcyon and *m*-Halcyon plans relative to *c*-Truebeam, respectively.

Table 5.4 Evaluation of plan delivery metrics for lung SBRT validation cases including original *c*-Truebeam plans.

Parameter	<i>k</i> -Halcyon	<i>m</i> -Halcyon	<i>c</i> -Truebeam	<i>k</i> -Halcyon vs. <i>m</i> -Halcyon	<i>k</i> -Halcyon vs. <i>c</i> -Truebeam	<i>m</i> -Halcyon vs. <i>c</i> -Truebeam
Total MU	4076 ± 608	3126 ± 745	3137 ± 873	p < 0.001	p < 0.001	p = n. s.
MF	4.08 ± 0.6	3.12 ± 0.7	3.14 ± 0.9	p < 0.001	p < 0.001	p = n. s.
BOT (min)	5.10 ± 0.8	3.90 ± 0.9	2.24 ± 0.6	p < 0.001	p < 0.001	p < 0.001
MC 2 nd check results (%)	98.6 ± 1.9	99.9 ± 2.4	98.4 ± 2.0	p = n. s.	p = n. s.	p = 0.03

5.3.4 Left Upper Lobe Example Case

Figure 5.4 presents an example patient with a left upper lobe lesion with the typical findings. The cumulative dose-volume histogram and corresponding 3-plane view through the isocenter are presented for each plan. As shown in the DVH, the *k*-Halcyon plan (triangle) is able to escalate the GTV minimum dose when compared to both *m*-Halcyon (circles) and *c*-Truebeam (squares). In this case, relative to *c*-Truebeam, GTV minimum dose was escalated by 4.6 Gy with minimal to no additional cost to OAR sparing. For example, the esophagus (blue) is the most proximal OAR to the target.

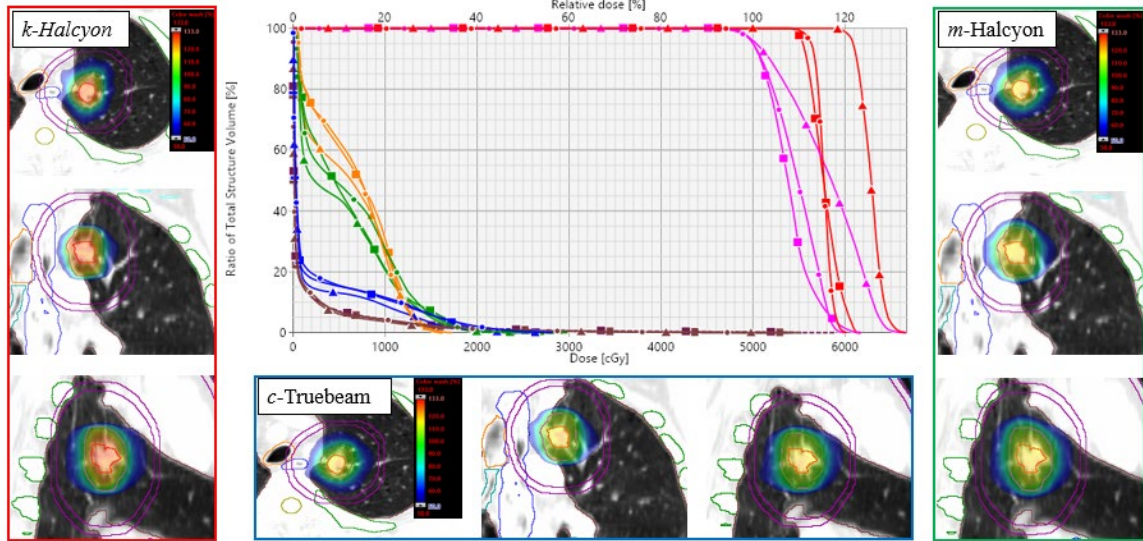


Figure 5.4 Cumulative dose-volume histogram and corresponding 3-plane view for an example LUL patient.

Cumulative dose-volume histogram and corresponding 3-views for an example LUL patient are presented. The cumulative DVH displays selected OAR and targets that include: GTV (red), PTV (pink), trachea (orange), ribs (green), esophagus (blue) and lungs-PTV (brown) for the *k*-Halcyon (triangles), *m*-Halcyon (circles) and *c*-Truebeam plan (squares). In this case, the *k*-Halcyon plan was able to significantly increase GTV dose while maintaining similar or better OAR sparing with similar intermediate dose spillage relative to both *m*-Halcyon and *c*-Truebeam plan.

The *k*-Halcyon plan provided at least 1.3 Gy lower maximal esophageal dose compared to the *c*-Truebeam plan. This dose sparing was accomplished in conjunction with a clinically significant GTV dose escalation. Similar intermediate dose spillage can be seen (Figure 5.4) for all three plans, with D2cm values reported to be 45% for both *k*-Halcyon and *m*-Halcyon plans compared to 46% in the *c*-Truebeam plan.

5.4 Discussion

This study appears to be the first to evaluate the use of a knowledge-based planning model for SBRT treatment of centrally located early-stage NSCLC patients using the ring-mounted coplanar Halcyon Linac. While manually generated lung SBRT plans on Halcyon were dosimetrically comparable to clinically treated plans on SBRT-dedicated Truebeam

Linac, the lung SBRT KBP model (originally trained and validated using non-coplanar Truebeam VMAT plans) was able to generate high-quality coplanar plans on Halcyon. This was accomplished with a much shorter treatment planning time and eliminated inter-planner variability. This KBP model offers a viable alternative to a SBRT-dedicated C-arm linac for selected lung SBRT patients. Additionally, dose to normal lung was significantly improved in *k*-Halcyon compared to both *m*-Halcyon and *c*-Truebeam plans.

A commercially available treatment planning system RayStation (RaySearch Laboratories, Stockholm, Sweden) offers a unique feature termed “fall-back (FB)” planning module for adaptive replanning.³⁸ This module enables generation of 3D-CRT, IMRT or VMAT plans based on reference plans for any treatment modality using a dose-mimicking algorithm with minimal planner time and effort. Recently, a few investigators have demonstrated that the FB planning module can convert Helical Tomotherapy plans to C-arm linac for various sites including conventionally fractionated treatment to brain tumors, head and neck, pelvis, prostate and lung tumors.^{34,35} It was reported that these FB plans were dosimetrically comparable to the original clinical plans and allowed for the fast and easy transfer of patients between treatment modalities during an unforeseen period of machine downtime.^{39,40} For instance, Yuan *et al.* showed that FB plans would typically be generated on average for 1 to 5 fractions of the conventionally fractionated treatment course in the event of machine breakdown.⁴⁰ Furthermore, their results suggested that an overall < 1% dose variation can be achieved on target coverage and dose to OAR on FB plans. These FB plans were typically generated in 10 to 20 min per case so that the patient can be treated on another machine. As of now, this feature is not available in Varian Eclipse. In the case of longer machine downtime, a full re-plan on another machine would

be required, resulting in significant treatment course delay. Our KBP model could emulate the ability of the RayStation FB planning module and enable our clinic to transfer lung SBRT patients between Halcyon and Truebeam Linacs (if required) by generating a similar quality plan in less than 30 minutes planning time. Furthering this thought, various treatment units in busy and larger clinics are often not beamed matched nor commissioned to golden beam data. Therefore, utilizing a KBP model would be vital to transferring these patients between the modalities the same or next day –reducing the chance of delaying the treatment course.

There are some limitations to this study and to the Halcyon Linac. An important limitation is that, at the time of this manuscript preparation, our clinic has treated a limited number of centrally located lung SBRT patients on Halcyon. In the future, as more lung SBRT patients are treated on Halcyon, it would be interesting and useful to include these patients in the training dataset to form a hybrid model with the clinical Truebeam SBRT plans. This may further improve the *k*-Halcyon’s model performance and may potentially create even higher-quality lung SBRT plans for prospective patients. Mechanically speaking, our Truebeam Linac is equipped with a perfect pitch couch with 6-degree of freedom (6DOF) couch corrections that allows for more accurate target localization compared to the Halcyon Linac. Additionally, for 6MV-FFF beam, the Truebeam Linac allows for a higher dose rate of maximum up to 1400 MU/min while the Halcyon maximum achievable dose rate of 800MU/min (increasing the beam-on time). This dose-rate discrepancy allows for treatments to not be clinically impractical as a 5-fraction treatment scheme required lower MU per fraction to be delivered the prescribed dose. Meaning, this added BOT can be offset with regard to overall treatment time using the Halcyon’s “one-

step patient set-up” capabilities as described above. However, as of now, Halcyon may not be suitable to treat lung SBRT patients with other commonly used extremely large fraction sizes (e.g., 54–60 Gy in 3 fractions or 30–34 Gy in 1 fraction) ⁴¹⁻⁴³ due to relatively longer treatment time. Future work will include investigating the feasibility of utilizing KBP models to generate lung SBRT plans with other fractionation schemes for both centrally and peripherally located lung tumors on Halcyon Linac.

5.5 Conclusion

This study reports on the plausibility of generating lung SBRT plans for centrally located early-stage NSCLC patients on ring-mounted Halcyon Linac using a previously trained and validated Truebeam KBP model. It has been demonstrated that the KBP model can be used to generate high-quality lung SBRT plans on the Halcyon Linac that are dosimetrically equivalent or better quality when compared to manually generated Halcyon and SBRT-dedicated Truebeam plans. This lung SBRT model is capable of quickly generating SBRT plans to support a curative SBRT program for centers by assuring that treatments are delivered in a safe and consistent manner potentially allowing for offline adaptive re-planning, if needed. Additionally, the results of this study indicate that KBP models can be cross-compatible between SBRT dedicated C-arm and O-ring linacs for lung SBRT. It is clinically useful to enable a clinic’s ability to facilitate a smooth transfer of patients between treatment machines as it will ensure minimal to no treatment course disruption. This model can be shared and may provide confidence in centers equipped solely with the Halcyon Linac in the treatment of lung SBRT in the future. It may also be a great option for diverse centers with a high SBRT volume, or for patients who require an immediate SBRT treatment.

Copyright © Justin David Visak 2021
<https://orcid.org/0000-0002-8674-5657>

CHAPTER 6. INNOVATIONS AND CLINICAL IMPACT

6.1 Chapter 2: Clinical Evaluation of Photon Optimizer (PO) MLC Algorithm for Stereotactic, Single-Dose of VMAT Lung SBRT

Chapter 2 explains the dosimetric evaluation of a newly configured PO-MLC positioning optimization algorithm in the Varian Eclipse TPS that is mandatory for generating RapidPlan models. All dosimetric comparisons were against its predecessor the PRO for two different calculation grid-size (CGS). **We hypothesized that the PO MLC algorithm would not clinically affect final plan quality but may be subject to more intermediate dose spillage.** The study found that the PO 1.25 mm CGS yielded acceptable plan quality compared to the PRO MLC algorithm. However, while minimally and not clinically relevant, a slight increase of intermediate dose-spillage was observed. For example, PO 1.25 mm CGS reported an average maximal dose 2 cm away from the target in any direction to be $50.03 \pm 6.94\%$ whereas the PRO 2.5 mm CGS reports $47.4 \pm 4.6\%$. The PO algorithm is currently used for all prospective lung SBRT patient's treatments in the clinic.

Clinical Innovation #1: PO-MLC algorithm can be used for RapidPlan modeling in Eclipse TPS.

Many of the previously treated lung SBRT patient's plans were optimized using the PRO algorithm which fundamentally functions differently than the PO-MLC algorithm. For the PO algorithm, the structures, dose-volume histogram calculations, and dose sampling are defined spatially using a single matrix over the image instead of a point-cloud model defining structures that was used in the PRO algorithm. This was of the great interest

to characterize as it was necessary to understand the benefits and limitations of the new PO algorithm for lung SBRT planning. Meaning, if the PO was underperforming compared to previously generated plans (with PRO algorithm) that needed to be taken in account in optimization and plan selection for prospective RapidPlan modeling to be successfully completed. The study indicated that the PO 1.25 mm CGS plans can be used for RapidPlan modeling.

6.2 Chapter 3: Development and Clinical Validation of a Robust KBP Model for SBRT of Centrally Located Lung Tumors

Chapter 3 describes the development and clinical validation of a robust knowledge-based planning model for SBRT treatments of centrally located lung tumors using a non-coplanar VMAT technique. The new KBP model was created using 86 previously treated lung SBRT training plans and validated with 20 independent plans. Additionally, it was further evaluated for its ability to improve clinical workflow and offline adaptive replanning capabilities by varying the CGS of the PO optimizer. **We hypothesized that this new KBP model would create high-quality lung SBRT plans faster, compliant with RTOG standards and would allow for slight dose escalation (50 to 55 Gy in 5 fractions) in tumors near adjacent OAR.** The results of this study show that KBPs were similar or better to manually generated clinical plans based on extensive target and dosimetric metrics in a shorter clinically relevant time. For instance, KBPs provided better normal lung sparing for an average minimum GTV dose increase of 1.1 Gy ($p = 0.05$).

Clinical Innovation #1: Significant reduction of ‘simulation-to-treatment’ start time from 7 to 3 working days.

The standard time it takes a patient to receive their initial CT simulation to the start time of their first treatment is approximately 7 working days using a manual planning process. This study reported that the average time it takes a fully dedicated, experienced SBRT planner to manually generate a high-quality lung SBRT plan is 129 minutes. However, in our clinic and others likewise, the majority of the planners (dosimetrists) are required to split their time between multiple patients’ plans and therefore are typically given at least 3 of those 7 working days to complete a lung SBRT plan. Patients who present for retreatment of same or adjacent treatment sites, difficult geometry (tumor size and location), or avoidance areas may require even more planning time. In addition to the superior plan quality, the KBP model generated in this study is the first to offer the significant reduction of the ‘simulation-to-treatment’ time down to 3 working days as it can generate a high-quality lung SBRT plan in under 30 minutes with minimal planner burden. Meaning, rather than meticulously adjusting constraints over multiple optimizations, a planner can now simply run the automatic optimization process and be confident in most cases that after one optimization the plan is ready for a physician’s evaluation. By quickening the planning process, this still allows for at least 2 working days for other required processes (e.g., contouring, plan review, approval and physics 2nd checks, and quality assurance check) to be performed under a reasonable timeline. Thus, offering optimal lung SBRT treatments to the patients in a timely manner. This will benefit a busy clinic and improve their capacity to safely treat more lung SBRT patients in the future.

Clinical Innovation #2: Enabled offline adaptive re-planning capabilities for lung SBRT.

Along with the development of a novel KBP model for lung SBRT of centrally located lesions, this study was also the first to evaluate the CGS effects in the context of KBP and offline adaptive re-planning. It was found that by increasing the CGS to 2.5 mm (in lieu of 1.25 mm CGS), minimal negative dosimetric impact occurred for faster plan generation time. On average, plans could be generated in under 5 minutes enabling the ability to perform same or next day of offline adaptive replanning, if needed. In select cases, offline adaptive replanning is warranted to account for patient weight loss, poor daily set-up, or tumor size shrinkage/expansion during the course of lung SBRT treatment. Without a KBP model, the standard ‘simulation to treatment’ time still applies and may negatively impact patient treatment.

6.3 Chapter 4: An Automated KBP Routine for SBRT of Peripheral Lung Tumors via DCA-Based VMAT

Chapter 4 discusses the development of a KBP routine for SBRT of peripherally located early-stage NSCLC tumors via dynamic conformal arc (DCA)-based VMAT. This routine required the development of a KBP model and was trained with 70 previously treated, high quality clinical plans and validated with another 20 independent clinical lung SBRT plans. **It was hypothesized that by incorporating traditional DCA-based dose before VMAT optimization, this hybrid KBP routine would help mitigate plan complexity and create high-quality VMAT lung SBRT plans in a clinically relevant shorter time to manual planning.** As with the centrally located KBP model, the results of this routine created plans of similar or better quality than clinically treated plans. Importantly, when compared to clinical plans, the KBPs that were not generated using the

proposed routine increased total MU on average by 1316 ($p < 0.001$) whereas when the routine was deployed total MU was on average decreased by 1114 MU in these plans—significantly improving plan complexity and delivery efficiency.

Clinical Innovation #1: Development of a novel automated planning routine for peripheral lung SBRT.

An automated planning routine was developed that couples the benefits of a traditional DCA-based dose technique with an automated modern knowledge-based VMAT optimization engine with minimal deviation from traditional planning workflow. To begin, dynamic conformal arcs and collimator angles are first manually selected by the planner. An MLC is then added to each arc and fit with a 2 mm margin around the PTV. A new MLC aperture shaper controller (ACS) found in the most recent PO-MLC algorithm is then adjusted from its default setting of ‘low’ to ‘very high’ strength and a 3D-DCA-based dose is calculated. If necessary, field weights are adjusted to give a practical starting point for future KBP-VMAT optimization. Once the base dose is adjusted (if necessary), the VMAT optimization window is launched and the DVH-estimations starts with objectives and associated priorities as previously created by the KBP model. This proposed method can easily be adopted by any planner and could enhance the final plan quality with less burden than manual planning, by generating lung SBRT plans faster enabling the potential of offline adaptive replanning.

Clinical Innovation #2: Reduction of plan complexity associated with lung SBRT KBP model due to the DCA-based VMAT routine.

As indicated by the previously generated model, KBP in the context of lung SBRT planning has the tendency to increase total MU and increase overall plan complexity. This may lead to unintended treatment delivery errors such as the interplay effect or small field dosimetry errors. Conversely, initial planning approach via DCA-based dose significantly reduces the total MU, improves treatment delivery confidence as it utilized larger MLC aperture openings and keeps the target in the open beamlets throughout the treatment duration. This proposed routine helps take advantage of the benefits of both KBP and more traditional techniques through its ability to lower overall plan complexity and improve treatment delivery accuracy. This will benefit the patient's treatment by improving safety, treatment accuracy and reduce the overall treatment time on the table.

6.4 Chapter 5: Fast Generation of Lung SBRT Plans with KBP model on O-ring

Halcyon Linac

Chapter 5 discusses the fast treatment planning feasibility of SBRT for centrally located lung tumors on the ring-mounted Halcyon Linac via a previously validated C-arm's KBP model. This novel KBP model was adapted from the model described in **Chapter 3** to optimally generate lung SBRT plans on Halcyon linac and was further validated with another set of 20 independent lung SBRT patient's plans. **We hypothesized that using the KBP model, prospective coplanar VMAT lung SBRT plans on the novel O-ring Halcyon linac will have similar or better-quality plans to SBRT-dedicated Truebeam plans.** The results of this study confirmed that when compared to manually generated Halcyon plans, the KBP model generated plans were similar or better quality when compared to the clinically treated plans on the C-arm Truebeam linac. Additionally, KBPs increased maximal target dose by 2.9 Gy ($p < 0.001$) while uniformly lowering normal

lung tissue dose compared to clinical plans indicating that coplanar restrictions on the Halcyon can be overcome while using the previously generated KBP model.

Clinical Innovation #1: KBP training data is cross-compatible between an SBRT-dedicated C-arm linac and a novel O-ring Halcyon linac.

There is no current literature available that describes training datasets and clinically validating a KBP model for lung SBRT with the Halcyon Linac. Meaning, being a new treatment platform, there is a lack of clinical training dataset used to develop a KBP model solely based on Halcyon treatments. Therefore, a KBP model originally built for non-coplanar VMAT treatments on a Truebeam linac was successfully adapted for use on the Halcyon linac. This model outperformed manually generated plans for the Halcyon linac and plan quality was similar or even better than corresponding clinical Truebeam plans. This is of great interest to many clinics that do not have training datasets available for multiple treatment machines but wish to deploy a KBP model across their clinic.

Clinical Innovation #2: KBP model could facilitate a smooth transfer of lung SBRT patients between two treatment platforms – potentially overcoming unanticipated longer machine downtime.

While in most cases the SBRT-dedicated Truebeam linac is the preferred treatment modality of the treating physicians, the results of this study suggest that the Halcyon is a viable alternative treatment option for selected lung SBRT patients. This is important as it enables a clinic to account for unintended longer machine downtime or relieve a single machine's burden in a busy SBRT clinic. By enabling both modalities for lung SBRT treatment options, this will lessen the chance of treatment course disruption. Moreover, in

these high-volume SBRT clinics, fast generation (< 30 min) of a KBP model could help distribute workload equally across machines allowing access to high-quality lung SBRT care to more patients, especially to those requiring immediate treatments. Moreover, for centers equipped solely with the Halcyon linac or are inexperienced planners in lung SBRT treatments, this model can be a tremendous help to increase their confidence in treatments.

Copyright © Justin David Visak 2021
<https://orcid.org/0000-0002-8674-5657>

CHAPTER 7. STUDY LIMITATIONS AND FUTURE RESEARCH DIRECTIONS

7.1 Study Limitations

There is full confidence that the KBP models created as part of this dissertation will produce high-quality, VMAT lung SBRT plans for prospective patients in a clinically shorter planning time than manually generated plans on both treatment platforms. However, each study presented in this dissertation is subject to some limitations that should be mentioned.

In **Chapter 2**, the PO-MLC algorithm was dosimetrically characterized and validated against its predecessor PRO algorithm. This dosimetric evaluation was exclusively compared for patients who received 30 Gy in 1 fraction in hopes of better highlighting any clear dosimetric deficiencies in the algorithm configuration. The major drawback of this method was there was limited patient datasets available for this dosing scheme. The single fraction SBRT is not the most common fractionation scheme used in our clinic; therefore, the study may not have enough power to meaningfully interpret the statistics presented. However, we believe that other treatment schemes for lung SBRT will have similar dosimetric characteristic of the PO-MLC algorithm, as demonstrated by satisfying all the RTOG compliance criteria with the KBPs.

Both **Chapters 3** and **4** developed and validated new KBP models for lung SBRT for either centrally or peripherally located tumors. In both cases, the development and characterization of the models were furthered whereas **Chapter 3** investigated CGS effects with KBP modeling and **Chapter 4** proposes a routine to minimize plan complexity associated with KBP while using a DCA-based VMAT approach. Due to the similarities of these models, both studies demonstrated similar limitations and therefore will be

discussed concurrently. The most important limitation to each chapter is that some patients presented anatomical geometries that were simply too difficult for each KBP model to perfectly predict an optimal lung SBRT plan. While this is rarely the case, it does limit the full robustness of these models. There is minimal training data available for these exceptionally difficult cases, so a combination of knowledge-based and manual planning is recommended and feasible with the newly generated KBP models. In terms of model development, we are confident that we chose an appropriate amount of training datasets for each KBP model. However, due to limited available literature and resources (besides manufacture guidelines), it cannot be said for certain this was the exact number of treatment plans needed to ensure the highest performing model. A robust study slowly stepping the number of training plans is warranted. Another limitation to this work is if these KBP models are to be shared and adapted with other clinics; it will be necessary they have an identical or a newer version of our treatment planning system. This includes dose calculation algorithms, licensure for the commercialized knowledge-based planning software, and training for the planners. Although, an important thing to note is that most clinics operate on the same treatment planning system as the University of Kentucky Medical Center, therefore we anticipate only a few major institutions would not have the system requirements to adapt the lung SBRT models. Lastly, only the model described in **Chapter 3** has been deployed clinically for a few patients' treatments in our center. Therefore, the studies presented in these chapters do not include patient follow-up results for a comparison of the treatment outcomes corresponding to the lung SBRT treatments delivered by manually generated plans.

Chapter 5 describes the dosimetric evaluation of a KBP model that was adapted from the one presented in **Chapter 3**. Specifically, it sought to investigate if a KBP model can be utilized to generate prospective lung SBRT treatments on the new O-ring Halcyon Linac. While some limitations are common to the ones presented for **Chapters 3** and **4**, the change of modalities presents unique limitations to the study. As a recently installed new machine, the first limitation was the lack of training datasets available for lung SBRT treatments on Halcyon platform. As of now, minimal clinical data exist for lung SBRT on the Halcyon and this may ultimately affect the final model performance because the model is not learning what is feasible on Halcyon. Additionally, the Halcyon has two important system limitations compared to a SBRT-dedicated Truebeam linac that should be mentioned. Mechanically, the Halcyon's highest achievable dose rate is limited to 800 MU/min (compared to 1400 MU/min for 6MV-FFF Truebeam) and will significantly increase beam-on-time potentially decreasing the overall treatment delivery efficiency. This may affect more extreme hypofractionated treatment schemes rendering longer beam-on-times that may not be clinically optimal for treating lung SBRT patients on Halcyon. Additionally, target localization may be impacted relative to Truebeam treatments as the Halcyon is not equipped with a 6 degrees-of-freedom couch (6-DOF) yet. Rather, the Halcyon can only account for 3-degrees of translational corrections. While not always available on C-arm linacs, many physicians prefer the use of the 6-DOF couch corrections as it improves the target localization accuracy for lung SBRT.

7.2 Future Research Directions

This dissertation laid the fundamental groundwork for expanding a lung SBRT program in many different clinically relevant and important directions. The first and

foremost expansion of this dissertation is as these KBP models are deployed clinically, patient follow-up data should be recorded to evaluate the positive clinical impact of these KBP models. While it is not expected to observe a significant change, it is important to ensure that KBPs at least maintain or improves the local control observed in manual planning a lung SBRT treatment. However, any marginal increase of tumor local control or decrease in normal lung tissue toxicity (i.e., radiation induced pneumonitis) will have significant impact on patients' outcomes if they require radiation treatment in the future.

The next direction is to continue expanding KBP lung SBRT modeling for more robust uses in busy SBRT centers. This work solely encompasses single lesion modeling, but there is growing interest in the treatment of synchronous oligometastatic multi-lesion lung SBRT. Recently, many patients have received multi-lesion lung SBRT treatments at the University of Kentucky Medical Center.^{1,2} Therefore, utilizing the validated models as a baseline, it is possible to inject select multi-lesion lung SBRT plans into the training datasets in aim to generate a submodel. This should enhance the predicting power of a KBP model in a synchronous multi-lesion setting. This will ultimately increase the use of lung SBRT KBP in the clinic, for the fast, safe and effective treatment of synchronous lung lesions. The adapted model described in **Chapter 5** solely used a C-arm Truebeam Linac training dataset for prospective treatment planning on the Halcyon Linac. In future, as physicians treats more lung SBRT patients on Halcyon, clinical lung SBRT training datasets will slowly be accumulated and can be used for further KBP development. An interesting and relevant study related to this dissertation would be to use these newfound datasets for the creation and development of a sole Halcyon trained model. While potentially tedious, it would also be of great interest to slowly replace the C-arm training

datasets in the currently developed model with new clinical plans treated on the Halcyon. This should effectively characterize the cross-compatibility of the training data between Halcyon and Truebeam linacs. Meaning, as training plans were replaced, an observation can be made of the dosimetric impacts between prospectively generated Halcyon and Truebeam lung SBRT plans.

Along with different modality and multi-lesion data becoming available, there is also more data available for patients treated at 30 Gy in 1 fraction than at the start of this dissertation. If the single treatment planning datasets were utilized for a sub-model generation from the KBP model described in **Chapter 4**, perhaps it could then be used to cover multiple prescriptions (depending on tumor size and geographical location). Moreover, the proposed DCA-based VMAT planning routine can be deployed to see the dosimetric advantages between manually generated clinical plans and the new DCA-KBP plans for single-dose of lung SBRT treatments. The most interesting expansion of this dissertation will be the adaptation and further development of a model designed to treat large lung tumors (>5 cm in diameter) with a simultaneous integrated boost (SIB) technique –potentially escalating higher dose to the hypoxic tumor core. Traditionally, lung SBRT is limited to tumors less than 5 cm, as anything larger presents difficulty in dose escalation because of normal tissue toxicity considerations. However, if the dose can be escalated via a KBP-SIB approach (i.e., 60 Gy to GTV and 50 Gy to PTV in 5 fractions) while respecting dose tolerances to the adjacent OAR, these concerns can be partially mitigated and curative SBRT treatments can be offered to this patient cohort. At the University of Kentucky Medical Center, a few patients have been manually planned and treated using this proposed approach, with clinical follow-up results actively being accrued. It is very difficult to

manually generate these lung SBRT plans, however, it may be significantly easier to plan with a combination of manual and KBP approaches. A full hybrid approach should be developed to assist in managing these difficult and complex patients.

In addition to expanding lung KBP modeling capabilities, the proposed routine in **Chapter 4** can be expanded in the future to support full automation of the entire treatment planning process. As of now, the routine only partially automates the lung SBRT planning process during the inverse optimization phase. To improve the overall planning time, the first step can be to incorporate an atlas-based auto-contouring feature of select OAR. Many structures (e.g., heart, spinal cord, total lung) do not heavily deviate between patients, yet require slice by slice delineation by the planner or the treating physician. This would significantly further shorten ‘simulation-to-treatment’ time and may only require physician intervention to contour the target structures. After contouring is done, a fully automated script can be written that will automatically deploy the isocenter location to the target center and auto-deploy beams/arc geometry from a template on a per-patient basis. In many cases, arc geometry and collimator angles are similar and therefore can become an automated process with the option of manual tweaking. Additionally, the DVH-estimation can be generated automatically with scripting and a fixed number of optimizations can be set for generating optimal lung SBRT plans. This will significantly reduce a planner’s burden, standardize the treatment geometry, and allow for increased confidence in treatments as the total number of optimizations is controlled. Paired with fully automating a treatment planning routine or a sole KBP model, a full plan evaluation and integration of an offline adaptive replanning process merits future investigation. Offline adaptive replanning is a condensed conventional planning workflow designed to address the gradual

changes of patient's treatment throughout the treatment course. There are many uncertainties and questions that need to be answered before fully implementing offline adaptive replanning in the clinic. This includes developing recommendations as to how often and when to make the decision to adapt and re-plan the treatment course. For instance, it should be decided what criteria of changes should trigger a re-plan (e.g., tumor size change, patient weight change, automatically after a certain number of fractions or difficulty in reproducing patient set up). Additionally, a complete study characterizing the clinical benefits of replanning the patient's treatment is required. When this information is gathered and analyzed, the proposed routine should be deployed on a limited basis with patient follow-up data ascertained.

In line with exploring the benefits of KBP for lung SBRT treatments via offline adaptive replanning, beyond this dissertation a study should be completed to explore the quality assurance (QA) benefits of a KBP model. For example, a lung SBRT KBP can be used for prospective patient-specific QA checks. Since a KBP model is derived from historical high-quality planning datasets, all prospective manually planned treatments should fall into some margin of agreement with a KBP DVH estimate. It would be necessary to define these cut-off values (e.g., total MU tolerance, OAR dose limits, plan complexity) to help maintain generating consistent plan quality and to further reduce inter-planner variability for manual planning (if needed). Lastly, developing and validating these KBP models for lung SBRT treatments as part of this dissertation serves as the basis for the transition of modern-day automated treatment planning. In the near future, multi-criteria optimization (MCO) will be utilized by planners to generate hundreds of plans at a time based on a clinical model library.⁴ In this dissertation, the KBP models produced are

only capable of generating only one plan at a time for a physician's review. However, when MCO becomes widely available clinically, multiple plans will now be able to be adapted in real-time to better suit the patient and physician's needs. For example, a slider bar window would be available to adjust the dose to an OAR or for the better target coverage on-the-fly rather than requiring another full optimization series which may delay the patient's treatment. In summary, developing and further validating KBP models for lung SBRT treatments as part of this dissertation successfully laid the groundwork for important and interesting future research endeavors. These potential routes will better serve complex patients, optimize clinic workflow, and provide important information to the greater medical physics community for the highest quality of patient care.

Copyright © Justin David Visak 2021
<https://orcid.org/0000-0002-8674-5657>

CHAPTER 8. CLOSING ARGUMENTS

The research presented in this dissertation describes the generation of novel KBP models for SBRT treatments of both centrally and peripherally located tumor locations using a non-coplanar VMAT geometry. These models also support treatments with a traditional C-arm linac and a newly installed O-ring Halcyon Linac; ultimately expanding a robust lung SBRT program at the University of Kentucky Medical Center. One of the parallel goals with model development was to eliminate the issues associated with manually planning and condense the current lung SBRT clinical workflow to support a timelier treatment manner. These models, in many cases, enhance tumor core dose with no additional cost to adjacent critical structures sparing. Meaning, they are able to generate plans with excellent quality relative to clinically treated plans. The models described in this dissertation eliminate inter-planner variability by standardizing a clinic's thoracic lung SBRT program, thus increasing patient safety. Moreover, by generating these high-quality plans, a clinic's workload capacity can be increased to provide the highest quality of care to more patients in the future. This is accomplished by using the KBP models generated in this dissertation to shorten the overall 'simulation-to-treatment' time to as few as 3 working days from traditional 7 days. In select cases, these KBP models may help condense this time down even quicker to support offline adaptive replanning that allows a clinician to account for physiological changes in a patient during the course of treatment. Overall, this dissertation enables standardization of a lung SBRT program and provides a basic modeling framework for other clinics (as well as other disease sites) to emulate or simply adapt these sharable lung SBRT models. With fast generation of KBPs (< 30 min), the model has the potential to transfer lung SBRT patients to the O-ring Halcyon to account

for unforeseen longer machine downtime and complete the patient's treatment course in a timely manner. The tools and techniques developed in this dissertation may potentially help inexperienced or busy centers provide more high-quality patient care to select prospective early-stage NSCLC patients who require SBRT treatments in a timely manner.

Copyright © Justin David Visak 2021
<https://orcid.org/0000-0002-8674-5657>

APPENDICES

APPENDIX 1. GLOSSARY

Glossary of Common Terms. A list of common acronyms used throughout this dissertation with corresponding definitions is presented.

3DCRT	3-Dimensional Conformal Radiation Therapy
6DOF	6 Degrees of Freedom
AAA	Analytical Anisotropic Algorithm
BOT	Beam-on-Time
c-Truebeam	Clinical Truebeam VMAT Lung SBRT Plan
CGS	Calculation Grid Size
CI	Conformity Index
CT	Computed Tomography
DCA	Dynamic Conformal Arcs
DLO	Dose Limiting Organs
DVH	Dose Volume Histogram
ESAPI	Eclipse Scripting Application Programming Interface
FFF	Flattening Filter Free
GD	Gradient Distance
GED	Geometry Expected Dose
GI	Gradient Index
GTV	Gross Tumor Volume
GY	Gray
HI	Heterogeneity Index
iCBCT	Iterative Cone-Beam Computed Tomography
IMRT	Intensity Modulated Radiation Therapy
IRB	Institutional Review Board
ITV	Internal Target Volume
k-DCA	DCA-Based VMAT Lung SBRT Plan
k-Halcyon	Knowledge-Based Optimized Halcyon Lung SBRT Plan
KBP	Knowledge-Based Planning/Plan
LINAC	Linear Accelerator
LLL	Left Lower Lobe
LUL	Left Upper Lobe
m-Halcyon	Manually Optimized Halcyon Lung SBRT Plan
MF	Modulation Factor
MIP	Maximum Intensity Projection

MLC	Multi-Leaf Collimator
MLD	Mean Lung Dose
MU	Monitor Units
n-VMAT	Clinical Truebeam VMAT Lung SBRT Plan
NSCLC	Non-Small-Cell-Lung-Cancer
OAR	Organs at Risk
PCA	Principal Component Analysis
PCS	Principal Component Score
PO	Photon Optimizer
PO-VMAT	Photon Optimizer Lung SBRT Plan
PRO	Progressive Resolution Optimizer
PRO-VMAT	Progressive Resolution Optimizer Lung SBRT Plan
PTV	Planning Target Volume
QA	Quality Assurance
RLL	Right Lower Lobe
RTOG	Radiation Therapy Oncology Group
RUL	Right Upper Lobe
SBRT	Stereotactic Body Radiation Therapy
SRS	Stereotactic Radiosurgery
STD	Standard Deviation
TPS	Treatment Planning system
VMAT	Volumetric Modulated Arc Therapy

Plan Selection and Matching Window: This diagram provides a summary to the user of which plans were added to the model via External Beam Planning. Additionally, the user may choose which structures contoured on the original clinical plan will be included in the model initially and after outlier verification.

Plans of the DVH Estimation Model							Number of Plans: 86	?
#	Patient ID/Course ID/Plan ID	Plan Prescription	Structure Matching	Include	Extracted	In Model		
18		5000.0 cGy	Target: 2/2 Other: 10/10	<input checked="" type="checkbox"/>	Yes	15.6.06	X	
19		5000.0 cGy	Target: 2/2 Other: 9/10	<input checked="" type="checkbox"/>	Yes	15.6.06	X	
20		5500.0 cGy	Target: 2/2 Other: 9/10	<input checked="" type="checkbox"/>	Yes	15.6.06	X	
21		5000.0 cGy	Target: 2/2 Other: 9/10	<input checked="" type="checkbox"/>	Yes	15.6.06	X	
22		5000.0 cGy	Target: 2/2 Other: 9/10	<input checked="" type="checkbox"/>	Yes	15.6.06	X	
23		5500.0 cGy	Target: 2/2 Other: 10/10	<input checked="" type="checkbox"/>	Yes	15.6.06	X	
24		5000.0 cGy	Target: 2/2 Other: 9/10	<input checked="" type="checkbox"/>	Yes	15.6.06	X	
25		5000.0 cGy	Target: 2/2 Other: 9/10	<input checked="" type="checkbox"/>	Yes	15.6.06	X	
26		5000.0 cGy	Target: 2/2 Other: 9/10	<input checked="" type="checkbox"/>	Yes	15.6.06	X	
27		5000.0 cGy	Target: 2/2 Other: 8/10	<input checked="" type="checkbox"/>	Yes	15.6.06	X	
28		5000.0 cGy	Target: 2/2 Other: 9/10	<input checked="" type="checkbox"/>	Yes	15.6.06	X	

Summary of Training Results Tab: The model reports the overall fitting statistics for each trained structure set. This includes the number of structures that reported an in-field volume along with the corresponding potential plan outlier number.

Model: Summary of training results							?
Structure	Trained	R ²	χ ²	Matched	In-field	Outliers	
Brachial Plexus	Yes	0.000	0.000	24	13	0	
Bronchial Tree	Yes	0.956	1.005	79	66	47	
Cord	Yes	0.880	1.025	82	81	6	
D2cm	Yes	0.860	1.059	71	71	11	
Esophagus	Yes	0.892	1.012	81	81	6	
GTV	N/A			82			
Heart	Yes	0.934	1.017	82	75	3	
Lungs	Yes	0.955	1.024	88	88	10	
PTV	N/A			82			
Ribs	Yes	0.933	1.020	81	81	49	
Skin	Yes	0.949	1.000	82	82	9	
Trachea	Yes	0.962	1.018	81	43	6	

Summary of Outlier Statistics Tab: The DVH algorithm flags what it interprets to be the largest outlier plans with the corresponding statistics (most critical in red). The user should manually review these recommendations and conclude whether or not it is a true outlier.

Model: Summary of outlier statistics

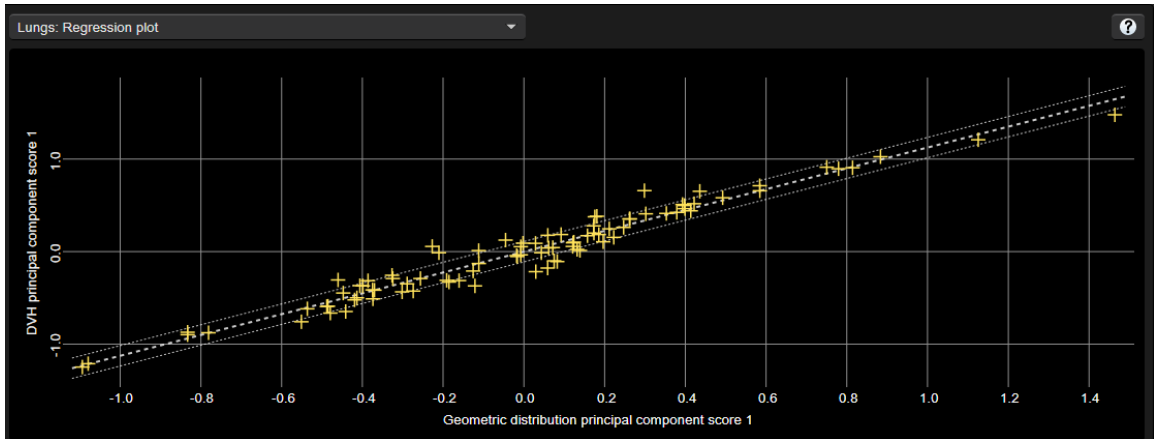
Plan #	Brachial Pl...	Bronchial...	Cord	D2cm	Esophagus	Heart	Lungs	Ribs	Skin	Trachea
38		3.007	2.612	1.369	1.692	2.695	2.136	7.290	1.601	2.213
20		3.642	2.167	1.802	2.107	2.035	7.203	2.035	2.078	2.596
16		6.901	1.605	2.177	1.430	0.815	1.044	0.971	2.430	2.681
82			1.753		5.655	5.716	3.798	1.553	2.147	2.684
55	1	1.061	1.041	1.191	1.075	0.999	1.051	5.673	0.987	1.064
57		4.437	2.762	1.896	1.754	1.861	1.856	1.692	1.729	1.903
59	0.662922	1.192	1.657		1.233	1.220	1.313	4.411	2.824	1.302
74		1.988	4.319	1.493	1.473	0.946	1.126	1.834	3.705	1.835
36		4.107	3.322	0.783	2.592	2.449	0.707	2.335	3.079	3.078
70			1.417	1.028	1.470	1.566	0.920	3.908	1.515	2.684
79		1.213	2.325	0.661	1.192	1.876	2.242	3.676	3.082	2.178
35	1.21475	3.494	1.035	0.497	1.554	1.908	1.058	3.185	1.590	1.566

APPENDIX 3. EXAMPLE PLOTS AND STATISTICS

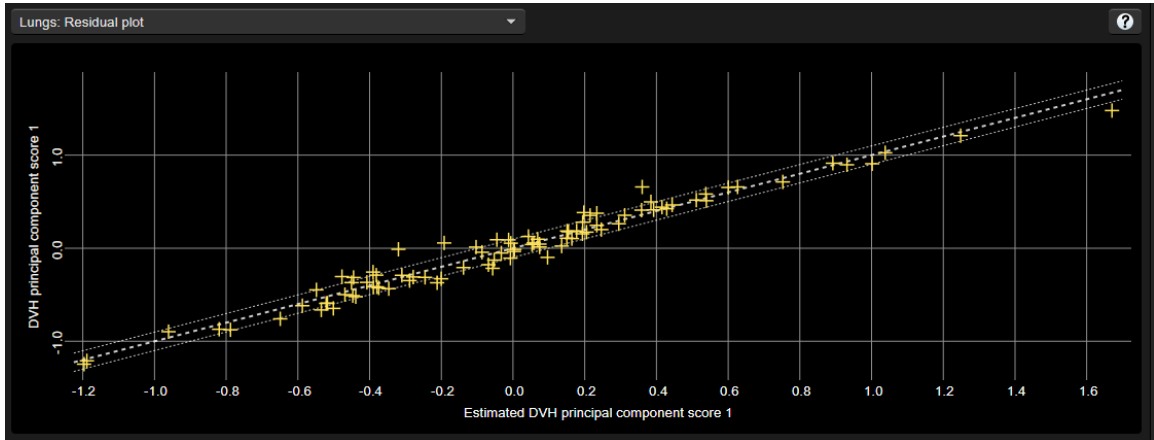
Geometric Plot for Normal Lung Structure: The geometric plot displays the distribution of all relevant statistics and volumes for the user to review. The primary purpose of this part of the process is to identify the geometric outliers. In statistically perfect model, all data points ideally would fall within the 10 and 90 percentile distribution. However, in practice this is not clinically feasible.



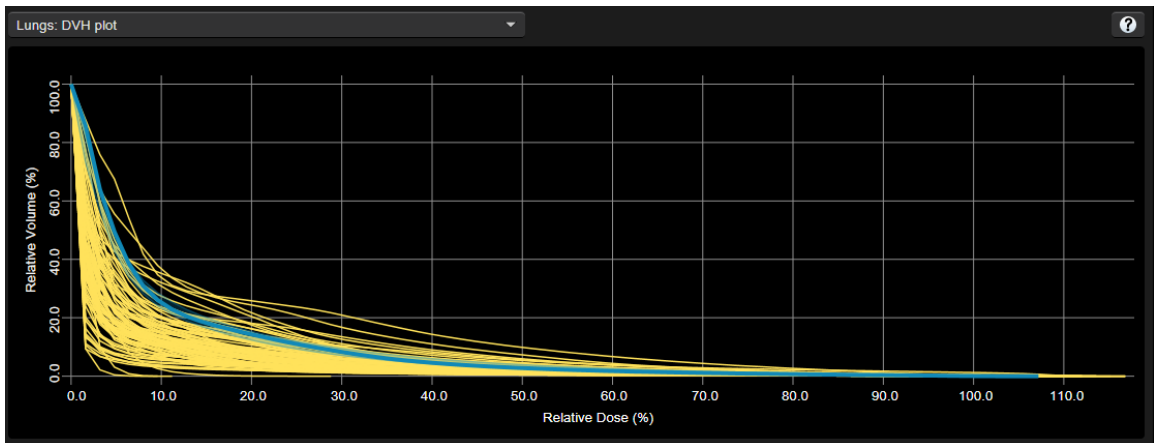
Regression Plot for Normal Lung Structure: The regression plot for a selected structure is shown below that provides correlation between the first DVH PCS and geometric PCS. In practice, all data points should fall within a reasonable margin of the standard deviation line and should mostly remain relatively grouped along the X-axis. This is a powerful tool to identify geometric outliers as well.



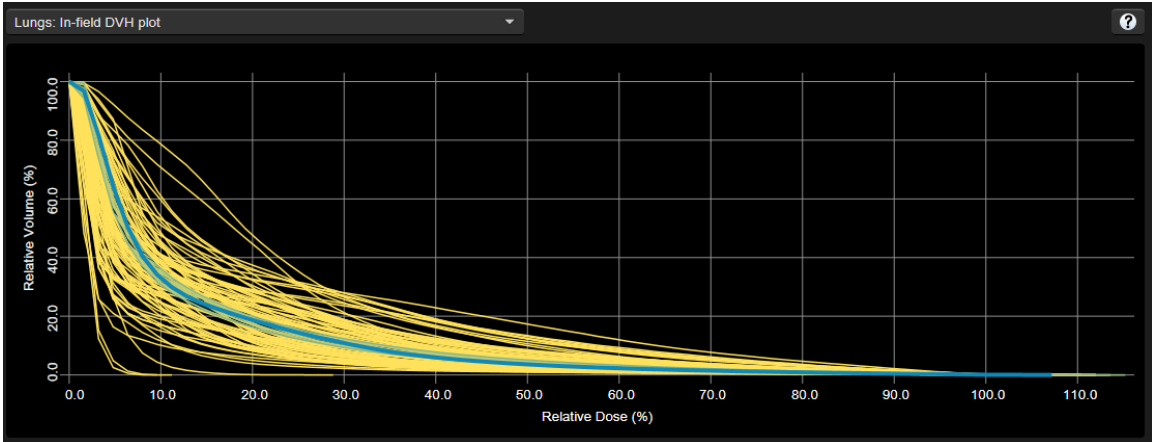
Residual Plot for Normal Lung Structure: The residual plot shown below is an important tool for not only identifying dosimetric outliers, but to also evaluate how well the DVH estimate is representing the actual training datasets. Meaning, similar to the geometric plot, a perfect model all data points would fall exactly (or within a STD) of the regression line.



Dose Volume Histograms for Normal Lung Structure: All DVHs for all plans that are included in the model are presented to the user (**Chapter 4** model). As stated by the vendor, the primary purpose of this window is to ensure there are no incorrect structure matches and all DVHs mostly are similar.



In-Field Region Dose Volume Histograms for Normal Lung Structure: The DVHs for in-field regions of all plans corresponding to that structure are presented to the user (Chapter 4 model). When selected, a plan will display its predicted DVH band and the actual plot should fall somewhere within that band. This provides confidence to the user the model is performing optimally.

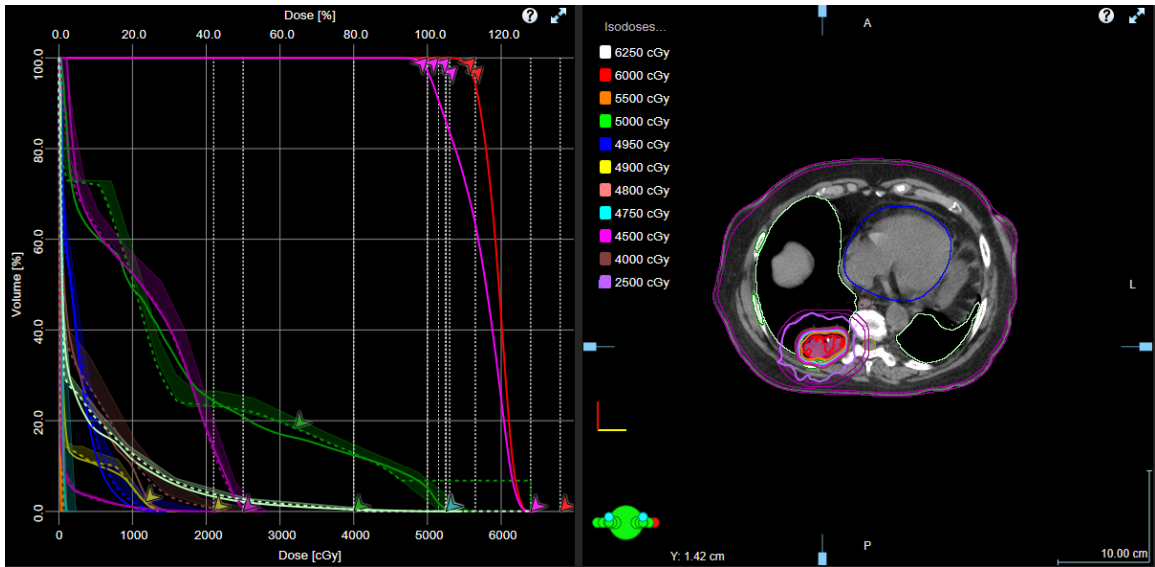


Summary of Outlier Statistics for Normal Lung Structure: The DVH estimation will provide important fitting statistics to help the user gauge and remove potential dosimetric and geometric outliers. Per vendor information, the following statistics and corresponding definitions are presented. Cook’s distance (CD) represents which plans are most influencing a model’s performance (shown in red). Modified Z-score (mZ) measured the difference of an individual structure from the training sample’s median value. The student residual (SR) correlates effectively the absolute difference between the original data and the estimated data using only the in-field DVH estimates. Lastly, the areal difference of estimate (dA) measures the difference between the original and reconstructed data, meaning, how much area remains between predicted and actual DVH normalized by a STD. Essentially, it is similar to the SR, but it considers the entire structure DVH.

Plan #	Structure	CD	SR	mZ	dA
4	Lungs-PTV	11.119	1.716	2.764	1.528
15	Lungs-PTV	7.825	1.594	2.395	1.594
51	Lungs-PTV	3.652	0.429	5.090	0.953
41	Lungs-PTV	3.169	2.257	2.586	2.230
62	Lungs-PTV	2.211	1.241	0.982	0.959
1	Lungs-PTV	2.014	1.405	1.014	1.030
18	Lungs-PTV	1.996	1.346	2.081	1.094
9	Lungs-PTV	1.771	2.319	1.986	2.489
52	Lungs-PTV	1.666	2.310	3.834	1.790

APPENDIX 4 EXAMPLE PATIENT WITH DVH AND ESTIMATION

Example KBP Optimization DVH and Axial View: Target (red = GTV, pink = PTV) and select OAR (green = ribs, purple = D2cm+5mm, light green = lungs-PTV, yellow = cord, blue = heart) with their actual DVH and predicted STD (including automatically generated optimization objectives) are shown. For most patients, the OAR DVH should fall somewhere within the predicted DVH estimation band (see bottom left of the DVHs).



REFERENCES

CHAPTER 1

1. American Cancer Society. Key Statistics for Lung Cancer. 2020:1-15.
2. Detterbeck FC. The eighth edition TNM stage classification for lung cancer: What does it mean on main street? *J Thorac Cardiovasc Surg.* 2018;155(1):356-359.
3. Hirsch FR, Scagliotti GV, Mulshine JL, et al. Lung cancer: current therapies and new targeted treatments. *Lancet.* 2017;389(10066):299-311.
4. Timmerman R, Paulus R, Galvin J, et al. Stereotactic body radiation therapy for inoperable early-stage lung cancer. *Jama.* 2010;303(11):1070-1076.
5. McDonald F, De Waele M, Hendriks LE, Faivre-Finn C, Dingemans AC, Van Schil PE. Management of stage I and II non-small cell lung cancer. *Eur Respir J.* 2017;49(1).
6. Grills IS, Yan D, Martinez AA, Vicini FA, Wong JW, Kestin LL. Potential for reduced toxicity and dose escalation in the treatment of inoperable non-small-cell lung cancer: a comparison of intensity-modulated radiation therapy (IMRT), 3D conformal radiation, and elective nodal irradiation. *Int J Radiat Oncol Biol Phys.* 2003;57(3):875-890.
7. Donington JS, Kim YT, Tong B, et al. Progress in the Management of Early-Stage Non-Small Cell Lung Cancer in 2017. *J Thorac Oncol.* 2018;13(6):767-778.
8. Navarra P, Ascolese AM, Mancosu P, et al. Volumetric modulated arc therapy with flattening filter free (FFF) beams for stereotactic body radiation therapy (SBRT) in patients with medically inoperable early-stage non-small cell lung cancer (NSCLC). *Radiother Oncol.* 2013;107(3):414-418.
9. Jeppesen SS, Schytte T, Jensen HR, Brink C, Hansen O. Stereotactic body radiation therapy versus conventional radiation therapy in patients with early stage non-small cell lung cancer: an updated retrospective study on local failure and survival rates. *Acta Oncol.* 2013;52(7):1552-1558.
10. Wu A. Physics and Dosimetry of the Gamma Knife. *Neurosurgery Clinics of North America.* 1992;3(1):35-50.
11. Lax I, Blomgren H, Näslund I, Svanström R. Stereotactic radiotherapy of malignancies in the abdomen. Methodological aspects. *Acta Oncol.* 1994;33(6):677-683.
12. Blomgren H, Lax I, Göranson H, et al. Radiosurgery for Tumors in the Body: Clinical Experience Using a New Method. *Journal of Radiosurgery.* 1998;1(1):63-74.
13. Blomgren H, Lax I, Näslund I, Svanström R. Stereotactic high dose fraction radiation therapy of extracranial tumors using an accelerator. Clinical experience of the first thirty-one patients. *Acta Oncol.* 1995;34(6):861-870.

14. Timmerman R, Papiez L, McGarry R, et al. Extracranial stereotactic radioablation: results of a phase I study in medically inoperable stage I non-small cell lung cancer. *Chest*. 2003;124(5):1946-1955.
15. Timmerman RD, Hu C, Michalski J, et al. Long-term Results of RTOG 0236: A Phase II Trial of Stereotactic Body Radiation Therapy (SBRT) in the Treatment of Patients with Medically Inoperable Stage I Non-Small Cell Lung Cancer. *International Journal of Radiation Oncology, Biology, Physics*. 2014;90(1).
16. Onishi H, Shirato H, Nagata Y, et al. Stereotactic body radiotherapy (SBRT) for operable stage I non-small-cell lung cancer: can SBRT be comparable to surgery? *Int J Radiat Oncol Biol Phys*. 2011;81(5):1352-1358.
17. Fakiris AJ, McGarry RC, Yiannoutsos CT, et al. Stereotactic body radiation therapy for early-stage non-small-cell lung carcinoma: four-year results of a prospective phase II study. *International Journal of Radiation Oncology* Biology* Physics*. 2009;75(3):677-682.
18. Timmerman R, McGarry R, Yiannoutsos C, et al. Excessive toxicity when treating central tumors in a phase II study of stereotactic body radiation therapy for medically inoperable early-stage lung cancer. *Journal of clinical oncology*. 2006;24(30):4833-4839.
19. McGarry RC, Song G, des Rosiers P, Timmerman R. Observation-only management of early stage, medically inoperable lung cancer: poor outcome. *Chest*. 2002;121(4):1155-1158.
20. Moghanaki D, Hagan M. Strategic Initiatives for Veterans with Lung Cancer. *Fed Pract*. 2020;37(Suppl 4):76-S80.
21. RTOG 0618. A Phase II Trial of Stereotactic Body Radiation Therapy (SBRT) in the Treatment of Patients with Operable Stage I/II Non-Small Cell Lung Cancer. 2007.
22. Bezjak A, Papiez L, Bradley J, et al. Radiation Therapy Oncology Group RTOG 0813 seamless Phase I/II study of stereotactic lung radiotherapy (SBRT) For early stage, centrally located, non-small cell lung cancer (NSCLC) in medically inoperable patients. Update. 2009.
23. Videtic GM, Hu C, Singh AK, et al. A randomized phase 2 study comparing 2 stereotactic body radiation therapy schedules for medically inoperable patients with stage I peripheral non-small cell lung cancer: NRG Oncology RTOG 0915 (NCCTG N0927). *International Journal of Radiation Oncology Biology Physics*. 2015;93(4):757-764.
24. Pokhrel D, Sanford L, Dhanireddy B, Molloy J, Randall M, McGarry RC. Flattening filter free VMAT for a stereotactic, single-dose of 30 Gy to lung lesion in a 15-min treatment slot. *J Appl Clin Med Phys*. 2020.
25. Videtic GM, Stephans KL, Woody NM, et al. 30 Gy or 34 Gy? Comparing 2 single-fraction SBRT dose schedules for stage I medically inoperable non-small cell lung cancer. *Int J Radiat Oncol Biol Phys*. 2014;90(1):203-208.
26. Benedict SH, Yenice KM, Followill D, et al. Stereotactic body radiation therapy: the report of AAPM Task Group 101. *Med Phys*. 2010;37(8):4078-4101.

27. Pokhrel D, Halfman M, Sanford L. A simple, yet novel hybrid-dynamic conformal arc therapy planning via flattening filter-free beam for lung stereotactic body radiotherapy. *J Appl Clin Med Phys*. 2020;21(6):83-92.
28. Das IJ, Ding GX, Ahnesjo A. Small fields: nonequilibrium radiation dosimetry. *Med Phys*. 2008;35(1):206-215.
29. Cai J, Malhotra HK, Orton CG. Point/Counterpoint. A 3D-conformal technique is better than IMRT or VMAT for lung SBRT. *Med Phys*. 2014;41(4).
30. Ong CL, Verbakel WF, Cuijpers JP, Slotman BJ, Lagerwaard FJ, Senan S. Stereotactic radiotherapy for peripheral lung tumors: a comparison of volumetric modulated arc therapy with 3 other delivery techniques. *Radiother Oncol*. 2010;97(3):437-442.
31. Merrow CE, Wang IZ, Podgorsak MB. A dosimetric evaluation of VMAT for the treatment of non-small cell lung cancer. *J Appl Clin Med Phys*. 2012;14(1)
32. Vanderstraeten B, Goddeeris B, Vandecasteele K, van Eijkeren M, De Wagter C, Lievens Y. Automated Instead of Manual Treatment Planning? A Plan Comparison Based on Dose-Volume Statistics and Clinical Preference. *Int J Radiat Oncol Biol Phys*. 2018;102(2):443-450.
33. Fogliata A, Reggiori G, Stravato A, et al. RapidPlan head and neck model: the objectives and possible clinical benefit. *Radiat Oncol*. 2017;12(1):73.
34. Wang J, Hu W, Yang Z, et al. Is it possible for knowledge-based planning to improve intensity modulated radiation therapy plan quality for planners with different planning experiences in left-sided breast cancer patients? *Radiat Oncol*. 2017;12(1):85.
35. Li N, Carmona R, Sirak I, et al. Highly Efficient Training, Refinement, and Validation of a Knowledge-based Planning Quality-Control System for Radiation Therapy Clinical Trials. *Int J Radiat Oncol Biol Phys*. 2017;97(1):164-172.
36. Fogliata A, Belosi F, Clivio A, et al. On the pre-clinical validation of a commercial model-based optimisation engine: application to volumetric modulated arc therapy for patients with lung or prostate cancer. *Radiother Oncol*. 2014;113(3):385-391.
37. Liu X, Liang Y, Zhu J, et al. A Fast Online Replanning Algorithm Based on Intensity Field Projection for Adaptive Radiotherapy. *Front Oncol*. 2020.
38. Peng C, Chen G, Ahunbay E, Wang D, Lawton C, Li XA. Validation of an online replanning technique for prostate adaptive radiotherapy. *Physics in Medicine and Biology*. 2011;56(12):3659-3668.
39. Fogliata A, Nicolini G, Clivio A, et al. A broad scope knowledge based model for optimization of VMAT in esophageal cancer: validation and assessment of plan quality among different treatment centers. *Radiat Oncol*. 2015;10:220.
40. Chanyavanich V, Das SK, Lee WR, Lo JY. Knowledge-based IMRT treatment planning for prostate cancer. *Med Phys*. 2011;38(5):2515-2522.

41. Moore KL, Brame RS, Low DA, Mutic S. Experience-based quality control of clinical intensity-modulated radiotherapy planning. *Int J Radiat Oncol Biol Phys.* 2011;81(2):545-551.
42. Chin Snyder K, Kim J, Reding A, et al. Development and evaluation of a clinical model for lung cancer patients using stereotactic body radiotherapy (SBRT) within a knowledge-based algorithm for treatment planning. *J Appl Clin Med Phys.* 2016;17(6):263-275.
43. Castriconi R, Fiorino C, Broggi S, et al. Comprehensive Intra-Institution stepping validation of knowledge-based models for automatic plan optimization. *Phys Med.* 2019;57:231-237.
44. Krayenbuehl J, Zamburlini M, Ghandour S, et al. Planning comparison of five automated treatment planning solutions for locally advanced head and neck cancer. *Radiat Oncol.* 2018;13(1):170.
45. Nelms BE, Robinson G, Markham J, et al. Variation in external beam treatment plan quality: An inter-institutional study of planners and planning systems. *Practical Radiation Oncology.* 2012;2(4):296-305.
46. Wu H, Jiang F, Yue H, Li S, Zhang Y. A dosimetric evaluation of knowledge-based VMAT planning with simultaneous integrated boosting for rectal cancer patients. *J Appl Clin Med Phys.* 2016;17(6):78-85.
47. Schubert C, Waletzko O, Weiss C, et al. Intercenter validation of a knowledge based model for automated planning of volumetric modulated arc therapy for prostate cancer. The experience of the German RapidPlan Consortium. *PLoS One.* 2017;12(5).
48. Younge KC, Marsh RB, Owen D, et al. Improving Quality and Consistency in NRG Oncology Radiation Therapy Oncology Group 0631 for Spine Radiosurgery via Knowledge-Based Planning. *Int J Radiat Oncol Biol Phys.* 2018;100(4):1067-1074.
49. Tseng H-H, Luo Y, Ten Haken RK, El Naqa I. The Role of Machine Learning in Knowledge-Based Response-Adapted Radiotherapy. *Frontiers in Oncology.* 2018;8(266).
50. Kavanaugh JA, Holler S, DeWees TA, et al. Multi-Institutional Validation of a Knowledge-Based Planning Model for Patients Enrolled in RTOG 0617: Implications for Plan Quality Controls in Cooperative Group Trials. *Pract Radiat Oncol.* 2019;9(2):218-227.
51. Berry SL, Ma R, Boczkowski A, Jackson A, Zhang P, Hunt M. Evaluating inter-campus plan consistency using a knowledge based planning model. *Radiother Oncol.* 2016;120(2):349-355.
52. Eclipse Photon and Electron Algorithms 13.7 Reference Guide. 2018.
53. Delaney AR, Tol JP, Dahele M, Cuijpers J, Slotman BJ, Verbakel WF. Effect of Dosimetric Outliers on the Performance of a Commercial Knowledge-Based Planning Solution. *Int J Radiat Oncol Biol Phys.* 2016;94(3):469-477.
54. Zhu X, Ge Y, Li T, Thongphiew D, Yin FF, Wu QJ. A planning quality evaluation tool for prostate adaptive IMRT based on machine learning. *Med Phys.* 2011;38(2):719-726.

55. Eclipse and Electron Algorithms 15.5 Instructions for Use. 2017.
56. Ouyang Z, Liu Shen Z, Murray E, et al. Evaluation of auto-planning in IMRT and VMAT for head and neck cancer. *J Appl Clin Med Phys*. 2019;20(7):39-47.
57. Scaggion A, Fusella M, Roggio A, et al. Reducing inter- and intra-planner variability in radiotherapy plan output with a commercial knowledge-based planning solution. *Phys Med*. 2018;53:86-93.
58. Fogliata A, Nicolini G, Bourgier C, et al. Performance of a Knowledge-Based Model for Optimization of Volumetric Modulated Arc Therapy Plans for Single and Bilateral Breast Irradiation. *PLoS One*. 2015;10(12)
59. Rice A, Zoller I, Kocos K, et al. The implementation of RapidPlan in predicting deep inspiration breath-hold candidates with left-sided breast cancer. *Med Dosim*. 2019;44(3):210-218.
60. Yu G, Li Y, Feng Z, et al. Knowledge-based IMRT planning for individual liver cancer patients using a novel specific model. *Radiat Oncol*. 2018;13(1):52.
61. Yu S, Xu H, Sinclair A, Zhang X, Langner U, Mak K. Dosimetric and planning efficiency comparison for lung SBRT: CyberKnife vs VMAT vs knowledge-based VMAT. *Med Dosim*. 2020.
62. Hof SV, Delaney AR, Tekatli H, et al. Knowledge-Based Planning for Identifying High-Risk Stereotactic Ablative Radiation Therapy Treatment Plans for Lung Tumors Larger Than 5 cm. *Int J Radiat Oncol Biol Phys*. 2019;103(1):259-267.
63. Delaney AR, Dachele M, Tol JP, Slotman BJ, Verbakel WF. Knowledge-based planning for stereotactic radiotherapy of peripheral early-stage lung cancer. *Acta Oncol*. 2017;56(3):490-495.
64. Visak J, Ge GY, McGarry RC, Randall M, Pokhrel D. An Automated knowledge-based planning routine for stereotactic body radiotherapy of peripheral lung tumors via DCA-based volumetric modulated arc therapy. *Journal of Applied Clinical Medical Physics*. 2020.
65. Visak J, McGarry RC, Randall ME, Pokhrel D. Development and clinical validation of a robust knowledge-based planning model for stereotactic body radiotherapy treatment of centrally located lung tumors. *J Appl Clin Med Phys*. 2020.
66. Landberg T, Chavaudra J, Dobbs J, et al. Report 62. *Journal of the International Commission on Radiation Units and Measurements*. 2016;os32(1)
67. Pokhrel D, Halfman M, Sanford L. FFF-VMAT for SBRT of lung lesions: Improves dose coverage at tumor-lung interface compared to flattened beams. *J Appl Clin Med Phys*. 2020;21(1):26-35.
68. Sanford L, Molloy J, Kumar S, Randall M, McGarry R, Pokhrel D. Evaluation of plan quality and treatment efficiency for single-isocenter/two-lesion lung stereotactic body radiation therapy. *Journal of applied clinical medical physics*. 2019;20(1):118-127.

69. Sanford L, Pokhrel D. Improving treatment efficiency via photon optimizer (PO) MLC algorithm for synchronous single-isocenter/multiple-lesions VMAT lung SBRT. *Journal of applied clinical medical physics*. 2019;20(10):201-207.
70. Varian Halcyon Physics Reference Guide. Palo Alto, CA. 2019.
71. Pokhrel D, Visak J, Critchfield LC, et al. Clinical validation of ring-mounted halcyon linac for lung SBRT: comparison to SBRT-dedicated C-arm linac treatments. *Journal of applied clinical medical physics*. 2020.
72. Fogliata A, Cayez R, Garcia R, et al. Technical Note: Flattening filter free beam from Halcyon linac: Evaluation of the profile parameters for quality assurance. *Med Phys*. 2020.
73. Tamura M, Matsumoto K, Otsuka M, Monzen H. Plan complexity quantification of dual-layer multi-leaf collimator for volumetric modulated arc therapy with Halcyon linac. *Phys Eng Sci Med*. 2020.
74. Gay SS, Netherton TJ, Cardenas CE, et al. Dosimetric impact and detectability of multi-leaf collimator positioning errors on Varian Halcyon. *J Appl Clin Med Phys*. 2019;20(8):47-55.
75. Jarema T, Aland T. Using the iterative kV CBCT reconstruction on the Varian Halcyon linear accelerator for radiation therapy planning for pelvis patients. *Phys Med*. 2019;68:112-116.
76. Cozzi L, Fogliata A, Thompson S, et al. Critical Appraisal of the Treatment Planning Performance of Volumetric Modulated Arc Therapy by Means of a Dual Layer Stacked Multileaf Collimator for Head and Neck, Breast, and Prostate. *Technol Cancer Res Treat*. 2018
77. O'Grady F, Barsky AR, Anamalayil S, et al. Increase in Superficial Dose in Whole-Breast Irradiation With Halcyon Straight-Through Linac Compared With Traditional C-arm Linac With Flattening Filter: In vivo Dosimetry and Planning Study. *Adv Radiat Oncol*. 2020;5(1):120-126.
78. Flores-Martinez E, Cervino LI, Pawlicki T, Kim GY. Assessment of the use of different imaging and delivery techniques for cranial treatments on the Halcyon linac. *J Appl Clin Med Phys*. 2020;21(1):53-61.
79. Kim H, Huq MS, Lalonde R, Houser CJ, Beriwal S, Heron DE. Early clinical experience with varian halcyon V2 linear accelerator: Dual-isocenter IMRT planning and delivery with portal dosimetry for gynecological cancer treatments. *J Appl Clin Med Phys*. 2019;20(11):111-120.
80. Pokhrel D, Tackett T, Stephen J, et al. Prostate SBRT using O-Ring Halcyon Linac—Plan quality, delivery efficiency, and accuracy. *Journal of Applied Clinical Medical Physics*. 2020.
81. Knutson NC, Kennedy WR, Reynoso FJ, et al. Intracranial Stereotactic Radiation Therapy With a Jawless Ring Gantry Linear Accelerator Equipped With New Dual Layer Multileaf Collimator. *Advances in Radiation Oncology*. 2020;5(3):482-489.

82. Li T, Irmen P, Liu H, et al. Dosimetric Performance and Planning/Delivery Efficiency of a Dual-Layer Stacked and Staggered MLC on Treating Multiple Small Targets: A Planning Study Based on Single-Isocenter Multi-Target Stereotactic Radiosurgery (SRS) to Brain Metastases. *Front Oncol.* 2019; 9:7.

CHAPTER 2

1. Timmerman R, Paulus R, Galvin J, *et al*, “Stereotactic body radiation therapy for inoperable early stage lung cancer,” *JAMA* (2010) 303:1070–76
2. Onishi H, Shirato H, Nagata Y, *et al*, “Stereotactic body radiotherapy (SBRT) for operable stage I non-small-cell lung cancer: Can SBRT be comparable to surgery?” *Int. J. Radiation Oncology Biol. Phys.*, (2011); 81; 1352–1358
3. Zimmermann F, Geinitz H, Schill S, *et al*, “Stereotactic hypofractionated radiation therapy for stage I non-small cell lung cancer,” *Lung Cancer* 2005; 48:107-14.
4. Timmerman R, McGarry R, Yiannoutsos C, *et al*, "Excessive toxicity when treating central tumors in a phase II study of stereotactic body radiation therapy for medically inoperable early-stage lung cancer," *J Clin Oncol* 2006; 24:4833–9.
5. Sandhu A, Lau S, Rahn D, *et al*, “Stereotactic body radiation therapy in octogenarians with stage I lung cancer,” *Clin Lung Cancer.* (2014);15:131–135
6. Benedict S, Yenice K, Followill D, *et al*, “Stereotactic body radiation therapy: the report of AAPM Task Group 101,” *Med Phys.* (2010);37:4078–4101
7. A Randomized Phase II Study Comparing 2 Stereotactic Body Radiation Therapy (SBRT) Schedules For Medically Inoperable Patients with Stage I Peripheral Non-Small Cell Lung Cancer; RTOG 0915 (2014) 1-67
8. Videtic G, Paulus R, Singh A, *et al*, “Long-term follow-up on NRG Oncology RTOG 0915 (NCCTG N0927): A randomized phase 2 study comparing 2 stereotactic body radiation therapy schedules for medically inoperable patients with stage I peripheral non-small cell lung cancer,” *Int J Radiat Oncol Biol Phys* (2019) 103, 1077–1084
9. Videtic G, Stephans K, Woodly N, *et al*, “30 Gy or 34 Gy? Comparing 2 single-fraction SBRT dose schedules for stage I medically inoperable non-small cell lung cancer,” *Int J Radiat Oncol Biol Phys* 2014; 90; 203-208
10. Merrow, C, Wang I, and Podgorsak M, “A dosimetric evaluation of VMAT for the treatment of non-small cell lung cancer,” *J Appl Clin Med Phys*, (2012) 14: p. 4110.
11. Xiao Y, Kry S, Popple R, *et al*, “Flattening filter-free accelerators: a report from the AAPM therapy emerging technology assessment work group,” *J. Appl. Clin. Med. Phys.* (2015), 16, 12
12. Navarria P, Ascolese AM, Mancosu P, *et al*, “Volumetric modulated arc therapy with flattening filter free (FFF) beams for stereotactic body radiation therapy (SBRT) in patients

with medically inoperable early stage non-small cell lung cancer (NSCLC),” *Radiation Oncology* (2013); 107:414

13. Scorsetti M, Alongi F, Castiglioni S, *et al*, "Feasibility and early clinical assessment of flattening filter free (FFF) based stereotactic body radiotherapy (SBRT) treatments,” *Radiation Oncology* (2011); 6:113

14. Eclipse Photon and Electron Algorithms 13.7 Reference Guide, 2018

15. Shende R, Gupta G, Patel G and Kumar S, “Assessment and performance evaluation of photon optimizer (PO) vs. dose volume optimizer (DVO) for IMRT and progressive resolution optimizer (PRO) for RapidArc planning using a virtual phantom,” *Int. Jour. of Cancer Therapy and Oncology* (2016) 4:437 1-12

16. Binny D, Kairn T, Lancaster C, *et al*, "Photon optimizer (PO) vs progressive resolution optimizer (PRO): a conformality- and complexity-based comparison for intensity-modulated arc therapy plans," *Medical Dosimetry*, (2017) 43; 267-275

17. Jiang F, Wu H, Yue H, *et al*, “Photon Optimizer (PO) prevails over Progressive Resolution Optimizer (PRO) for VMAT planning with or without knowledge-based solution,” *J Appl Clin Med Phys* (2017) 18; 9-14

18. Liu H, Sintay B, Pearman K, *et al*, “Comparison of the progressive resolution optimizer and photon optimizer in VMAT optimization for stereotactic treatments,” *J Appl Clin Med Phys* (2018) 19; 155-162

19. Kry S F, Bednarz B, Howell R M, *et al*, "AAPM TG 158: Measurement and calculation of doses outside the treated volume from external-beam radiation therapy," *Med Phys* 2017; 44; e391-e492

20. Baker R, Han G, Sarangkasiri S, *et al*, “Clinical and dosimetric predictors of radiation pneumonitis in a large series of patients treated with stereotactic body radiation therapy to the lung,” *Int J Radiat Oncol Biol Phys* (2013) 85:190–5.

21. Vassiliev O, Wareing T, McGhee J, *et al*, “Validation of a new grid-based Boltzmann equation solver for dose calculation in radiotherapy with photon beams,” *Phys Med Biol*. (2010);55:581–98

22. Bush K, Gagne I, Zavgorodni S, *et al*, “Dosimetric validation of Acuros® XB with Monte Carlo methods for photon dose calculations,” *Med. Phys.* (2011); 38, 2208–21

23. Kroon P, Hol S and Essers M, *et al*, “Dosimetric accuracy and clinical quality of Acuros XB and AAA dose calculation algorithm for stereotactic and conventional lung volumetric modulated arc therapy plans,” *Radiat. Oncol.* (2013), 8, 149

24. Huang B, Wu L, Lin P, *et al*, “Dose calculation of Acuros XB and Anisotropic Analytic Algorithm in lung stereotactic body radiotherapy treatment with flattening filter free beams and the potential role of calculation grid size,” *Radiation Oncology* (2015) 10:53

25. Vanetti E, Nicolini G, Nord J, *et al*, “On the role of the optimization algorithm of RapidArc((R)) volumetric modulated arc therapy on plan quality and efficiency,” *Med. Phys.* (2011);38:5844

26. Chin Snyder, K, Kim J, Reding A, *et al*, “Development and evaluation of a clinical model for lung cancer patients using stereotactic body radiotherapy (SBRT) within a knowledge-based algorithm for treatment planning,” *J Appl Clin Med Phys*, 2016. 17(6): p. 263-275.

CHAPTER 3

1. Benedict SH, Yenice KM, Followill D, *et al*. Stereotactic body radiation therapy: the report of AAPM Task Group 101, *Med Phys*. 2010; 37:4078-4101.
2. Timmerman R, Paulus R, Galvin J, *et al*. Stereotactic body radiation therapy for inoperable early stage lung cancer. *JAMA*. 2010; 303:1070-1076.
3. Grills IS, Yan D, Martinez AA, Vicini FA, Wong JW, Kestin LL. Potential for reduced toxicity and dose escalation in the treatment of inoperable non-small-cell lung cancer: a comparison of intensity-modulated radiation therapy (IMRT), 3D conformal radiation, and elective nodal irradiation. *Int J Radiat Oncol Biol Phys*. 2003;57:875-890.
4. Navarria P, Ascolese AM, Mancosu P, *et al*. Volumetric modulated arc therapy with flattening filter free (FFF) beams for stereotactic body radiation therapy (SBRT) in patients with medically inoperable early stage non small cell lung cancer (NSCLC). *Radiother Oncol*. 2013;107:414-418.
5. Xiao Y, Kry SF, Popple R, *et al*. Flattening filter-free accelerators: a report from the AAPM Therapy Emerging Technology Assessment Work Group. *J Appl Clin Med Phys*. 2015;16:12-29.
6. Pokhrel D, Halfman M, Sanford L. FFF-VMAT for SBRT of lung lesions: Improves dose coverage at tumor-lung interface compared to flattened beams. *J Appl Clin Med Phys*. 2020;21(1):26-35.
7. Group RTOG. A seamless phase I/II study of stereotactic lung radiotherapy SBRT for early stage, centrally located, non-small cell lung cancer (NSCLC) in medically inoperable patients, RTOG-0813. 2014:1-21.
8. Fogliata A, Reggiori G, Stravato A, *et al*. RapidPlan head and neck model: the objectives and possible clinical benefit. *Radiat Oncol*. 2017;12:73.
9. Berry SL, Ma R, Boczkowski A, Jackson A, Zhang P, Hunt M. Evaluating inter-campus plan consistency using a knowledge based planning model. *Radiother Oncol*. 2016;120:349-355.
10. Vanderstraeten B, Goddeeris B, Vandecasteele K, van Eijkeren M, De Wagter C, Lievens Y. Automated Instead of Manual Treatment Planning? A Plan Comparison Based on Dose-Volume Statistics and Clinical Preference. *Int J Radiat Oncol Biol Phys*. 2018;102:443-450.
11. Li N, Carmona R, Sirak I, *et al*. Highly Efficient Training, Refinement, and Validation of a Knowledge-based Planning Quality-Control System for Radiation Therapy Clinical Trials. *Int J Radiat Oncol Biol Phys*. 2017;97:164-172.

12. Systems VM. Eclipse Photon and Electron Algorithms 13.7 Reference Guide. 2018.
13. Chanyavanich V, Das SK, Lee WR, Lo JY. Knowledge-based IMRT treatment planning for prostate cancer. *Med Phys*. 2011;38:2515-2522.
14. Chin Snyder K, Kim J, Reding A, et al. Development and evaluation of a clinical model for lung cancer patients using stereotactic body radiotherapy (SBRT) within a knowledge-based algorithm for treatment planning. *J Appl Clin Med Phys*. 2016;17:263-275.
15. Delaney AR, Dahele M, Tol JP, Slotman BJ, Verbakel WF. Knowledge-based planning for stereotactic radiotherapy of peripheral early-stage lung cancer. *Acta Oncol*. 2017;56:490-495.
16. Fogliata A, Nicolini G, Bourgier C, et al. Performance of a Knowledge-Based Model for Optimization of Volumetric Modulated Arc Therapy Plans for Single and Bilateral Breast Irradiation. *PLoS One*. 2015:1-12.
17. Hof SV, Delaney AR, Tekatli H, et al. Knowledge-Based Planning for Identifying High-Risk Stereotactic Ablative Radiation Therapy Treatment Plans for Lung Tumors Larger Than 5 cm. *Int J Radiat Oncol Biol Phys*. 2019;103:259-267.
18. Younge KC, Marsh RB, Owen D, et al. Improving Quality and Consistency in NRG Oncology Radiation Therapy Oncology Group 0631 for Spine Radiosurgery via Knowledge-Based Planning. *Int J Radiat Oncol Biol Phys*. 2018; 100:1067-1074.
19. Bush K, Gagne IM, Zavgorodni S, Ansbacher W, Beckham W. Dosimetric validation of Acuros XB with Monte Carlo methods for photon dose calculations. *Med Phys*. 2011; 38:2208-2221.
20. Kroon PS, Hol S, Essers M. Dosimetric accuracy and clinical quality of Acuros XB and AAA dose calculation algorithm for stereotactic and conventional lung volumetric modulated arc therapy plans. *Radiat Oncol*. 2013; 8:149.
21. Visak J, McGarry RC, Pokhrel D. Clinical evaluation of photon optimizer (PO) MLC algorithm for stereotactic, single-dose of VMAT lung SBRT. *Medical Dosimetry*.
22. Delaney AR, Tol JP, Dahele M, Cuijpers J, Slotman BJ, Verbakel WF. Effect of Dosimetric Outliers on the Performance of a Commercial Knowledge-Based Planning Solution. *Int J Radiat Oncol Biol Phys*. 2016; 94:469-477.
23. Yamaguchi S, Ohguri T, Ide S, et al. Stereotactic body radiotherapy for lung tumors in patients with subclinical interstitial lung disease: the potential risk of extensive radiation pneumonitis. *Lung Cancer*. 2013; 82:260-265.
24. Baker R, Han G, Sarangkasiri S, et al. Clinical and dosimetric predictors of radiation pneumonitis in a large series of patients treated with stereotactic body radiation therapy to the lung. *Int J Radiat Oncol Biol Phys*. 2013;85:190-195.
25. Barriger RB, Forquer JA, Brabham JG, et al. A dose-volume analysis of radiation pneumonitis in non-small cell lung cancer patients treated with stereotactic body radiation therapy. *Int J Radiat Oncol Biol Phys*. 2012; 82:457-462.

26. Pokhrel D, Visak J, Sanford L. A novel and clinically useful dynamic conformal arc (DCA)-based VMAT planning technique for lung SBRT. *J Appl Clin Med Phys*. 2020.

CHAPTER 4

1. Benedict S, Yenice K, Followill D, et al. Stereotactic body radiation therapy: the report of AAPM Task Group 101. *Med Phys*. 2010;37(8):4078-4101.
2. Zimmermann F, Geinitz H, Schill S, et al. Stereotactic hypofractionated radiation therapy for stage I non-small cell lung cancer. *Lung Cancer*. 2005;48(1):107-114.
3. Timmerman R, Paulus R, Galvin J, et al. Stereotactic body radiation therapy for inoperable early stage lung cancer. *Jama*. 2010;303(11):1070-1076.
4. Ong CL, Verbakel WF, Cuijpers JP, et al. Stereotactic radiotherapy for peripheral lung tumors: a comparison of volumetric modulated arc therapy with 3 other delivery techniques. *Radiother Oncol*. 2010;97(3):437-442.
5. Grills IS, Yan D, Martinez AA, et al. Potential for reduced toxicity and dose escalation in the treatment of inoperable non-small-cell lung cancer: a comparison of intensity-modulated radiation therapy (IMRT), 3D conformal radiation, and elective nodal irradiation. *Int J Radiat Oncol Biol Phys*. 2003;57(3):875-890.
6. Navarra P, Ascolese AM, Mancosu P, et al. Volumetric modulated arc therapy with flattening filter free (FFF) beams for stereotactic body radiation therapy (SBRT) in patients with medically inoperable early stage non small cell lung cancer (NSCLC). *Radiother Oncol*. 2013;107(3):414-418.
7. Pokhrel D, Halfman M, Sanford L. FFF-VMAT for SBRT of lung lesions: Improves dose coverage at tumor-lung interface compared to flattened beams. *J Appl Clin Med Phys*. 2020;21(1):26-35.
8. Xiao Y, Kry SF, Popple R, et al. Flattening filter-free accelerators: a report from the AAPM Therapy Emerging Technology Assessment Work Group. *J Appl Clin Med Phys*. 2015;16(3):5219.
9. Fogliata A, Reggiori G, Stravato A, et al. RapidPlan head and neck model: the objectives and possible clinical benefit. *Radiat Oncol*. 2017; 12(1):73.
10. Berry SL, Ma R, Boczkowski A, Jackson A, Zhang P, Hunt M. Evaluating inter-campus plan consistency using a knowledge-based planning model. *Radiother Oncol*. 2016;120(2):349-355.
11. Fogliata A, Cozzi L, Reggiori G, et al. RapidPlan knowledge-based planning: iterative learning process and model ability to steer planning strategies. *Radiat Oncol*. 2019;14(1):187.
12. Yu S, Xu H, Sinclair A, et al. Dosimetric and planning efficiency comparison for lung SBRT: CyberKnife vs VMAT vs knowledge based VMAT. *Med Dosim*. 2020.

13. Chanyavanich V, Das S, Lee W, Lo J. Knowledge-based IMRT treatment planning for prostate cancer. *Med Phys*. 2011;38 (5):2515-2522.
14. Fogliata A, Nicolini G, Bourgier C, et al. Performance of a Knowledge-Based Model for Optimization of Volumetric Modulated Arc Therapy Plans for Single and Bilateral Breast Irradiation. *PLoS One*. 2015;10(12):e0145137.
15. Younge KC, Marsh RB, Owen D, et al. Improving Quality and Consistency in NRG Oncology Radiation Therapy Oncology Group 0631 for Spine Radiosurgery via Knowledge-Based Planning. *Int J Radiat Oncol Biol Phys*. 2018;100(4):1067-1074.
16. Chin Snyder K, Kim J, Reding A, et al. Development and evaluation of a clinical model for lung cancer patients using stereotactic body radiotherapy (SBRT) within a knowledge-based algorithm for treatment planning. *J Appl Clin Med Phys*. 2016;17(6):263-275.
17. Delaney AR, Dachele M, Tol JP, Slotman BJ, Verbakel WF. Knowledge-based planning for stereotactic radiotherapy of peripheral early-stage lung cancer. *Acta Oncol*. 2017;56(3):490-495.
18. Hof SV, Delaney AR, Tekatli H, et al. Knowledge-Based Planning for Identifying High-Risk Stereotactic Ablative Radiation Therapy Treatment Plans for Lung Tumors Larger Than 5 cm. *Int J Radiat Oncol Biol Phys*. 2019;103(1):259-267.
19. Cai J, Malhotra HK, Orton CG. Point/Counterpoint. A 3D-conformal technique is better than IMRT or VMAT for lung SBRT. *Med Phys*. 2014;41(4):040601.
20. Das IJ, Ding GX, Ahnesjo A. Small fields: nonequilibrium radiation dosimetry. *Med Phys*. 2008;35(1):206-215.
21. Pokhrel D, Visak J, Sanford L. A novel and clinically useful dynamic conformal arc (DCA)-based VMAT planning technique for lung SBRT. *J Appl Clin Med Phys*. 2020.
22. Bush K, Gagne IM, Zavgorodni S, Ansbacher W, Beckham W. Dosimetric validation of Acuros XB with Monte Carlo methods for photon dose calculations. *Med Phys*. 2011;38(4):2208-2221.
23. Kroon P, Hol S, Essers M. Dosimetric accuracy and clinical quality of Acuros XB and AAA dose calculation algorithm for stereotactic and conventional lung volumetric modulated arc therapy plans. *Radiat Oncol*. 2013;8:149.
24. Handsfield L, Jones R, Wilson D, Siebers J, Read P, Chen Q. Phantomless patient-specific TomoTherapy QA via delivery performance monitoring and a secondary Monte Carlo dose calculation. *Med Phys*. 2014;41(10):101703.
25. Chen Q, Oldland T, Sanford L, Johnson E, Molloy J. Cloud Based Monte Carlo Independent Dose Calculation Tool for Varian Linac: Implementation and Validation. *Medical Physics*. 2019; 46(6):E278.
26. Peng C, Chen G, Ahunbay E, Wang D, Lawton C, Li XA. Validation of an online re-planning technique for prostate adaptive radiotherapy. *Physics in Medicine and Biology*. 2011; 56(12):3659-3668.

27. Salvat F, Fernández-Varea J, Sempau J, Penelope. A code system for Monte Carlo simulation of electron and photon transport. NEA Data Bank, Workshop Proceeding, Barcelona. 2007:4-7.
28. Yamaguchi S, Ohguri T, Ide S, et al. Stereotactic body radiotherapy for lung tumors in patients with subclinical interstitial lung disease: the potential risk of extensive radiation pneumonitis. *Lung Cancer*. 2013;82(2):260-265.
29. Baker R, Han G, Sarangkasiri S, et al. Clinical and dosimetric predictors of radiation pneumonitis in a large series of patients treated with stereotactic body radiation therapy to the lung. *Int J Radiat Oncol Biol Phys*. 2013;85(1):190-195.
30. Barriger R, Forquer J, Brabham J, et al. A dose-volume analysis of radiation pneumonitis in non-small cell lung cancer patients treated with stereotactic body radiation therapy. *Int J Radiat Oncol Biol Phys*. 2012; 82(1):457-462.
31. Pokhrel D, Sanford L, Dhanireddy B, Molloy J, Randall M, McGarry R. Flattening filter free VMAT for a stereotactic, single-dose of 30 Gy to lung lesion in a 15-min treatment slot. *J Appl Clin Med Phys*. 2020, 1-6
32. Ong CL, Dahele M, Slotman BJ, Verbakel WF. Dosimetric impact of the interplay effect during stereotactic lung radiation therapy delivery using flattening filter-free beams and volumetric modulated arc therapy. *Int J Radiat Oncol Biol Phys*. 2013; 86(4):743-748.
33. Kubo K, Monzen H, Ishii K, et al. Dosimetric comparison of RapidPlan and manually optimized plans in volumetric modulated arc therapy for prostate cancer. *Physica Medica*. 2017; 44:199-204

CHAPTER 5

1. Onishi H, Shirato H, Nagata Y, et al. Stereotactic body radiotherapy (SBRT) for operable stage I non-small-cell lung cancer: can SBRT be comparable to surgery? *Int J Radiat Oncol Biol Phys*. 2011;81(5):1352-1358.
2. Navarria P, Ascolese A, Mancosu P, et al. Volumetric modulated arc therapy with flattening filter free (FFF) beams for stereotactic body radiation therapy (SBRT) in patients with medically inoperable early stage non-small cell lung cancer (NSCLC). *Radiother Oncol*. 2013;107(3):414-418.
3. Zimmermann F, Geinitz H, Schill S, et al. Stereotactic hypofractionated radiation therapy for stage I non-small cell lung cancer. *Lung Cancer*. 2005;48(1):107-114.
4. Timmerman R, Paulus R, Galvin J, et al. Stereotactic body radiation therapy for inoperable early stage lung cancer. *JAMA*. 2010;303(11):1070-1076.
5. Benedict S, Yenice K, Followill D, et al. Stereotactic body radiation therapy: the report of AAPM Task Group 101. *Med Phys*. 2010;37(8):4078-4101.

6. Ong C, Verbakel W, Cuijpers J, et al. Stereotactic radiotherapy for peripheral lung tumors: a comparison of volumetric modulated arc therapy with 3 other delivery techniques. *Radiother Oncol*. 2010;97(3):437-442.
7. Cai J, Malhotra HK, Orton CG. Point/Counterpoint. A 3D-conformal technique is better than IMRT or VMAT for lung SBRT. *Med Phys*. 2014;41(4):040601.
8. Merrow CE, Wang IZ, Podgorsak MB. A dosimetric evaluation of VMAT for the treatment of non-small cell lung cancer. *J Appl Clin Med Phys*. 2012;14(1):4110.
9. Pokhrel D, Halfman M, Sanford L. FFF-VMAT for SBRT of lung lesions: Improves dose coverage at tumor-lung interface compared to flattened beams. *J Appl Clin Med Phys*. 2020;21(1):26-35.
10. Scorsetti M, Alongi F, Castiglioni S, et al. Feasibility and early clinical assessment of flattening filter free (FFF) based stereotactic body radiotherapy (SBRT) treatments. *Radiat Oncol*. 2011;6:113.
11. Xiao Y, Kry SF, Popple R, et al. Flattening filter-free accelerators: a report from the AAPM Therapy Emerging Technology Assessment Work Group. *J Appl Clin Med Phys*. 2015; 16:12-29.
12. Varian Medical Systems. Halcyon Physics. Palo Alto, CA 2019.
13. Fogliata A, Cayez R, Garcia R, et al. Technical Note: Flattening filter free beam from Halcyon linac: Evaluation of the profile parameters for quality assurance. *Med Phys*. 2020. 1-8
14. Tamura M, Matsumoto K, Otsuka M, et al. Plan complexity quantification of dual-layer multi-leaf collimator for volumetric modulated arc therapy with Halcyon linac. *Phys Eng Sci Med*. 2020.1-10
15. Gay S, Netherton T, Cardenas C, et al. Dosimetric impact and detectability of multi-leaf collimator positioning errors on Varian Halcyon. *J Appl Clin Med Phys*. 2019;20(8):47-55.
16. Jarema T and Aland T. Using the iterative kV CBCT reconstruction on the Varian Halcyon linear accelerator for radiation therapy planning for pelvis patients. *Phys Med*. 2019; 68:112-116.
17. Berry S, Ma R, Boczkowski A, et al. Evaluating inter-campus plan consistency using a knowledge-based planning model. *Radiother Oncol*. 2016;120(2):349-355.
18. Li N, Carmona R, Sirak I, et al. Highly Efficient Training, Refinement, and Validation of a Knowledge-based Planning Quality-Control System for Radiation Therapy Clinical Trials. *Int J Radiat Oncol Biol Phys*. 2017;97(1):164-172.
19. Vanderstraeten B, Goddeeris B, Vandecasteele K, et al. Automated Instead of Manual Treatment Planning? A Plan Comparison Based on Dose-Volume Statistics and Clinical Preference. *Int J Radiat Oncol Biol Phys*. 2018;102(2):443-450.

20. Fogliata A, Belosi F, Clivio A, et al. On the pre-clinical validation of a commercial model-based optimization engine: application to volumetric modulated arc therapy for patients with lung or prostate cancer. *Radiother Oncol.* 2014;113(3):385-391.
21. Chin Snyder K, Kim J, Reding A, et al. Development and evaluation of a clinical model for lung cancer patients using stereotactic body radiotherapy (SBRT) within a knowledge-based algorithm for treatment planning. *J Appl Clin Med Phys.* 2016;17(6):263-275.
22. Hof S, Delaney A, Tekatli H, et al. Knowledge-Based Planning for Identifying High-Risk Stereotactic Ablative Radiation Therapy Treatment Plans for Lung Tumors Larger Than 5 cm. *Int J Radiat Oncol Biol Phys.* 2019;103(1):259-267.
23. Delaney A, Dahele M, Tol J, et al. Knowledge-based planning for stereotactic radiotherapy of peripheral early-stage lung cancer. *Acta Oncol.* 2017;56(3):490-495.
24. Yu S, Xu H, Sinclair A, et al. Dosimetric and planning efficiency comparison for lung SBRT: CyberKnife vs VMAT vs knowledge-based VMAT. *Med Dosim.* 2020; 1-8
25. Visak J, McGarry RC, Randall ME, Pokhrel D. Development and clinical validation of a robust knowledge-based planning model for stereotactic body radiotherapy treatment of centrally located lung tumors. *J Appl Clin Med Phys.* 2020; 1-10
26. Cozzi L, Fogliata A, Thompson S, et al. Critical Appraisal of the Treatment Planning Performance of Volumetric Modulated Arc Therapy by Means of a Dual Layer Stacked Multileaf Collimator for Head and Neck, Breast, and Prostate. *Technol Cancer Res Treat.* 2018
27. Flores-Martinez E, Kim G, Yashar C, et al. Dosimetric study of the plan quality and dose to organs at risk on tangential breast treatments using the Halcyon linac. *J Appl Clin Med Phys.* 2019;20(7):58-67.
28. Flores-Martinez E, Cervino L, Pawlicki T et al. Assessment of the use of different imaging and delivery techniques for cranial treatments on the Halcyon linac. *J Appl Clin Med Phys.* 2020;21(1):53-61.
29. A seamless phase I/II study of stereotactic lung radiotherapy SBRT for early stage, centrally located, non-small cell lung cancer (NSCLC) in medically inoperable patients, RTOG-0813. 2014:1-21.
30. Hallemeier C, Stauder M, Miller R, et al. Lung stereotactic body radiotherapy using a coplanar versus a non-coplanar beam technique: a comparison of clinical outcomes. *J Radiosurg SBRT.* 2013;2(3):225-233.
31. Pokhrel, D, Visak, J, Critchfield L, et al. Clinical Validation of Ring-Mounted Halcyon Linac for Lung SBRT: Comparison to SBRT-dedicated C-arm linac treatments. *J Appl Clin Med Phys.* 2020;(Article-in-Press).
32. Bush K, Gagne I, Zavgorodni S, et al. Dosimetric validation of Acuros XB with Monte Carlo methods for photon dose calculations. *Med Phys.* 2011;38(4):2208-2221.

33. Kroon P, Hol S, Essers M. Dosimetric accuracy and clinical quality of Acuros XB and AAA dose calculation algorithm for stereotactic and conventional lung volumetric modulated arc therapy plans. *Radiat Oncol*. 2013; 8:149.
34. Chen Q, Oldland T, Sanford L, et al. Cloud Based Monte Carlo Independent Dose Calculation Tool for Varian Linac: Implementation and Validation. *Medical Physics*. 2019; 46(6): E278.
35. Baker R, Han G, Sarangkasiri S, et al. Clinical and dosimetric predictors of radiation pneumonitis in a large series of patients treated with stereotactic body radiation therapy to the lung. *Int J Radiat Oncol Biol Phys*. 2013;85(1):190-195.
36. Barriger R, Forquer J, Brabham J, et al. A dose-volume analysis of radiation pneumonitis in non-small cell lung cancer patients treated with stereotactic body radiation therapy. *Int J Radiat Oncol Biol Phys*. 2012;82(1):457-462.
37. Dupic G, Biau J, Molnar I, et al. Significant Correlation Between Overall Survival and Mean Lung Dose in Lung Stereotactic Body Radiation Therapy (SBRT). *Front Oncol*. 2020; 10:1577.
38. Bodensteiner D. RayStation: External beam treatment planning system. *Med Dosim*. 2018;43(2):168-176.
39. Zhang X, Penagaricano J, Narayanasamy G, et al. Helical tomotherapy to LINAC plan conversion utilizing RayStation Fallback planning. *J Appl Clin Med Phys*. 2017;18(1):178-185.
40. Yuan Z, Nair CK, Benedict SH, et al. Converting Treatment Plans from Helical Tomotherapy to L-Shape Linac: Clinical Workflow and Dosimetric Evaluation. *Technol Cancer Res Treat*. 2018;17 :1533033818785279.
41. NRG-RTOG: A Phase II Trial of Stereotactic Body Radiation Therapy (SBRT) in the Treatment of Patients with Operable Stage I/II Non-Small Cell Lung Cancer, RTOG-0618, 2014; 1-66
42. Pokhrel D, Sanford L, Dhanireddy B, *et al*, “Flattening filter free VMAT for a stereotactic, single-dose of 30 Gy to lung lesion in a 15-min treatment slot,” *J Appl Clin Med Phys*. 2020, 1-6
43. NRG-RTOG: A Randomized Phase II Study Comparing 2 Stereotactic Body Radiation Therapy (SBRT) Schedules for Medically Inoperable Patients with Stage I Peripheral Non-Small Cell Lung Cancer, RTOG-0915. 2014; 1-67

CHAPTER 7

1. Sanford L, Molloy J, Kumar S, Randall M, McGarry R, Pokhrel D. Evaluation of plan quality and treatment efficiency for single-isocenter/two-lesion lung stereotactic body radiation therapy. *Journal of applied clinical medical physics*. 2019;20(1):118-127.

2. Sanford L, Pokhrel D. Improving treatment efficiency via photon optimizer (PO) MLC algorithm for synchronous single-isocenter/multiple-lesions VMAT lung SBRT. *Journal of applied clinical medical physics*. 2019;20(10):201-207.
4. Miguel-Chumacero, E., Currie, G., Johnston, A. et al. Effectiveness of Multi-Criteria Optimization-based Trade-Off exploration in combination with RapidPlan for head & neck radiotherapy planning. *Radiat Oncol* 13, 229 (2018).

VITA

Justin David Visak

Education

University of Kentucky, Lexington, KY

Doctor of Philosophy, Radiation and Radiological Sciences Expected Spring 2021

Dissertation: “Development and Clinical Validation of Knowledge-Based Planning Models for Stereotactic Body Radiotherapy of Early-Stage Non-Small-Cell Lung Cancer Patients”

Thesis Advisor: Dr. Damodar Pokhrel

University of Kentucky, Lexington, Ky

Master of Science, Radiological Medical Physics 2019

University of Kentucky, Lexington, Ky

Bachelor of Science, Physics 2017

Minor: Mathematics

Professional Experience

Medical Physics Assistant

Department of Radiation Oncology at the University of Kentucky 2019-current

Teaching Assistant

Department of Radiation Oncology at the University of Kentucky. 2019-current

Peer-Reviewed Journals Relevant to this Thesis (5)

1. **Visak J**, McGarry RC, Pokhrel D. Clinical evaluation of photon optimizer (PO) MLC algorithm for stereotactic, single-dose of VMAT lung SBRT. *Med Dosim.* 2020; 45(4):321-326
2. **Visak, J**, McGarry RC, Randall M, Pokhrel, D. Development and Clinical Validation of a Robust Knowledge-Based (KBP) Model for Stereotactic Body Radiotherapy (SBRT) of Centrally Location Lung Tumors. *J Appl Clin Med Phys.* 2020; 22(1); 1-10
3. **Visak J**, Ge G, McGarry RC, Randall M, and Pokhrel D. An Automated Knowledge-Based Planning Routine for Stereotactic Body Radiotherapy of Peripheral Lung Tumors via DCA-Based Volumetric Arc Therapy. *J Appl Clin Med Phys.* 2020; 22(1); 1-10
4. Pokhrel D, **Visak J**, Sanford L. A novel and clinically useful dynamic conformal arc (DCA)-based VMAT planning technique for lung SBRT. *J Appl Clin Med Phys.* 2020; 21(7); 1-8
5. Pokhrel D, **Visak J**, Critchfield L, Stephenson J, et al. Clinical Validation of Ring-Mounted Halcyon Linac for Lung SBRT: Comparison to SBRT-dedicated C-arm Linac Treatments. *J Appl Clin Med Phys.* 2020; 22(1); 1-9

Submitted Peer-Reviewed Journals Related to Thesis (2)

1. **Visak J**, Webster A, Bernard ME, et al. Fast Generation of Lung SBRT Plans with a Knowledge-Based Planning Model on Ring-Mounted Halcyon Linac. (**Under Review**, *J Appl Clin Med Phys*, submitted on January 10, 2021).
2. Critchfield L, **Visak J**, Bernard, M, et al. Automation and Integration of Restricted Single-Isocenter Stereotactic Body Radiotherapy (RESIST) Method for Synchronous Multiple Lung Lesions. (**Under Review**, *J Appl Clin Med Phys*, **Revised** on January 15, 2021).

Other Peer-Reviewed Journal Publications (1)

1. Pokhrel D, Tackett T, Stephen J, **Visak J**. et al. Prostate SBRT using O-Ring Halcyon Linac- Plan Quality, Delivery Efficiency and Accuracy. *J Appl Clin Med Phys*. 2020; 22(1); 1-7

Abstracts and Presentations (6)

1. Kenamond M, Pokhrel D, **Visak J** and McGarry RC. Escalating Tumor Dose via Simultaneous Integrated Boost (SIB) Stereotactic Body Radiation Therapy (SBRT) for Large (> 5 cm) Lung Masses. [Abstract] Submitted to ASTRO Annual Meeting, March 1, 2021.
2. **Visak J**, Webster A, Kudrimoti M, McGarry RC, Randall M and Pokhrel D. Demonstrating the Practical Limitation of Previously Validated Knowledge-Based Planning Model for SIB Lung SBRT of Large (> 5 cm) Tumors. [Abstract] Submitted to AAPM Annual Meeting, March 3, 2021.
3. **Visak J**, McGarry RC, Randall M, McGarry RC and Pokhrel D. On the Use of Knowledge-Based Planning for the Treatment of Lung Stereotactic Body Radiation Therapy with Halcyon Linac. AAPM ORVC Oral Presentation, (Virtual Meeting) October 2020
4. **Visak J**, McGarry RC, Randall M, McGarry RC and Pokhrel D. Development and Clinical Validation of a Robust Knowledge-based Planning (KBP) Model for SBRT Treatment of Centrally Located Lung Tumors. Med. Phys. [Abstract] AAPM Annual Meeting & Exhibition 2020 (ePoster Presentation)
5. Gei M, **Visak J** and Pokhrel D. Evaluating iCBCT Image Quality at Halcyon Linac for Patient Set Up Verification. Med. Phys. [Abstract] AAPM Annual Meeting & Exhibition 2020 (ePoster Presentation)
6. **Visak J**, Molloy J, Randall M, McGarry RC and Pokhrel D. Clinical Validation of Photon Optimizer (PO) Algorithm Against Progressive Resolution Optimizer (PRO) in the Treatment of Single-Dose Lung SBRT. Med. Phys. [Abstract] AAPM Annual Meeting & Exhibition 2019 (Moderated Campus ePoster Presentation)